THE ROLE OF MITOPHAGY IN MUSCLE STEM CELL FATE AND FUNCTION DURING MUSCLE REGENERATION

Madhavee Thumiah-Mootoo

A thesis submitted in partial fulfilment of the requirements for the
Master's degree in Cellular and Molecular Medicine

Department of Cellular and Molecular Medicine
Faculty of Medicine
University of Ottawa

ABSTRACT

Skeletal muscles have a remarkable capacity to repair and regenerate in response to injury by virtue of their unique population of resident muscle stem cells (MuSCs). Recently, several studies have reported that mitochondria are important regulators of fate and function in various types of stem cells including MuSCs. Furthermore, emerging evidence has shown that accumulation of dysfunctional mitochondria leads to stem cell aging, premature commitment and impaired self-renewal. Preliminary evidence from publicly available transcriptomics datasets processed by our lab showed that Phosphatase and tensin homolog (PTEN)-induced putative kinase 1(PINK1) and Parkin/PARK2 genes, two key regulators of mitophagy are expressed in quiescent MuSCs and are transiently down-regulated as MuSCs activate. This led us to hypothesize that maintenance of an optimally functioning population of mitochondria through mitophagy would be important for self-renewal and muscle repair. *In vitro* single myofiber cultures isolated from mitophagy reporter mice (*mito*-QC mice), show that mitophagy is active in quiescent MuSCs and is transiently decreased upon MuSCs activation. We also show that mitophagy is re-activated in differentiating and self-renewing MuSCs. To further study muscle regeneration, we used a cardiotoxin (CTX) injury model of the Tibialis anterior (TA) muscle in mouse models harboring a knockout (KO) of PINK1 and Parkin. We show that loss of PINK1 *in vivo* promotes commitment of MuSCs in response to acute injury and ultimately leads to depletion of the MuSC pool and impaired muscle regeneration compared to wild type (WT) mice following repetitive injuries. Similarly, loss of Parkin in MuSCs *in vivo* impaired their self-renewal capacity. Consistent with these results, *in vitro* single myofiber cultures isolated from PINK1-deficient mice showed increased MuSCs commitment and impaired self-renewal. *In vitro* preliminary results from MuSCs-specific KO of Parkin revealed altered lineage progression, differentiation and self-renewal of MuSCs. Together, these findings suggest that PINK1/Parkin-dependent mitophagy acts as an important mitochondrial

quality control mechanism which could be required for regulating MuSCs fate and function during muscle regeneration.

Keywords: Mitophagy, PINK1, Parkin/PARK2, *mito*-QC, mitochondria, stem cells, MuSCs, muscle regeneration.

ACKNOWLEDGMENTS

First and foremost, I would like to thank my supervisors, Dr. Yan Burelle and Dr. Mireille Khacho for their support and invaluable guidance throughout this research. Their passion, vision, dynamism and motivation have deeply inspired me.

I would also like to express my gratitude to my thesis advisory committee, Dr. Keir Menzies and Dr. Jeff Dilworth for their continued support, encouragement and insightful comments.

I am extending my heartfelt thanks to my husband, Roody for his support, love and patience for the last 2 years of work. My biggest thanks to my beloved pet, Ellie for her unconditional love, care and joy she brought to my life during the thesis period.

I am extremely grateful to my parents and family for their love, prayers, care and continuing support to complete this research work.

Special thanks go to our lab technician, Nikita Larionov for technical support on animal handling, procedures and tissue sectioning, as well as for his encouragement throughout the project. I would like to express my most sincere gratitude to my dear labmate, Nicole Baker for her time and patience in training me and also for her kind words and support. I would also like to thank all my fellow labmates in particular Dr. George Cairns for his help, guidance and encouragement throughout this research.

My special thanks and appreciation to my friends and everyone who have provided their support and love in completing this endeavor.

Funding for this work was supported by an NSERC-CREATE MATRIX Scholarship.

TABLE OF CONTENTS

LIST OF ABBREVIATIONS

ACVS	Animal care and veterinary service
AFSC	Amniotic fluid stem cell
AMBRA1	Autophagy and beclin 1 regulator 1
AMPK	Adenosine monophosphate-activated protein kinase
AMPKα1	Adenosine monophosphate-activated protein kinase alpha-1
ANOVA	Analysis of variance
ATG12	Autophagy related 12
ATG5	Autophagy related 5
ATP	Adenosine triphosphate
$BaCl_2$	Barium chloride
BCL2	B-cell leukemia/lymphoma 2
bFGF	Basic fibroblast growth factor
BH3	Bcl-2 homology 3
BMSC	Bone marrow mesenchymal stem cell
BNIP3	BCL2 interacting protein 3
BNIP3L	BCL2 Interacting Protein 3 Like
BRCA1	Breast cancer gene 1
BSA	Bovine serum albumin
CCCP	Carbonyl cyanide m-chlorophenylhydrazone
CD11b	Cluster of differentiation 11b
CD31	Cluster of differentiation 31
CD34	Cluster of differentiation 34
CD45	Cluster of differentiation 45
CDK	Cyclin-dependent kinase
CHK	Checkpoint kinase
CI	Complex I

CIV	Complex IV
CO_2	Carbon dioxide
COX	Cytochrome c oxidase
CSA	Cross-sectional area
CSC	Cancer stem cell
CTX	Cardiotoxin
D.melanogaster	*Drosophila melanogaster*
DAB	3,3'-diaminobenzidine
DAPI	4′,6-diamidino-2-phenylindole
DLL1	Delta-like protein 1
DMEM	Dulbecco's modified eagle's medium
DNA	Deoxyribonucleic acid
DPI	Days post-injury
DPX	Dibutylphthalate polystyrene xylene
DRP1	Dynamin-related protein 1
DSHB	Developmental studies hybridoma bank
EDL	Extensor digitorum longus
EDTA	Ethylenediaminetetraacetic acid
EGF	Epidermal growth factor
eMyHC	Embryonic myosin heavy chain
ERK1/2	Extracellular signal-regulated kinase ½
ESAM	Endothelial cell-selective adhesion molecule
ESC	Embryonic stem cell
FACS	Fluorescence-activated cell sorting
FAO	Fatty acid oxidation
FBS	Fetal bovine serum
FGF2	Fibroblast growth factor 2

FIS1	Mitochondrial fission protein 1
Flx	Floxed
FoxK1	Forkhead box K1
FUNDC1	FUN14 domain containing 1
GABAA	γ-Aminobutyric acid type A
GABARAP	γ-Aminobutyric acid type A (GABAA) receptor-associated protein
GEO	Gene expression omnibus
GFP	Green fluorescent protein
H&E	Hematoxylin and eosin
Hes1	Hes family BHLH transcription factor 1
Hey1	Hes related family BHLH transcription factor with YRPW Motif 1
HeyL	Hes related family BHLH transcription factor with YRPW Motif Like
HGF	Hepatocyte growth factor
Hh	Hedgehog
HSC	Hematopoietic stem cell
IF	Immunofluorescence
IGF-1	Insulin-like growth factor-1
IGF-2	Insulin-like growth factor 2
IL34	Interleukin 34
IMM	Inner mitochondrial membrane
iPSC	Induced-pluripotent stem cell
JAK	Janus kinase
JC-1	1st J-aggregate-forming cationic
KO	Knockout
LC3	Light chain 3
LC3B	Light chain 3B
LIR	LC3-interacting region

LoxP	Locus of X-over P1
LSC	Leukemia stem cell
MACS	Magnetic-activated cell sorting
MAP1LC3A-II	Microtubule associated protein 1 light chain 3 alpha-II
MAPK	Mitogen-activated protein kinase
MCP-1	Monocyte chemoattractant protein-1
MFN1	Mitofusin 1
MFN2	Mitofusin 2
MIP-1	Macrophage inflammatory protein-1
miR-31	Micro-ribonucleic acid 31
miR-489	Micro-ribonucleic acid 489
miRNA/miR	Micro-ribonucleic acid
mito-SQSTM1	Mito-sequestosome 1
MMP	Mitochondrial membrane potential
MRF	Myogenic regulatory factor
MRF	Myogenic regulatory factor 4
mRNA	Messenger ribonucleic acid
MSC	Mesenchymal stem cell
mtDNA	Mitochondrial DNA
MUL1	Mitochondrial E3 ubiquitin protein ligase 1
MuSC	Muscle stem cell
Myf5	Myogenic factor 5
MyHC/MYH	Myosin heavy chain
MyoD	Myoblast determination protein
MyoG	Myogenin
N-CAM	Neural cell adhesion molecule
NaCl	Sodium chloride

NADH	1,4-Dihydronicotinamide adenine dinucleotide
NBR1	Neighbor of breast cancer gene 1 (BRCA1) gene 1
NBT	Nitro blue tetrazolium
NDP52	Nuclear domain 10 protein 52
NSC	Neural stem cell
°C	Degree Celsius
OMM	Outer mitochondrial membrane
OPA1	Optic atrophy 1
OXPHOS	Oxidative phosphorylation
P62	Nucleoporin 62
PARK2	Parkinson disease 2
PARL	Presenilin-associated rhomboid-like protein
PAX3	Paired box 3
PAX7	Paired box 7
PBS	Phosphate buffered saline
PDGF-BB	Platelet-derived growth factor-BB
PE	Phycoerythrin
PE-Cy7	Phycoerythrin-cyanine7
PFA	Paraformaldehyde
PGAM5	Mitochondrial phosphatase PGAM family member 5
PINK1	Phosphatase and tensin homolog (PTEN)-induced putative kinase 1
PPAR	Peroxisome proliferator-activated receptor
PPARδ	Peroxisome proliferator-activated receptor δ
qPCR	Quantitative polymerase chain reaction
QSC	Quiescent muscle stem cell
RNA	Ribonucleic acid
ROS	Reactive oxygen species

Sca-1	Stem cell antigen-1
SEM	Standard error of the mean
SIRT3	Sirtuin 3
SIX1	Sine oculis homeobox homolog 1
SPB	Sodium phosphate buffer
Spry1	Sprouty1
SQSTM1	Sequestosome 1
STAT3	Signal transducer and activator of transcription 3
T0	Timepoint 0 (0 hours post isolation)
T0.5	Timepoint 0.5 (0.5 hours post isolation)
T1	Timepoint 1 (1 hours post isolation)
T24	Timepoint 24 (24 hours post isolation)
T48	Timepoint 48 (48 hours post isolation)
T72	Timepoint 72 (72 hours post isolation)
TA	Tibialis anterior
TGF-β1	Transforming growth factor beta 1
TMRE	Tetramethylrhodamine, ethyl ester
TNF-α	Tumor necrosis factor alpha
TOMM70A	Translocase of outer mitochondrial membrane 70 homolog A
Ub	Ubiquitin
ULK1	Unc-51 like autophagy activating kinase 1
VCAM-1	Vascular adhesion molecule-1
WT	Wild type

LIST OF TABLES

LIST OF FIGURES

1. INTRODUCTION

1.1. Adult skeletal muscle

Adult skeletal muscle is a dynamic and plastic tissue representing about 40% of the human body weight and over 50% of all body proteins[1; 2; 3; 4; 5]. It is primarily involved in contraction due to its characteristic properties such as strength, flexibility and plasticity therefore allowing organisms to generate force and facilitate voluntary movement to perform daily activities and be functionally independent[1; 4; 5]. Additionally, skeletal muscle also serves as a storage for amino acids and carbohydrates, assists in the maintenance of body temperature by generating heat and is required for oxygen and fuel consumption during physical activity[5]. This tissue is mainly composed of muscle fibers, also known as myofibers due to their elongated morphology[4; 5]. The skeletal muscle fiber is a multinucleated cylindrical cell with a varying length of 2 to 3 cm to up to 50 cm and can be between 10 and 100 μm thick[4; 6]. Muscle fibers are surrounded by a cell membrane called the sarcolemma which contains the cytoplasm termed sarcoplasm (**Fig. 1**)[4]. Each muscle fiber is composed of myofibrils which run parallel to the myofiber attached to the sarcolemma at each extremity thereby occupying majority of the intracellular space[4]. Consequently, cellular organelles, such as mitochondria and nuclei, are pushed towards the periphery of the sarcoplasm[4]. The myofibril is organized into a unique striated pattern and contains long myofilaments mainly made up of the proteins, actin and myosin[4]. These proteins are arranged into regions to form contractile units called sarcomeres which are delineated by Z-lines[4; 6]. Myofilaments are of two types, thick and thin filaments, the thick one consists of myosin and the thin filament is composed of actin, troponin, and tropomyosin[4; 7]. Muscle fibers are classified into fiber types with different contractile and metabolic profiles and are based on differential myosin heavy chain (MYH) gene expression[8]. Slow twitch fibers, also known as Type I fibers, expressing MYH1, MYH2, MYH4, have low maximal force, low shortening speed but are endurant and mostly oxidative with more mitochondria while fast twitch fibers, referred to as Type II fibers, expressing MYH7, have

high velocity and power, fast speed of fatigue and are mostly glycolytic with fewer mitochondria[8; 9]. Myofibers are formed during myogenesis which is a highly regulated process distinguished by a period of precursor cell proliferation followed by the expression of different muscle-specific transcription factors and finally the fusion of myocytes into myotubes[1; 10].

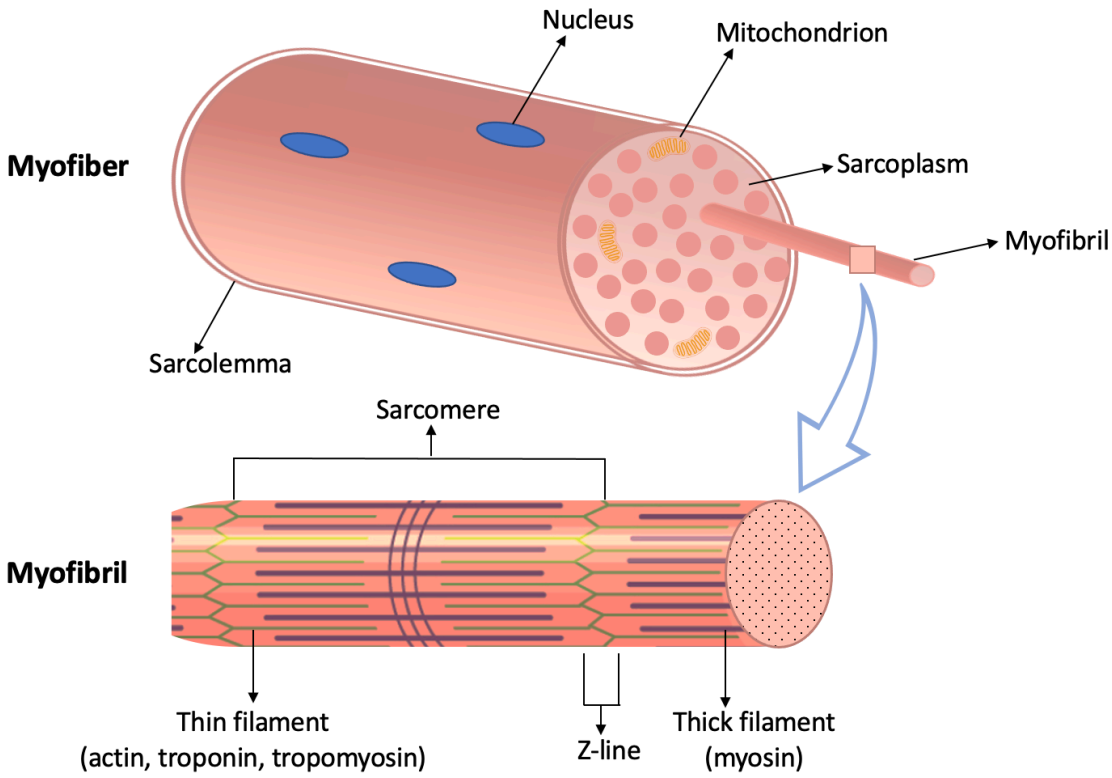

Fig. 1: Structure of a skeletal muscle fiber (adapted from Cretoiu *et al.*[4]).

Muscle health impacts life quality and is pivotal for allowing an individual to carry out normal daily activities. Therefore, research on factors influencing muscle plasticity in particular muscle regeneration for the long-term maintenance of muscle function and adaptability, is of great importance and scientific interest[11].

1.2. Muscle injury/degeneration and regeneration

The vital functions of skeletal muscle can be disturbed by injuries[12]. Adult skeletal muscle possesses the tremendous capacity to repair and regenerate in response to injury or muscle loss[1; 2; 3]. Muscle regeneration in humans starts 7-10 days after injury or degeneration whereas

in mice, it begins slightly earlier, during the first 4-5 days. Then, in both humans and mice, the process peaks around 14 days and then slowly decreases by 3 to 4 weeks[11; 13; 14; 15]. Significant changes occur in muscle cells and extracellular matrix upon muscle loss[11; 14]. Skeletal muscle injury or degeneration is initially characterized by a loss of intracellular calcium homeostasis within the injured myofiber resulting in the degradation of damaged proteins[16]. This degradative process is also associated with the rupture and rapid necrosis of the injured muscle fibers which involves the disruption of the sarcolemma of myofibers resulting in increased myofiber permeability[11]. This is followed by the formation of a hematoma and the expression of inflammatory cytokines and chemokines such as tumor necrosis factor alpha (TNF-α), macrophage inflammatory protein-1 (MIP-1), and monocyte chemoattractant protein-1 (MCP-1) occurring 6 hours post-injury and subsequently, the infiltration by inflammatory cells such as neutrophils, at 24 hours post-injury and macrophages peaking at 72 hours post-injury[11; 16; 17]. The inflammatory response has been reported to play a role in signaling the primary regenerative cells, a unique population of resident stem cells to participate in the regeneration process[16]. The last step of the muscle repair process involves fusion events of myogenic cells where the size of myofibers increase and myonuclei move to the periphery of the fiber due to the increase in contractile protein content and myofiber density to finally give the new muscle tissue the same morphological and functional properties as an uninjured muscle. Muscle repair can also result in fibrosis and formation of scar tissue[11; 14; 16]. A fine balance between these steps are essential for complete, effective regeneration and proper functioning of the muscle tissue[14].

1.3. Muscle stem cells

The primary regenerative cells involved in muscle regeneration are muscle stem cells (MuSCs), also known as satellite cells[11; 18]. Since all myofiber nuclei are terminally postmitotic, muscle repair is mediated by MuSCs[1]. MuSCs, discovered by Alexander Mauro in 1961, reside in a protected membrane-enclosed niche between the basal lamina and sarcolemma of muscle fibers

and comprise less than 5% of myonuclei in skeletal muscle tissue[19; 20; 21]. Skeletal muscle tissue has a low turnover with about 1-2% myonuclei per week. Therefore, the activity of MuSCs is more predominant during periods of remodeling secondary to physiological changes in workload or in response to episodes of injury or disease[1; 21]. MuSCs are mitotically quiescent until required for growth or repair[20; 22]. Following muscle injury, they are activated, start to proliferate and travel to the injury site to give rise to myoblasts that will fuse to each other or to existing myofibers to form terminally differentiated myofibers within a few days[13; 20; 23; 22; 24; 25]. During the repair response, new quiescent MuSCs are formed to replenish the MuSC pool[23; 26; 22; 24].

These different phases of MuSCs are determined by the expression of muscle-specific genes. Quiescent MuSCs express Paired box transcription factors (Pax3 and Pax7) whereas activated MuSCs retain the expression of Pax7 while also expressing proliferative and myogenic transcription factors, Myogenic factor 5 (Myf5), and Myoblast determination protein (MyoD)[10; 27; 28] (**Fig.2**). Most activated MuSCs then start to proliferate and are characterized by the expression the markers of proliferation, Ki67 and proliferating cell nuclear antigen (PCNA)[27; 29; 30]. Proliferating MuSCs can give rise to committed cells thus contributing to the regenerative process or return to quiescence thereby maintaining the MuSC pool[27; 31]. Self-renewing MuSCs retain the expression of Pax7 and repress MyoD ($Pax7^{high}/MyoD^{low}$) while committed cells down-regulate Pax7 and express MyoD ($Pax7^{low}/MyoD^{high}$). Committed cells, also referred to as differentiating myoblasts, express MyoD which later form myocytes, characterized by the expression of the late myogenic marker myogenin (MyoG)[27; 31; 32]. Regenerating muscle fibers express the embryonic form of myosin heavy chain (eMyHC) and finally, mature myofibers can be identified by the expression of adult myosin heavy chain (MyHC/MYH) isoforms[27; 33].

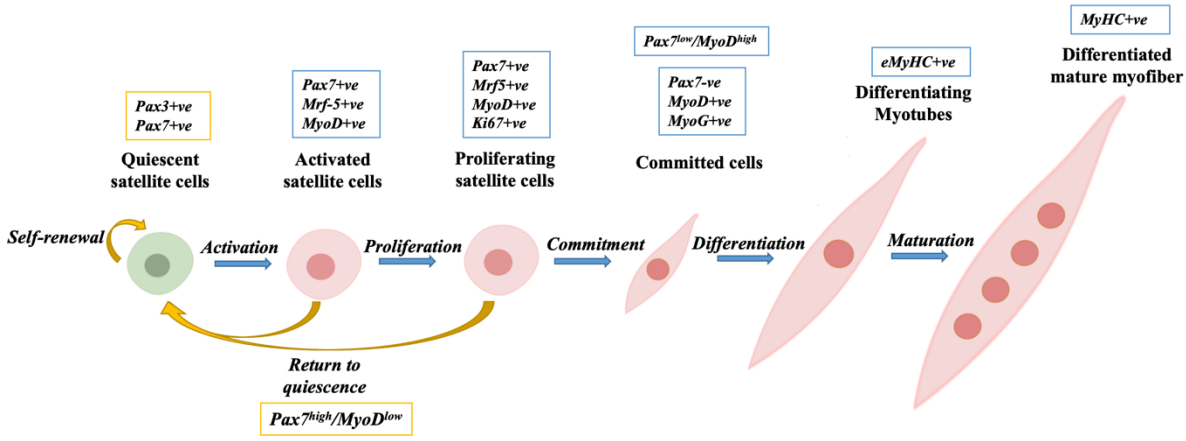

Fig.2: Regulation of MuSC activation and differentiation into myotubes[10; 28; 33].

1.3.1. MuSC quiescence

Quiescent MuSCs are generally spindle-shaped cells with minimal cytoplasm and few organelles[22; 34]. These cells do not undergo cell division and thus have a low metabolic demand and are also resistant to deoxyribonucleic acid (DNA) damage compared to myogenic progenitor cells[35; 36]. Due to their mitotically quiescent nature, quiescent MuSCs are said to be in a G_0 state which is described as a temporary and reversible cell cycle arrest within the G_1 phase[3; 37]. The quiescent state is important to maintain the pool of MuSCs since entry into the cell cycle may result in premature differentiation and depletion of the MuSC population[36].

Quiescence in MuSCs is maintained by a number of transcription factors which are involved in maintenance of a dormancy state and the inhibition of cell cycle entry[35; 38]. In addition to Pax genes, quiescent MuSCs are characterized by the high expression of cell-cell adhesion molecules namely vascular adhesion molecule-1 (VCAM-1), neural cell adhesion molecule (N-CAM), cluster of differentiation 34 (CD34) and endothelial cell-selective adhesion molecule (ESAM) and low expression of cell cycle genes such as cyclins, cyclin-dependent kinases (CDKs) and checkpoint kinases (CHKs)[35; 36; 38].

The molecular regulation of quiescent MuSCs has been extensively studied over the years. Strong evidence has shown that MuSC quiescence is a highly regulated state involving a number of critical regulators[25; 35; 36; 37; 38; 39]. Mourikis *et al.* identified the Notch signaling

pathway as the first regulator of quiescence in MuSCs[37; 40]. The high expression of Notch target genes such as Hes1, Hey1, and HeyL in quiescent MuSCs and their repression upon activation demonstrated the critical role of the notch signaling for the maintenance of a quiescence state in MuSCs[40; 41; 42]. Pax7 is a widely used marker for quiescent and activated MuSCs and has been shown to be essential for normal skeletal muscle growth and repair through its role in the maintenance and regulation of MuSCs[43; 44; 45]. Quiescent MuSCs can be distinguished as Pax7^{high} cells since down-regulation of Pax7 has been shown to be required for commitment and differentiation of MuSCs[32]. CD34, a known marker for hematopoietic stem cells (HSCs), has been reported to play an important role in the maintenance of quiescence in MuSCs[35; 46]. Beauchamp *et al*. showed that quiescent cells express CD34 suggesting its role in the maintenance of MuSC quiescence[46]. Similar to Pax7, high expression of CD34 in MuSCs has been linked to a quiescent state[47]. Sprouty1 (Spry1), a receptor tyrosine kinase inhibitor, is highly expressed in quiescent MuSCs and is down-regulated as MuSCs start to activate[36; 48]. It is well established that Spry1 is an important regulator of MuSC quiescence and maintenance of the MuSC pool during muscle regeneration[48]. Several other key regulators have been found to maintain MuSC quiescence namely MicroRNAs (miRNAs), Staufen1 and primary cilium-mediated repressive Hedgehog (Hh) signaling[36; 39; 49; 50].

Quiescence in MuSCs have been recently reported to exist in different states where they are either in deep quiescence or be primed for activation or commitment[37]. These states can be distinguished by the level of Pax7 expression whereby Pax7^{high} cells are more likely to be in a dormancy state and Pax7^{low} cells would be poised for cell cycle entry[32; 37; 51].

1.3.2. MuSC activation

Although MuSCs remain in their quiescent state, they are activated upon injury or any other damage[13]. MuSC activation is defined as the exit from quiescence in response to signals from a damaged environment[3]. Activated MuSCs are morphologically distinct from quiescent MuSCs, they are larger in size with an enlarged cytoplasm and more organelles[22; 52]. Activation

of MuSCs results in the expansion of the myogenic cell pool and thus triggers a highly orchestrated myogenic program that is controlled by a number of myogenic regulatory factors (MRFs) namely Myf5, MyoD, MyoG and myogenic regulatory factor 4 (MRF4), niche factors, miRNAs molecules and signaling pathways such as the Wnt and Notch[3; 53]. The extracellular matrix has also been found to contribute to MuSC activation through the release of growth factors and cytokines such as insulin-like growth factor-1 (IGF-1), insulin-like growth factor 2 (IGF-2), fibroblast growth factor 2 (FGF2), epidermal growth factor (EGF), platelet-derived growth factor-BB (PDGF-BB) and hepatocyte growth factor (HGF)[54; 55; 56; 57]. Activation of MuSCs is not only restricted to the injury site, all MuSCs on the same muscle fiber are activated and migrate to the regeneration site[3; 58].

1.4. MuSC fate

MuSCs are known to have the ability to choose their fate, they can either self-renew to replenish the MuSC pool or commit and differentiate to form a new muscle fiber[3; 59; 60; 61]. Regulation of MuSC fate decisions is crucial for the balance between muscle regeneration and the maintenance of the MuSC pool[62]. Therefore, identifying the underlying mechanisms that regulate MuSC fate will provide insight into potential treatment for diseases related to MuSC pool depletion and impaired muscle regeneration.

1.4.1. MuSC self-renewal

Self-renewal of MuSCs is a crucial process required for the maintenance of the MuSC pool in adult skeletal muscle[63]. During cell division, MuSCs have the ability to give rise to daughter cells with self-renewal properties thus becoming a new stem cell to replenish the MuSC pool[63; 64]. MuSCs may undergo both asymmetric and symmetric self-renewal to accomplish their role to expand the MuSC pool following injury or disease state[3]. It is also well known that during regenerative myogenesis, a small population of MuSC maintain an undifferentiated state and remain quiescent[63]. Many researchers showed great interest in elucidating the mechanisms regulating MuSC self-renewal. The most studied genes or pathways dictating MuSC self-

renewal are Pax3, Pax7, Myf5, MyoD, p38 α/β mitogen-activated protein kinase (MAPK) pathway, miRNA 489-Dek (miR-489-Dek) pathway, Spry1 and Sine oculis homeobox homolog 1 (SIX1)[43; 48; 50; 66; 67; 68; 69; 70].

1.4.2. MuSC commitment

MuSC commitment, also referred to as myogenic commitment, is described as the commitment of a MuSC into a myogenic progenitor to ensure efficient and complete muscle regeneration[36; 71]. To direct MuSC fate, MuSCs can divide asymmetrically to generate committed progeny to allow for muscle regeneration[32; 63; 64]. Several factors have been implicated in regulating MuSC commitment. Myogenic commitment is known to be directed by the myogenic regulatory factors, Myf5, MyoD and MyoG and previously studied pathways such as the p38α/β MAPK pathway[36; 69; 72; 73].

1.4.3. Mechanisms regulating MuSC fate decisions

Cell division is an important determinant of MuSC fate[74]. Generally, to regulate stem cell fate, stem cells can divide symmetrically and asymmetrically[27; 62; 75]. Symmetric division generates either two new stem cells allowing expansion of the stem cell pool or two committed progenitor cells resulting in the depletion of the stem cell population while asymmetric cell division gives rise to a new stem cell and a committed progenitor cell thereby maintaining the stem cell pool (**Fig.3**)[27; 60; 62]. Additionally, Ono and colleagues demonstrated a key role of cell division frequency in MuSC fate whereby slow-dividing activated MuSCs produced self-renewed cells and fast-dividing activated cells are poised towards MuSC commitment[65].

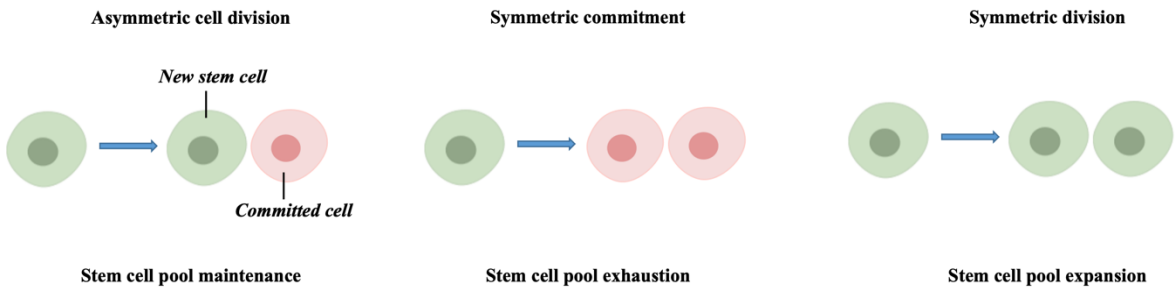

Fig.3: Asymmetric and symmetric cell division in MuSCs (adapted from Ito and Ito.[76]).

Pax7 and the MRFs namely Myf5, MRF4, MyoD and MyoG greatly participate in MuSC fate decisions. Numerous studies showed that MyoG down-regulates Pax7 expression at the transcription level to favor MuSC commitment thus showing a critical role of these transcription factors in MuSC fate determination[3; 77].

Scrib, a cell-polarity protein has been reported to govern MuSC fate based on its expression level in MuSCs possibly through ERK1/2 expression and c-Jun activation[78]. Scrib has been shown to be absent in quiescent MuSCs and is expressed in activated MuSCs to modulate their expansion[78].

miRNAs are small non-coding RNAs that control gene expression at post-transcription level. They play a crucial role at all stages in skeletal muscle myogenesis and thus in the regulation of fate decisions in MuSCs as well. miRNAs can influence the expression of MRFs, Pax factors and other transcripts such as Notch signaling, Wnt signaling, Janus kinase-Signal transducer and activator of transcription 3 (JAK-STAT3) signaling and thus participate in MuSC self-renewal or favor myogenic commitment[79]. Like many other researchers, Su *et al.* demonstrated the role of miRNAs in satellite fate determination. Here, the authors reported that hyperactivation of JAK-STAT3 signaling via the miRNA 31-Interleukin 34 (miR-31-IL34) axis in adult MuSCs favored asymmetric cell division during muscle repair thereby regulating MuSC fate[61].

Likewise, several pathways have been found to control MuSC fate decisions. As previously mentioned, the Notch signaling pathway, a key regulator of quiescence in MuSCs has been found to control MuSC fate[41]. Forkhead box K1 (FoxK1), a member of the forkhead/winged helix transcription factor family, is expressed in both quiescent and proliferating MuSCs and is thought to regulate MuSC fate[28; 80; 81]. Adenosine monophosphate-activated protein kinase alpha-1 (AMPKα1) has been reported to play a critical role in maintaining the balance between self-renewal for stem cell pool replenishment and commitment for efficient muscle repair[37; 82].

1.5. Mitochondria and stem cells

Mitochondria are essential organelles known to play a key role in the control of cell growth and death therefore showing that mitochondrial fitness is crucial for cellular homeostasis[75; 83]. Recently, stem cells have been reported to rely on mitochondria for stem cell identity, fate and to maintain their normal function[59; 75; 84; 85; 86]. Numerous studies demonstrated that improved mitochondrial function maintained stemness of many stem cell populations therefore emphasizing the importance of mitochondrial activity and metabolism in stem cell fate decisions[87;75; 84; 88; 89; 90; 91]. The link between mitochondria and stem cell function has attracted many researchers in the field of regenerative medicine and healthy aging[62; 84]. A study by Katajisto *et al*. demonstrated that during asymmetric cell division, the new stem cell received mostly young mitochondria whereas the committed cell retained aged mitochondria thus suggesting a crucial role of mitochondrial-linked signaling in stem cell function (**Fig. 4**)[62; 64]. Mitochondrial dynamics is thought to regulate stem cell identity and fate[75; 84; 88; 89; 90; 91]. The mitochondrial network is highly dynamic and therefore constantly undergoes mitochondrial fission and fusion to meet the specific cell requirements[92]. Most stem cells, including HSCs, mesenchymal stem cells (MSCs) and embryonic stem cells (ESCs) have few mitochondria with low complexity and poorly developed cristae, however, as they progress further down the lineage, their mitochondria become more complex with a more developed cristae and greater surface area for protein accommodation thereby sustaining the higher energy demand required for stem cell commitment and differentiation[87; 88; 93; 94]. Mitochondrial fusion proteins, mitofusin 1 (MFN1), mitofusin 2 (MFN2) and optic atrophy 1 (OPA1) are known to be required for differentiation of stem cells[92]. This suggests the key role of mitochondrial dynamics in regulating stem cell function[87; 88]. Several studies demonstrated that mitochondrial dynamics through the regulation of fission/fusion is important for the maintenance, commitment and differentiation of stem cells including various pluripotent stem cells and cancer stem cells (CSCs)[86; 88; 91; 95; 96].

The remodeling of mitochondria particularly cristae structure reflects the changes in mitochondrial bioenergetics[84; 85; 87]. Quiescent stem cells have a lower metabolic demand and are known to mostly rely on glycolysis while committed progenitors use oxidative phosphorylation (OXPHOS) therefore supporting the potential role of mitochondrial metabolism in stem cell fate and function[62]. A variety of stem cells including HSCs, ESCs and MSCs have been shown to have fewer and immature mitochondria at early stages due to their low energy demand and reliance on glycolysis[62]. However, some studies have shown that there are some exceptions whereby some stem cell types such as embryonic mouse neural stem cells (NSCs), MSCs, HSCs and CSCs utilize glycolysis for energy demands despite their fused and elongated mitochondrial morphology[84; 86; 92; 97; 98]. A metabolic shift from glycolysis to OXPHOS for energy production has been reported to be important for commitment and differentiation of several stem cells. Khacho *et al*. have shown that glycolytic uncommitted NSCs with elongated mitochondria undergo a metabolic shift to mitochondrial OXPHOS upon progenitor commitment as well as mitochondrial fragmentation and increase in mitochondrial oxygen consumption. The changes in mitochondrial dynamics in this study has been reported to regulate stem cell fate by modifying reactive oxygen species (ROS) signaling[84]. Many researchers speculated that decreased mitochondrial metabolism in quiescent stem cells serve as a protective role to maintain low levels of ROS and therefore actively regulate stem cell fate and function by conserving their stemness properties irrespective of their proliferative features[85; 88; 92; 99; 100; 101; 102]. Numerous studies demonstrated that improved mitochondrial function maintained stemness of many stem cell populations therefore emphasizing the importance of limited mitochondrial activity and metabolism in stem cell fate decisions[84; 87; 103; 104; 105; 106; 107]. ROS exert different roles at different stages of stem cell lineage progression. Low levels of ROS have been shown to maintain quiescence and the self-renewing capacity of stem cells while higher levels of ROS act as a signal and participate in stem cell fate determination by driving stem cell proliferation and differentiation[84; 87]. The role of mitochondria in stem cell commitment and differentiation has been greatly investigated where

the authors show increased mitochondrial activity, increased mitochondrial content and mitochondrial cytosolic distribution and efficiency in differentiating stem cells[84; 96; 98; 108; 109]. Additionally, mitochondria are primary sites of fatty acid oxidation (FAO) and mitochondrial FAO is known to be involved in the maintenance of the stem cell pool and function[110; 111; 112]. Fatty acid metabolism driven by mitochondrial bioenergetics and mitochondrial dynamics has been reported to be important for maintenance of the self-renewal trait of stem cells including NSCs and HSCs[110; 113]. Wang *et al*. reported that fatty acid synthesis via regulation of mitochondrial dynamics is pivotal for maintaining pluripotency of stem cells[110]. Alteration of FAO has been shown to result in symmetric commitment of HSCs thereby leading to a decline in the stem cell pool[111].

Mitochondria might be crucial for regulation of intracellular calcium for stem cell homeostasis since it plays a role in cell death and physiological signaling pathways[92]. Excessive calcium accumulation into the mitochondria can lead to apoptosis through the release of cytochrome c in the cytoplasm. Enhanced mitochondrial membrane potential (MMP) caused by increased intracellular calcium resulted in loss of HSCs after cell division thereby suggesting the important role of calcium-mitochondria axis in the maintenance of stem cells.[114]. The regulation of mitochondrial calcium has also been reported to be vital for the differentiation of stem cells including MSCs and NSCs.[92].

While many researchers have focused on growing evidence showing how mitochondrial structure, content and activity in stem cells dictate cell fate, the role of mitochondria in MuSCs fate is poorly understood and still needs to be explored.

1.6. Mitophagy

Emerging evidence has shown that accumulation of damaged and dysfunctional mitochondria leads to stem cell aging, premature commitment and impaired self-renewal and that timely degradation of aged and dysfunctional mitochondria is pivotal for cellular homeostasis[64; 115; 116]. It is therefore crucial to have optimally functional mitochondria for the proper functioning

and maintenance of stem cells. Mitophagy acting as an essential mitochondrial quality control mechanism by selectively degrading damaged mitochondria, could thus play a major role in the regulation of stem cell homeostasis(**Fig. 4**).[115]

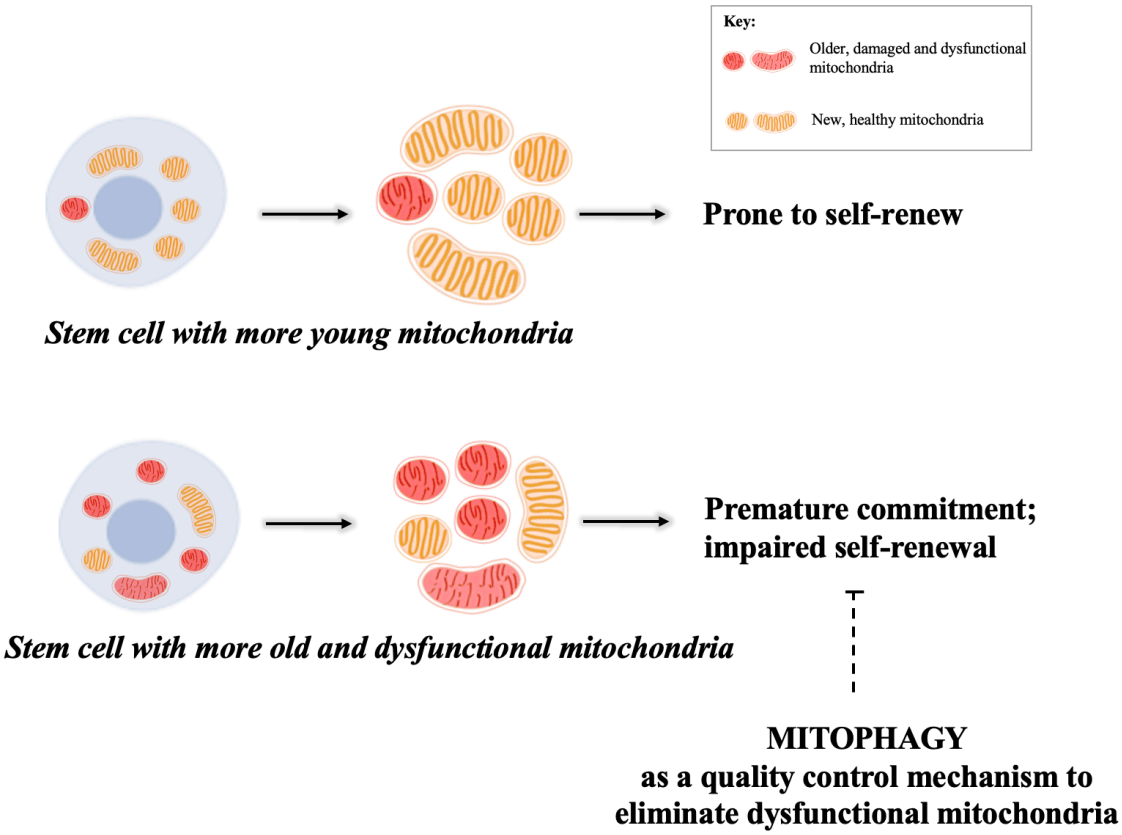

Fig.4: Fate of stem cells with two different mitochondrial properties[64].

Mitophagy is a cargo-specific form of autophagy, also known as mitochondrial autophagy which was first described by Lemasters and colleagues as a mitochondrial turnover mechanism that selectively targets and degrades damaged and dysfunctional mitochondria following reduced MMP[83; 117; 118]. Mitophagy involves the sensing, sequestration, and trafficking of defective mitochondria to the lysosome for degradation[119,120]. The two recognition signals necessary for mitochondrial clearance are ubiquitin (Ub)-adaptor- and receptor-driven mitochondrial interaction with LC3 (light chain 3) on the autophagosomes[121].

Mitochondrial priming is required for mitophagy to take place and this is mediated by mitophagy receptors which are essentially mitochondrial proteins. All known mitophagy receptors contain an LC3-interacting region (LIR) motif, which is responsible for their interaction with the LC3 protein and its homologs on the autophagosome[122]. Mitochondrial fission is also thought to be an important step in mitophagy whereby a typical mitochondrion needs to be structurally altered to fit within an autophagosome thus making mitochondrial dynamics pivotal for mechanics of mitophagy[122]. Upon mitochondrial fission, the mitochondria with reduced membrane potential is unlikely to rejoin the mitochondrial network and is more prone to mitophagy[122]. Mitophagy is normally initiated in response to cellular stresses such as depolarization, oxidative stress, starvation, hypoxia and several other damaging conditions[123; 124]. Impaired mitophagy has also been shown to occur under physiological and pathological processes such as differentiation, aging and diseases[123].

1.6.1. Pathways of mitophagy

1.6.1.1. Phosphatase and tensin homolog (PTEN)-induced putative kinase 1 (PINK1)/Parkin-mediated mitophagy

So far, the best characterized mechanism of mitophagy is initiation of the PINK1/Parkin-mediated mitophagy upon sensing of loss of MMP, a key indicator of mitochondrial health and injury[125; 126; 127]. PINK1/Parkin mediated mitophagy is also recognized as the main pathway of mitophagy activated under stress conditions[128]. PINK1 was isolated as one of the genes induced by the tumor suppressor PTEN and contains eight exons spanning 18 kb on chromosome 1p36.12. This gene encodes a protein of 581 amino acid residues with a mitochondrial targeting motif and a serine/threonine protein kinase domain[125; 126]. Parkin also known as Parkinson disease 2 (PARK2), is an E3 Ub ligase which is directly phosphorylated by PINK1 and acts as a signaling pathway to activate mitophagy in response to mitochondrial damage[129]. Under resting conditions, PINK1 is rapidly degraded after import into healthy mitochondria by the mitochondrial protease, presenilin-associated rhomboid-like protein

(PARL) in the inner mitochondrial membrane (IMM) (**Fig.5**). Conversely, loss of MMP leads to impairment of PINK1 proteolysis. Unprocessed PINK1 accumulates specifically at the outer mitochondrial membrane (OMM) of damaged mitochondria. PINK1 then promotes the recruitment of the E3-ligase, Parkin by phosphorylating it. Accumulated and activated Parkin on the OMM surface initiates the polyubiquitination of some proteins in the mitochondria membrane that act as an elimination signal. Different mitophagy adapters such as nucleoporin 62 (p62), neighbor of breast cancer gene 1 (BRCA1) gene 1 (NBR1), nuclear domain 10 protein 52 (NDP52), and optineurin recognize and bind these polyubiquitinated chains and simultaneously bind to LC3 to recruit the autophagic limiting membrane and finally engulf the targeted damaged mitochondria(**Fig.5**)[130].

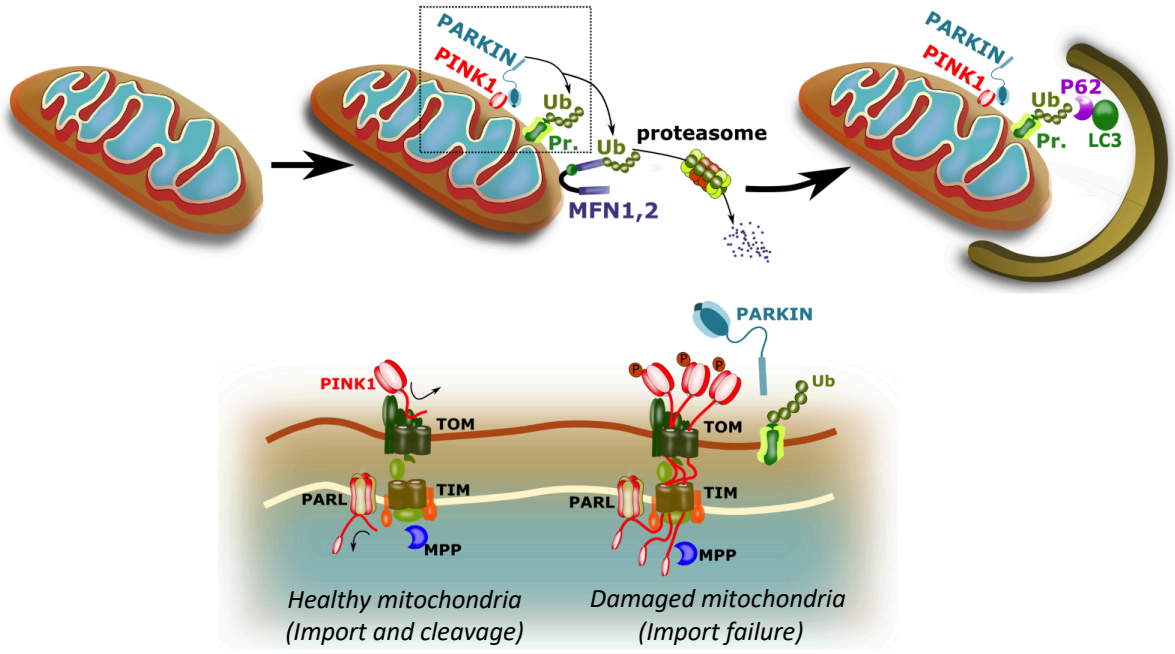

Fig.5: Schematic diagram of PINK1/Parkin mediated-mitophagy[131].

PINK1 is known to play an important role in cell respiration, protein folding, and degradation, and in various mitochondrial functions, such as fission/fusion dynamics, trafficking and calcium signaling[127]. PINK1 loss of function has been also reported to impair the mitochondrial respiratory chain and adenosine triphosphate (ATP) production[127]. The same study stated that PINK1 deficiency results in calcium overload within mitochondria, causing excessive ROS production in the mitochondria and cytosol. PINK1 has been widely linked with mitochondrial function where its deficiency in both *D. melanogaster* and mice was reported to lead to mitochondrial dysfunction and specific reduction of Complex I (CI) activity[132]. In addition, in mouse cell cultures, PINK1 deficiency was shown to affect MMP and fragmentation, and increase ROS in substantia nigra dopaminergic neurons [133]. Transient PINK1 knockdown has also been reported to cause a decrease in mitochondrial potential and to promote ROS levels [125]. Loss of PINK1 has been reported to lead to mitochondrial fragmentation, increased mitophagy in various mouse and human cell cultures and also influenced stem cells regenerative ability by causing a dramatic decrease in the speed and efficiency of induced pluripotent stem cell (iPSC) reprogramming[125; 127; 133; 134].

Even if other pathways could still maintain fidelity of mitochondria by inducing mitophagy of dysfunctional mitochondria, a reduction in PINK1-mediated mitophagy is nevertheless detrimental for cellular function and homeostasis and was reported to result in increased cell death [135].

1.6.1.2. PINK1/Parkin-independent mitophagy pathways

Although PINK1/Parkin-driven mitophagy has dominated the field in the recent years, PINK1/Parkin-independent mechanisms of mitophagy have also been of increasing interest to researchers in the context of cellular homeostasis.

1.6.1.2.1. BNIP3 and NIX-dependent mitophagy

B-cell leukemia/lymphoma 2 (BCL2) interacting protein 3 (BNIP3), encoded by the BNIP3 gene belongs to the BCL2 family of cell-death-regulating factors and is located at the OMM[136].

BNIP3 plays various key roles in cells as a signaling molecule in mitochondrial dysfunction, mitophagy and apoptosis[136]. The primary role of BNIP3 is the regulation of mitochondrial fragmentation and mitochondrial clearance through its interaction with LC3 and its related molecular receptors, therefore acting as a mitophagy receptor[121; 136].

Similar to BNIP3, NIX also known as BCL2 Interacting Protein 3 Like (BNIP3L), is an OMM protein belonging to the BH3 only domain proteins of the BCL2 family[123]. NIX is known to play a role in hypoxia-mediated mitophagy[137]. NIX has a LIR motif allowing its direct interaction with the LC3 protein or the LC3 homolog, γ-Aminobutyric acid type A (GABAA) receptor-associated protein (GABARAP)[123; 137]. This interaction mediates the recruitment of autophagosome to the damaged mitochondria[123; 137].

1.6.1.2.2. FUN-14 domain containing protein 1 (FUNDC1)-mediated mitophagy

FUNDC1 is localized to the OMM and functions as a mitophagy receptor in mitochondrial uncoupling-, and hypoxia-induced mitophagy[123]. FUNDC1 needs to be dephosphorylated by mitochondrial phosphatase PGAM family member 5 (PGAM5) therefore allowing the LIR domain of FUNDC1 to interact with LC3 and also increase mitochondrial fission[123; 137]. FUNDC1 then mediates the colocalization of LC3 to the targeted fragmented mitochondria thereby promoting mitophagy[137].

1.6.1.2.3. Other mitophagy receptors

Over the years, researchers have gained significant interest in exploring other mitophagy pathways. These include autophagy and beclin 1 regulator 1 (AMBRA1), Unc-51 like autophagy activating kinase 1 (ULK1) which is critical for PINK1/Parkin-mediated mitophagy as well as during hypoxia, adenosine monophosphate-activated protein kinase (AMPK) through AMPK/mitochondrial fission protein 1 (FIS1)-mediated mitophagy, mitochondrial E3 ubiquitin protein ligase 1 (MUL1) which is an E3-Ub ligase and Cardiolipin[122; 131; 138].

1.6.2. Mitophagy in stem cells

Recently, basal autophagic activity has been reported in quiescent MuSCs, which sustain skeletal muscle regeneration suggesting a potential role of mitochondrial autophagy in the maintenance of MuSCs in their healthy quiescent state[139]. Furthermore, failure of autophagy led to an accumulation of damaged mitochondria in MuSCs at old age, resulting in increased ROS levels and failure of MuSCs to regenerate with aging therefore suggesting a role of mitochondrial autophagy in muscle regeneration. García-Prat, L. *et al.* reported that defective autophagy in MuSCs increased mitochondrial dysfunction and oxidative stress, resulting in a decrease in the function and number of MuSCs[120; 140].

It has been previously demonstrated that traumatic muscle damage results in impaired mitochondrial content and is accompanied by an induction of mitophagy[140]. Mohiuddin *et al*. reported changes in mitophagy as assessed by mtKeima expression at different stages of muscle repair following injury thus suggesting its potential role in muscle regeneration[141].

Emerging evidence has highlighted an important role of mitophagy in stem cell homeostasis[142]. Vazquez-Martin and colleagues have demonstrated a key role of PINK1-mediated mitophagy in stem cell fate decisions whereby loss of PINK1 led to impaired mitochondrial rejuvenation and decreased the speed and efficiency of nuclear reprogramming of somatic cells into iPSCs[143]. This study therefore suggested a potential role of PINK1-mediated mitophagy in stemness acquisition in stem cells. Additionally, Ito *et al*. found that PINK1 and Parkin genes are up-regulated to promote the expansion of a purified Tie2+ HSCs population and thus maintain its pool. The authors demonstrated that silencing of PINK1 and Parkin attenuated the expansion and maintenance of this unique HSCs population by *in vitro* means as well as after transplantation where PINK1 knockout (KO) HSCs failed to survive[144]. Similarly, Pei *et al*. further supported the role of mitophagy in stem cell self-renewal by showing that up-regulation of FIS1-mediated mitophagy through AMPK activation facilitated the clearance of stressed mitochondria and thus preserved stemness in Leukemia stem cells (LSCs)[138]. In a recent study, BNIP3L/NIX-mediated mitophagy was stimulated by transforming growth factor beta 1 (TGF-

β1) and resulted in increased HSC growth and thus accelerated erythroid differentiation thus further suggesting a crucial role of mitophagy in stem cell differentiation[145].

Recent studies have emphasized on the protective role of mitophagy in stem cells. PINK1/Parkin-mediated mitophagy has been shown to protect transplanted bone marrow MSCs (BMSCs) against stress-induced apoptosis and senescence[59]. Moreover, modulation of PINK1/Parkin-mediated mitophagy protected MSCs from hyperglycemia-induced injury by rescuing mitochondrial dysfunction and decreasing apoptosis in endothelial cells of diabetic rats[146]. SIRT3 activated mitophagy attenuated mitochondrial dysfunction in amniotic fluid stem cells (AFSCs) and increased its survival against high glucose-induced apoptosis[147]. Yoon *et al*. also demonstrated that inducing mitophagy increased the survival of human MSCs exposed to oxidative stress therefore supporting its protective role in stem cells[148].

While up-regulation of mitophagy has been shown to be beneficial in stem cells, hyperactivated mitophagy has also been found to be detrimental to these cell populations, thus, a proper balance in the regulation of mitophagy is essential for the optimal stem cell function. Jin *et al*. have shown that hyperactivation of PINK1-mediated mitophagy increased HSC pool, impaired their differentiation and disturbed HSC homeostasis suggesting that a certain level of mitophagy is required for proper functioning of stem cells[149]. A recent study by Yin and colleagues supported this hypothesis by showing that regulation of mitophagy via the MAPK signaling pathway was required to increase the efficiency of transplanted BMSCs and subsequently to repair kidney injury[150].

While recent studies have shown how different pathways of mitophagy play a crucial role in the maintenance and proper functioning of various stem cells, the specific role of mitophagy as a mitochondrial quality control mechanism in MuSCs remains unclear and still needs to be investigated.

1.7. Hypothesis and Objectives

Mitochondria are important regulators of fate and function in various types of stem cells including MuSCs. Accumulation of damaged and dysfunctional mitochondria has been reported to lead to stem cell aging, premature commitment and impaired self-renewal. Thus, we hypothesized that maintaining an optimally functioning population of mitochondria is pivotal for stem cell homeostasis and that mitophagy acting as a mitochondrial quality control mechanism by selectively degrading damaged and dysfunctional mitochondria, could play an important role in MuSC fate determination during muscle regeneration.

The aim of this thesis was to examine the role of mitophagy in MuSC fate and function during muscle repair. The following three objectives were set to achieve our aim:

Objective 1:

Determine the response of mitophagy to muscle injury in MuSCs.

Objective 2:

Determine the effect of PINK1 loss of function on MuSC fate and function during muscle regeneration.

Objective 3:

Determine the effect of Parkin deficiency on MuSC fate and function in response to injury.

2. MATERIALS AND METHODS

2.1. Mouse model

2.1.1. *Mito*-QC mice

Mitophagy reporter mice (*Mito*-QC) mice were developed and obtained from Dr. Ian Ganley's Laboratory from the University of Dundee. 6-8 weeks old mice of both genders were used for MuSCs isolation. 10 weeks old mice of both genders were used for all other experimental procedures. Genotyping was confirmed at the time of weaning. DNA isolated from tail snips was amplified using primers as described in Table 1.

2.1.2. PINK1 KO mice

Germline PINK1 KO mice were obtained from Dr. David Park from the University of Ottawa to study the effect of PINK1 deficiency in MuSCs fate and function in response to cardiotoxin (CTX)-induced injury. 6-8 weeks old mice of both genders were used for MuSCs isolation. 10 weeks old mice of both genders were used for all other experimental procedures. Genotyping was confirmed at the time of weaning. DNA isolated from tail snips was amplified using primers as described in Table 1.

2.1.3. Parkin KO mice

$Parkin^{Flx/Flx}$ mice, in which exon 7 was flanked by loxP sites, were developed and obtained from Lexicon Pharmaceuticals. to study the effect of loss of Parkin in Pax7+ adult MuSCs. Our lab developed a Cre-flox conditional Parkin exon 7 KO model by crossing the $Parkin^{Flx/Flx}$ mice with Pax7 $CreER^{T2\ +/-}$ mice[151]. At 9 weeks of age, 200mg/kg of tamoxifen (Sigma T5648, 50mg/mL dissolved in corn oil) was administered to $Parkin^{WT/WT}$, Pax7 $Cre^{+/-}$ mice (wild type (WT)) and $Parkin^{Flx/Flx}$, Pax7 $Cre^{+/-}$ mice (Parkin KO) via gavage for five consecutive days to activate cre-recombinase, followed by three days of rest for efficient gene deletion. Both genders were used for all experimental procedures.

Genotyping was confirmed at the time of weaning. DNA isolated from tail snips was amplified using primers as described in Table 1. Confirmation of Parkin KO in MuSCs was performed by immunostaining on isolated cultured MuSCs and *in vitro* single fiber cultures.

2.2. CTX Preparation and Injections

CTX (Latoxan L8102) was prepared in saline (0.9% NaCl) at a final concentration of 10 μM[152]. PINK1 KO, Parkin KO and corresponding WT mice were injected with Buprenorphine subcutaneously prior to subsequent procedures and anesthetized by gas inhalation 30 minutes prior to CTX injection. Using an insulin-type disposable syringe, 50 μl of 10 μM CTX was injected 1-2 mm deep into the right tibialis anterior (TA) muscle. The contralateral uninjured muscle was used as a control. The injured mice were allowed to recover in a heated room and transferred to a clean cage until time of harvest.

All procedures were approved by the Animal care and veterinary service (ACVS) committee at the University of Ottawa and complied with the guidelines of the Canadian Council on Animal Care and the Animals for Research Act.

2.3. Muscle Tissue Harvest for Histology

At the time of harvest, mice were sacrificed by cervical dislocation. The TA muscle was immediately dissected, weighed and cut in half at the center in a cross-sectional orientation. Half of the TA was flash frozen in ice-cold isopentane using liquid nitrogen for 30 seconds and immediately stored at -80°C for sectioning and subsequent staining procedures. The other half of the TA muscle was dropped in freshly prepared cold 2% (w/v) paraformaldehyde (PFA) (Sigma P6148) and fixed for 30 minutes, shaking on ice. Following fixation, TA muscles were washed twice with phosphate buffered saline (PBS) for 5 minutes and twice with glycine for 10 minutes, then left in 5% (w/v) sucrose for 2 hours, followed by 20% sucrose (w/v) for 2-3 days to allow for cryopreservation of the tissue. TA muscle was frozen in ice-cold isopentane using liquid nitrogen for 30 seconds and immediately stored at -80°C for sectioning and subsequent staining procedures.

2.4. Single Myofiber Isolation

For *in vitro* single myofiber cultures, the extensor digitorum longus (EDL) muscles were harvested immediately following cervical dislocation and digested in 0.5% (w/v) collagenase B (Roche 11088815001) approximately 30-40 minutes at 37ºC.

0.5 hours post isolation (T0.5) for *mito*-QC mice: Each digested EDL muscle was immediately transferred to 800µL of 4% (w/v) PFA for 10 minutes on the shaker followed by three PBS washes to remove residual PFA[153]. The EDL muscle was then triturated in PBS using fetal bovine serum (FBS)-coated tips and plates to release individual muscle fibers. The isolated single myofibers were stored in PBS at 4°C until any subsequent staining procedures.

All other timepoints for all mice: The digested EDL muscle was then triturated in wash media (Dulbecco's Modified Eagle's Medium (DMEM) containing 4.5 g/L glucose and 1% (v/v) penicillin-streptomycin) to release single myofibers. Single myofibers were then washed three times in wash media to clean the myofibers from cellular debris. For T1 (timepoint 1 hour post isolation) for the PINK1- and Parkin- deficient mice, after trituration, the single myofibers were fixed in 2% (w/v) PFA for 10 minutes followed by three PBS washes to remove residual PFA. For timepoints 24, 48, 72 hours post isolation (T24, T48 and T72 respectively), after trituration, myofibers were allowed to recover in wash media for 45 minutes before being transferred to single myofiber culture media (DMEM 4.5 g/L glucose, 20% (v/v) FBS, 2% (v/v) chicken embryo extract, 1% (v/v) penicillin-streptomycin, 9.3ng/mL basic fibroblast growth factor (bFGF)). Cultured fibers were then incubated at 37ºC, 5% CO_2 for 24, 48 and 72 hours. After desired culture time, single myofibers were fixed in 2% (w/v) PFA for 10 minutes followed by three PBS washes to wash off any residual PFA and stored in PBS at 4°C until any subsequent staining procedures[134; 154].

2.5. MuSC Isolation

2.5.1. Standard Isolation of MuSCs, 3 hours post isolation (T3 MuSCs)

MuSCs were isolated by fluorescence activated cell sorting (FACS) using a published protocol[155]. Following cervical dislocation, hindlimb muscles were harvested and digested in 1% (w/v) Collagenase-B (Roche 11088831001) and 0.4% (w/v) Dispase II (Roche 04942078001) using the Milteny MACS Octo-dissociator SLICE_FACS program for 27 minutes. Following digestion, muscle slurry was filtered and centrifuged to obtain a cell pellet, which was then incubated with red blood cell lysis (Sigma R7757) for 30 seconds to remove any red blood cells, followed by a wash with 10 mL of PBS and subsequent spin at 600g for 10 minutes. The cell pellet was then resuspended in 1 mL of FACS buffer (3mM ethylenediaminetetraacetic acid (EDTA), 10% (v/v) FBS in 1xPBS) with conjugated antibodies (phycoerythrin (PE)-conjugated antibodies: stem cell antigen-1 (Sca-1) (BD Pharmingen, 553108), cluster of differentiation 45 (CD45) (BD Pharmingen, 553081), cluster of differentiation 31 (CD31) (BD Pharmingen, 553373) and cluster of differentiation 11b (CD11b) (eBiosciences, 12-0112-82) to remove non-MuSCs present in the population, and α-integrin-7 (Ablab, 67-0010-05) and VCAM-1 (Biolegend, 105720) to mark MuSCs). α-integrin-7 and VCAM-1 positive cells were finally sorted by FACS at the Flow Cytometry facility at the Ottawa Hospital Research Institute.

2.5.2. *In situ* fixed MuSCs (T0 MuSCs)

T0 MuSCs were isolated by FACS using a modified version of a published protocol[156]. Following cervical dislocation, hindlimb muscles were harvested and dropped in 0.5 % (w/v) PFA. The muscle was rapidly cut to 1-5 mm pieces. The PFA was then replaced with fresh 0.5 % (w/v) PFA and the muscle was chopped to a slurry followed by 1 hour gentle rotation at 4ºC. After fixation, the tube was centrifuged at 4°C for 5min/600g and the supernatant was discarded.

The fixed chopped muscles were washed twice in PBS with centrifugation at 4°C for 5min/600g to remove any residual PFA. The muscles were then digested in 2% (w/v) Collagenase-B (Roche 11088831001) and 0.8% (w/v) Dispase II (Roche 04942078001) using the Milteny MACS Octo-dissociator SLICE_FACS program for 27 minutes. Following digestion, muscle slurry was filtered using a 100 µm cell strainer and centrifuged at 4°C for 10min/600g. The cell pellet was resuspended in ice-cold DMEM and filtered using a 70 µm cell strainer followed by centrifugation at 4°C for 5min/50g. The supernatant containing MuSCs was then passed through a 50 µm cell strainer and centrifuged at 4°C for 5min/600g. The cell pellet was then resuspended in 1 mL of FACS buffer (3mM EDTA, 10% (v/v) FBS in 1xPBS) with conjugated antibodies (PE-conjugated antibodies: Sca-1 (BD Pharmingen, 553108), CD45 (BD Pharmingen, 553081), CD31 (BD Pharmingen, 553373) and CD11b (eBiosciences, 12-0112-82) to remove non-MuSCs present in the population, and α-integrin-7 (Ablab, 67-0010-05) and VCAM-1 (Biolegend, 105720) to mark MuSCs). α-integrin-7 and VCAM-1 positive cells were finally sorted by FACS at the Flow Cytometry facility at the Ottawa Hospital Research Institute.

2.6. Histology

2.6.1. Tissue Sectioning

Tissue was sectioned in a cross-sectional orientation at a thickness of 14 µm using the HM525NX Cryostat (University of Ottawa Histology Core) at -28ºC and placed on a charged slide (Fisher Scientific 12-550-15). Slides were stored at -80ºC until further processing.

2.6.2. Hematoxylin & Eosin Staining

Previously flash frozen muscle sections were immediately fixed in PFA for 30 minutes followed by three washes with PBS. The fixed tissue sections were stained for hematoxylin and eosin (H&E) by the Histology Core at the University of Ottawa. The stained tissues were imaged on the EVOS FLAuto2 microscope at the University of Ottawa.

2.6.3. Cytochrome c oxidase (COX)/Complex IV (CIV) Staining

Previously flash frozen muscle sections were allowed to dry at room temperature for about 1 hour. Tissue sections were stained with 50µL COX buffer (1X 3,3'-diaminobenzidine (DAB) and 100 µM cytochrome c in 0.1 mM sodium phosphate buffer (SPB) pH=7.0, 2 µg bovine catalase) for 45 minutes at 37ºC. After incubation, slides were washed thrice with SPB followed by dehydration in ethanol. Slides were then cleared with xylene for 10 minutes and mounted using dibutylphthalate polystyrene xylene (DPX)[157]. Stained tissue sections were imaged on the EVOS FLAuto2 microscope at the University of Ottawa.

2.6.4. CI Staining

Flash frozen muscle sections were allowed to dry at room temperature for about 1 hour. Tissue sections were stained with 50µL CI buffer (0.625mg/mL 1,4-Dihydronicotinamide adenine dinucleotide (NADH) in 1.875nM nitro blue tetrazolium (NBT)) for 45 minutes at 37ºC. After incubation, slides were washed thrice with SPB followed by dehydration in ethanol. Slides were then cleared with xylene for 10 minutes and mounted using DPX[158]. Stained tissue sections were imaged on the EVOS FLAuto2 microscope at the University of Ottawa.

2.6.5. Immunofluorescence Staining

2.6.5.1. Tissue sections

Tissue sections were sent for antigen retrieval (citrate buffer at pH=6.0) to the University of Ottawa Histology Core, followed by 1 hour blocking in 3% (w/v) bovine serum albumin (BSA) and primary antibody incubation overnight at 4ºC (Table 2). Secondary antibody staining was performed using a Biotin-Strepdavidin interaction (Biotin: Jackson Immunoresearch, 115-065-205, Strepdavidin: Jackson Immunoresearch, 016-160-084) and/or fluorescence-conjugated secondary antibody incubation (Refer to Table 2 for antibody information). Slides were mounted using Invitrogen™ ProLong™ Gold Antifade Mountant with 4′,6-diamidino-2-phenylindole (DAPI) (ThermoFisher Scientific P36935). Stained tissue sections were imaged on the EVOS FLAuto2 microscope at the University of Ottawa.

2.6.5.2. Single Myofibers

Single myofibers were permeabilized (0.1% (v/v) triton, 0.1M glycine in PBS) for 10 minutes at room temperature and blocked in 5% (v/v) horse serum, 2% (w/v) BSA and 0.1% (v/v) triton in PBS for 5 hours at room temperature. Following blocking, permeabilized individual myofibers were incubated with primary antibody overnight at 4^{o}C (Antibody concentration listed in Table 2). Secondary antibody was then added for 1 hour at room temperature, and then fibers were mounted using Invitrogen™ ProLong™ Gold Antifade Mountant with DAPI (ThermoFisher Scientific P36935) or Immumount (ThermoFisher 9990402) on a charged glass slide (Fisher Scientific, 12-550-15). *Mito*-QC myofibers were imaged on the LSM880 Airyscan Confocal Microscope, and all other stained fibers were imaged on the EVOS FLAuto2 microscope at the University of Ottawa.

2.6.5.3. FACS sorted isolated MuSCs

2.6.5.3.1. *Mito*-QC T0 MuSCs

Following FACS sorting, T0 *mito*-QC MuSCs were cytospined onto charged slides (Fisher Scientific, 12-550-15) and mounted using Invitrogen™ ProLong™ Gold Antifade Mountant with DAPI (ThermoFisher Scientific P36935). T0 *mito*-QC MuSCs were imaged on the LSM880 Airyscan Confocal Microscope at the Cell Biology Image Acquisition Core at the University of Ottawa.

2.6.5.3.2. *Mito*-QC T3 MuSCs

Following FACS sorting, isolated MuSCs were cytospined onto charged slides (Fisher Scientific, 12-550-15) and fixed with 4% (w/v) PFA for 15 minutes at room temperature.
Any residual PFA was washed off with three PBS washes 5 minutes each. The slides were then mounted using Invitrogen™ ProLong™ Gold Antifade Mountant with DAPI (ThermoFisher Scientific P36935). T3 *mito*-QC MuSCs were imaged on the LSM880 Airyscan Confocal Microscope at the Cell Biology Image Acquisition Core at the University of Ottawa.

2.6.5.3.3. PINK1 KO, Parkin KO, WT MuSCs

Following FACS sorting, isolated MuSCs were cytospined onto charged slides (Fisher Scientific, 12-550-15) and fixed with 4% (w/v) PFA for 15 minutes at room temperature. Any residual PFA was washed off with three PBS washes 5 minutes each. Fixed MuSCs were permeabilized (0.3% (v/v) triton in PBS) for 7 minutes at room temperature and blocked in 2% (w/v) BSA for 20 minutes at room temperature. Following blocking, permeabilized cells were incubated with primary antibody overnight at 4ºC (Antibody concentration listed in Table 2). Secondary antibody was then added for 1 hour at room temperature, and then slides were mounted using Invitrogen™ ProLong™ Gold Antifade Mountant with DAPI (ThermoFisher Scientific P36935) on a charged glass slide (Fisher Scientific, 12-550-15). Stained MuSCs were imaged on the EVOS FLAuto2 microscopeat the University of Ottawa.

2.7. Statistical analysis

Statistical analyses were realized using GraphPad Prism 8. Quantitative results were presented as means ± standard error of the mean (SEM). Statistical differences were assessed using an unpaired t-test for two groups and one-way analysis of variance (ANOVA) for multiple comparisons. Statistical significance is displayed as ns: not significant, *$p < 0.05$, **$p < 0.01$, ***$p < 0.001$, ****$p < 0.0001$. Minimum number of replicates per experiment varied across study (Please see individual figure legends).

Table 1. Primers for genotyping and quantitative polymerase chain reaction (qPCR).

Primer Name	Sequence (5'-3')		Method
	Forward	Reverse	
PINK1 KO	AGAGGATGCTAGTCCCTGTG AAGGG	ACCAAAGAAGGGAGCTTG	Genotyping
WT PINK1	AGAGGATGCTAGTCCCTGTG AAGGG	ACACTCAGTCCTTGGGCAA TGCTA	Genotyping
Parkin KO	AATGGATGAGTTCAAGGTTG CACAG	AACTCCAGAGCTAGGATAG GGCATA	Genotyping
WT Parkin	TTACGTCCATCGTGGACAGC	TGGGCTGGGTGTTAGCCTT	Genotyping
Cre	GAACCTGATGGACATGTTCA GG	AGTGCGTTCGAACGCTAGA GCCTGT	Genotyping
***Mito*-QC**	CAAAGACCCCAACGAGAAGC CCCAAGGCACACAAAAAACC CTCTTCCCTCGTGATCTGCAACTCC CATGTCTTTAATCTACCTCGATGG		Genotyping
Parkin	Forward primer GAGCTTCCGAATCACCTGAC Reverse primer CCATCTGGGAGCTAGGAATG		qPCR

Table 2. Antibodies used for FACS and Immunofluorescence (IF).

Antibody Name	Company/Cat no.	Dilution	Assay
PE rat anti-mouse CD31	BD Pharmingen 553373	2 µL/mouse	FACS
PE rat anti-mouse CD45	BD Pharmingen 553081	2 µL/mouse	FACS
PE rat anti-mouse CD11b	eBiosciences 12-0112-82	2 µL/mouse	FACS
PE rat anti-mouse Sca1	BD Pharmingen 553108	2 µL/mouse	FACS
PE-Cy7 conjugated CD106 (VCAM-1)	Biolegend 105720	10 µL/mouse	FACS
647 conjugated alpha integrin-7 (rat)	Ablab 67-0010-05	10 µL/mouse	FACS
Pax7 (mouse)	DHSB PAX7-S	1:8	IF Primary
Pax7 (rabbit)	Invitrogen PA1-117	1:100	IF Primary
MyoD (mouse)	SantaCruz sc-32758	1:50	IF Primary
MyoG (mouse)	DHSB F5D	1:6	IF Primary
Ki67 (rabbit)	Abcam ab15580	1:500	IF Primary
eMyHC (mouse)	DHSB F1.652-s	1:5	IF Primary
Parkin (mouse)	ab77924	1:200	IF Primary
Alexa-Fluor 488 (rabbit)	Invitrogen A11008	1:1000	IF Secondary
Brilliant Violet 421 (mouse)	Jackson 115-675-146	1:200	IF Secondary
Alexa-Fluor 647 (mouse)	Abcam AB-150107	1:200	IF Secondary
Alexa-Fluor 594 (mouse)	Invitrogen A11005	1:200	IF Secondary
Cy3 (mouse)	Jackson 715-165-150	1:1000	IF Secondary
Biotin	Jackson 115-065-205	1:200	IF Secondary
Cy3-Conjugated Streptavidin	Jackson 016-160-084	1:500	IF Secondary

3. RESULTS

3.1. Mitophagy is active in quiescent MuSCs

To determine the response of mitophagy to muscle injury in MuSCs, our lab processed three transcriptomics datasets obtained from publicly available GEO (Gene Expression Omnibus) datasets (GSE70376[139], GSE47177[159], GSE55490[51]) which were acquired by expression profiling by array. Here we compared quiescent MuSCs to activated MuSCs after CTX or Barium chloride ($BaCl_2$)-induced injury to assess any gene expression changes upon muscle injury. In **Fig. 6A**, we revealed that the two Ub-dependent mitophagy genes, PINK1 and Parkin/PARK2 are expressed in quiescent MuSCs and are transiently decreased as MuSCs activate in response to injury suggesting that PINK1/Parkin-dependent mitophagy could be required for the maintenance of quiescence in MuSCs. Interestingly, we show that receptor-dependent mitophagy genes such as BNIP3, BNIP3L and FUNDC1 are up-regulated as PINK1 and Parkin/PARK2 are repressed indicating that alternative pathways of mitophagy may be involved in MuSCs activation or lineage progression in the absence of PINK1/Parkin-mediated mitophagy.

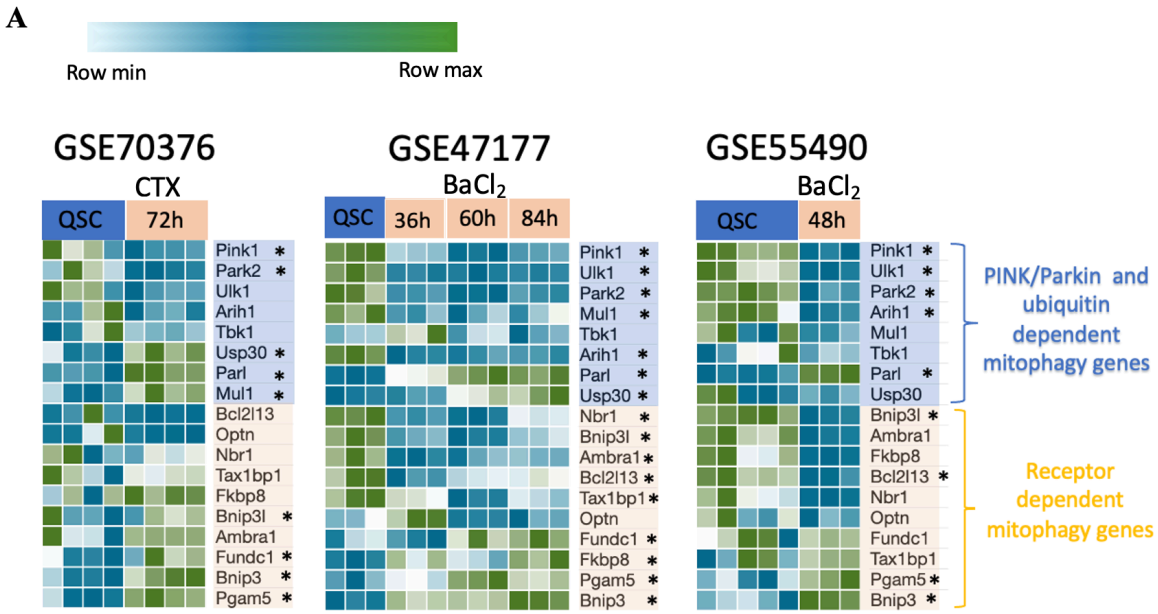
A
Row min
Row max
GSE70376
CTX
QSC
72h
GSE47177
BaCl2
QSC
36h
60h
84h
GSE55490
BaCl2
QSC
48h
Pink1 *
Park2 *
Ulk1
Arih1
Tbk1
Usp30 *
Parl *
Mul1 *
Bcl2l13
Optn
Nbr1
Tax1bp1
Fkbp8
Bnip3l *
Ambra1
Fundc1 *
Bnip3 *
Pgam5 *
Ulk1 *
Park2 *
Mul1 *
Arih1 *
Parl *
Nbr1 *
Bnip3l *
Ambra1 *
Bcl2l13 *
Tax1bp1 *
Fundc1 *
Fkbp8 *
Pgam5 *
PINK/Parkin and ubiquitin dependent mitophagy genes
Receptor dependent mitophagy genes

Fig. 6: PINK1 and Parkin/PARK2 are expressed in quiescent MuSCs

A, Heat maps of mitophagy genes obtained from expression profiling by array generated from GEO datasets GSE70376[139] (MuSCs in homeostatic conditions (QSC) or after CTX injury (72 hours)), GSE47177[159] (quiescent MuSCs (QSC) isolated from hindlimb muscles of uninjured mice and activated MuSCs isolated from hindlimb muscles of $BaCl_2$-injured mice (36, 60 and 84 hours after injury) of 2-3 months of age, GSE55490[51] (uninjured quiescent MuSCs (QSC) and activated MuSCs from contralateral $BaCl_2$-injured muscle).

3.2. Changes in mitophagy are detectable from MuSC quiescence to differentiation

Single myofibers isolated from the EDL muscle allow for the visualization and quantification of MuSCs in their physiological niche and can be used to analyse MuSC fate occurring during skeletal muscle regeneration as per described by B*run et al.*[134].

For this experiment, we used a previously developed mitophagy reporter mouse, *mito*-QC which is a transgenic mouse with a pH-sensitive fluorescent mitochondrial signal allowing the assessment of mitophagy through a binary-based fluorescence assay. This assay is based on the expression of mCherry-green fluorescent protein (GFP) tag fused to the mitochondrial targeting sequence of the OMM protein, FIS1[119]. Under steady-state conditions, the mitochondrial network expresses both mCherry and GFP markers. However, upon mitophagy, damaged mitochondria are engulfed by phagophores to form mitophagosomes which are then delivered to lysosomes where the fluorescence of mCherry remains stable but the GFP fluorescence becomes quenched by the acidic microenvironment. This eventually results in structures with a punctate mCherry-only fluorescence termed mitolysosomes (**Fig. 7**)[119].

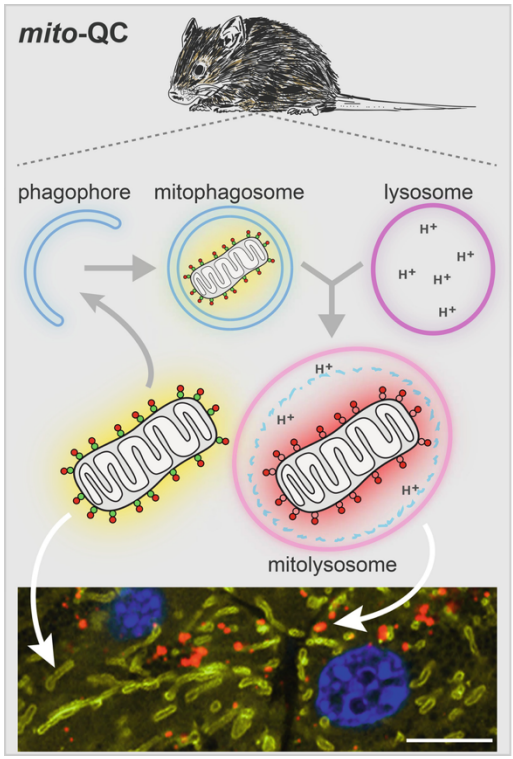

Fig.7: Principle of the *mito*-QC mouse model[160].

As a positive control for the assessment of mitophagy using the *mito*-QC mice, we first mimicked mitochondrial damage by experimentally depolarizing mitochondria to induce mitophagy in MuSCs from single myofiber cultures at T72 with 20µM uncoupler carbonyl cyanide m-chlorophenylhydrazone (CCCP) for 1 hour at 37ºC. We then assessed mitophagy by mitolysosomes quantification. CCCP significantly induced mitophagy as assessed by an increase in the number of mitolysosomes thus validating the *mito*-QC mouse model as an effective tool to assess mitophagy (**Fig. 8A-B**).

To assess changes in mitophagy after injury in MuSCs, we isolated *in vitro* single myofiber cultures from the *mito*-QC mice at different timepoints (0.5 hour post isolation (T0.5), T1, T24, T48, T72) as the MuSCs exit quiescence (T0.5, T1) to activate (T24), proliferate, commit and differentiate or self-renew (T48-T72). MuSCs were identified by immunolabeling with the MuSC specific transcription factor, Pax7. Changes in mitophagy rates were readily detectable from MuSC quiescence to MuSC differentiation/self-renewal as observed by a statistically significant difference among the different timepoints ($F(4,10) = 8.833$, $p = 0.0026$) (**Fig. 8D**). We reported that mitophagy is active in quiescent MuSCs (T0.5, T1) and is transiently down-regulated during MuSC activation (T24) followed by a gradual increase during early differentiation (T72) and self-renewal (T72) (**Fig. 8C-D**). As previously described by Brun *et al*. and Rocheteau *et al*., at T72, two populations of MuSCs can be identified based on their expression of Pax7[32; 134]. Rocheteau and colleagues described Pax7^{high} MuSCs as self-renewing MuSCs and Pax7^{low} MuSCs as differentiating MuSCs[32] (**Fig. 8E**). We therefore quantified the number of mitolysosomes in these two different populations at T72 and found that self-renewing MuSCs have a significantly higher degree of mitophagy than differentiating MuSCs (**Fig. 8F).** These findings suggest that mitophagy plays a considerable role in the maintenance of a quiescence state in MuSCs and potentially for their differentiation and self-renewal.

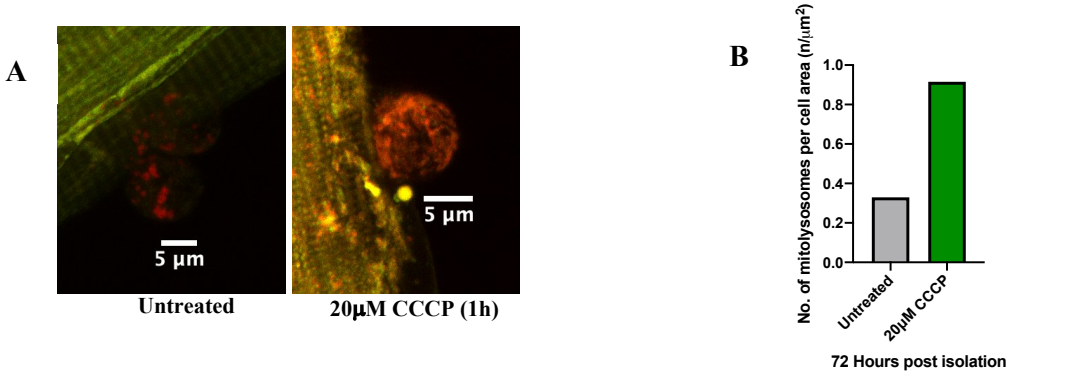
A
5 µm
5 µm
Untreated
20µM CCCP (1h)
B
No. of mitolysosomes per cell area (n/µm²)
1.0
0.8
0.6
0.4
0.2
0.0
Untreated
20µM CCCP
72 Hours post isolation

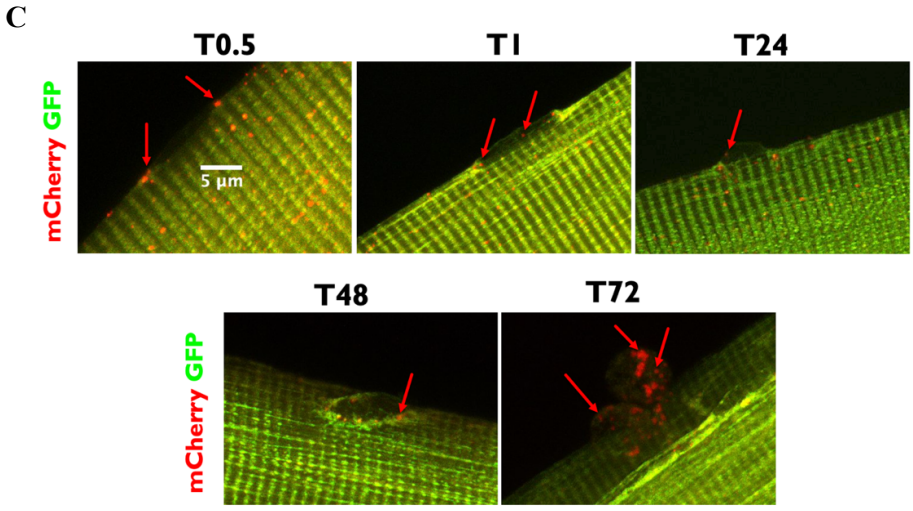
C
T0.5
T1
T24
mCherry GFP
5 µm
T48
T72
mCherry GFP

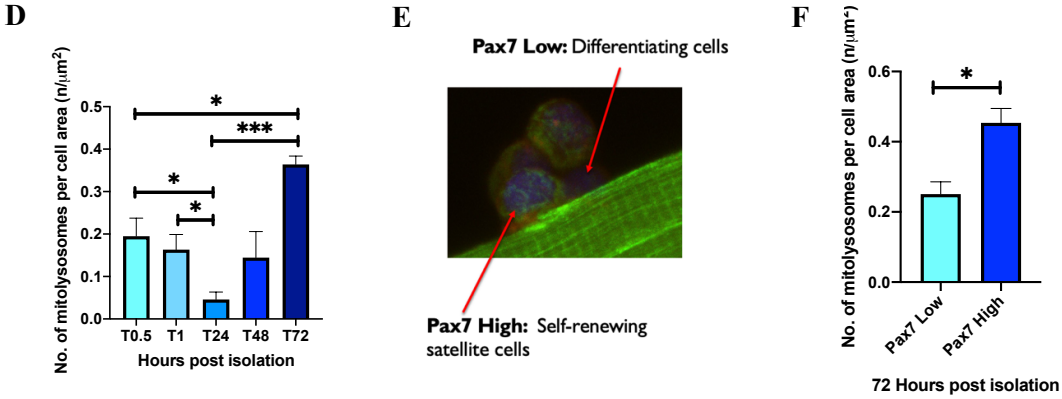
D
No. of mitolysosomes per cell area (n/µm²)
0.5
0.4
0.3
0.2
0.1
0.0
*
***
*
*
T0.5
T1
T24
T48
T72
Hours post isolation
E
Pax7 Low: Differentiating cells
Pax7 High: Self-renewing satellite cells
F
No. of mitolysosomes per cell area (n/µm²)
0.6
0.4
0.2
0.0
*
Pax7 Low
Pax7 High
72 Hours post isolation

Fig. 8: Mitophagy is active in quiescent, differentiating and self-renewing MuSCs

A, Representative confocal images of MuSCs on *mito*-QC EDL muscle fibers at T72 with and without 20μM CCCP. Magnification: 63X. **B**, Quantification of number of mitolysosomes per MuSC area (n/μm^2) at T72 with and without 20μM CCCP assessed by the *mito*-QC counter on ImageJ (n=1 independent experiment). **C**, Representative confocal images of MuSCs on *mito*-QC EDL muscle fibers at different isolation timepoints (T0.5, T1, T24, T48 and T72). Magnification: 63X. **D**, Quantification of number of mitolysosomes per MuSC area (n/μm^2) at different isolation timepoints assessed by the *mito*-QC counter on ImageJ (n=3 independent experiments). Statistically significant difference among timepoints as determined by one-way ANOVA ($F(4,10) = 8.833$, $p = 0.0026$). **E**, Representative confocal image of Pax7^{high} and Pax7^{low} labelled MuSCs on *mito*-QC EDL muscle fiber at T72. Magnification: 63X. **F**, Quantification of number of mitolysosomes per MuSC area in Pax7^{high} and Pax7^{low} labelled MuSCs (n/μm^2) assessed by the *mito*-QC counter on ImageJ (n=3 independent experiments). Statistics in D were realized using one-way ANOVA followed by an unpaired t test. Statistics in F were realized using an unpaired t test and statistical significance is displayed as *p < 0.05, **p < 0.01, ***p < 0.001, ****p < 0.0001. Data are presented as mean ± SEM (at least 10 cells analyzed per each timepoint).

3.3. Quiescent MuSCs exhibit a higher degree of mitophagic degradation than activated MuSCs

Next, we wanted to verify the level of mitophagy in quiescent MuSCs. We thus isolated *mito*-QC MuSCs by FACS. To analyze true quiescent MuSCs, we fixed the muscle immediately after dissection (T0 MuSCs) and compared it to 3 hours post isolated-MuSCs (T3 MuSCs). Gating of MuSCs was performed based on a double positive cell population of VCAM-1-PE-Cy7 and Integrin α7-Alexa Fluor 647, two commonly used MuSC surface markers (**Fig. 9A-B**). We first assessed changes in the length and area of the nuclei of T0 MuSCs and T3 MuSCs and found that as previously described by Machado *et al*., truly quiescent MuSCs have a slightly more elongated nuclei than activated MuSCs (**Fig. 9C-E**) and that they maintained their spindle-like shape while activated MuSCs started to adopt a round-shaped morphology[156] (**Fig. 9F**). Furthermore, consistent with our *in vitro* single myofiber cultures data from the *mito*-QC mice (**Fig. 8)**, we observed active mitophagy in T0 MuSCs followed by a relative decrease as the MuSCs activate, 3 hours post isolation through quantification of mitolysosomes therefore indicating that mitophagy may be necessary to maintain quiescence in MuSCs (**Fig. 9F-G**).

A

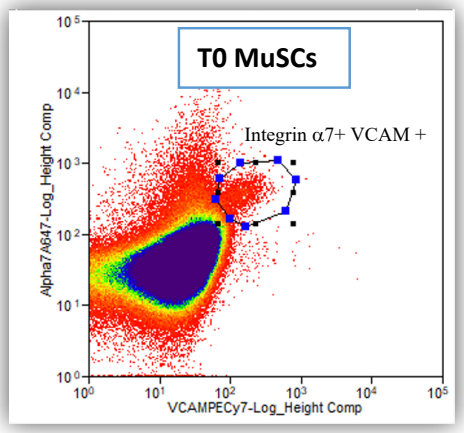
T0 MuSCs
Integrin α7+ VCAM +
Alpha7A647-Log_Height Comp
VCAMPECy7-Log_Height Comp

B

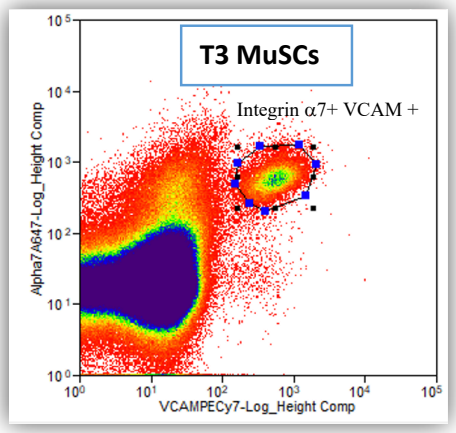
T3 MuSCs
Integrin α7+ VCAM +
Alpha7A647-Log_Height Comp
VCAMPECy7-Log_Height Comp

C

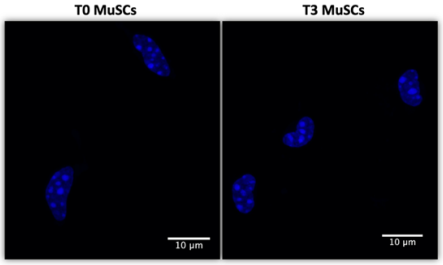
T0 MuSCs
T3 MuSCs
10 µm
10 µm

D

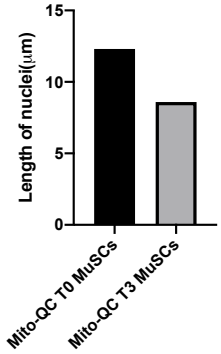
Length of nuclei(µm)
Mito-QC T0 MuSCs
Mito-QC T3 MuSCs

E

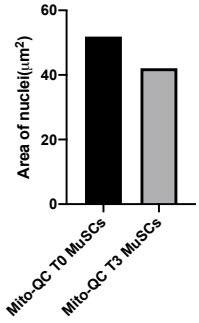
Area of nuclei(µm²)
Mito-QC T0 MuSCs
Mito-QC T3 MuSCs

F

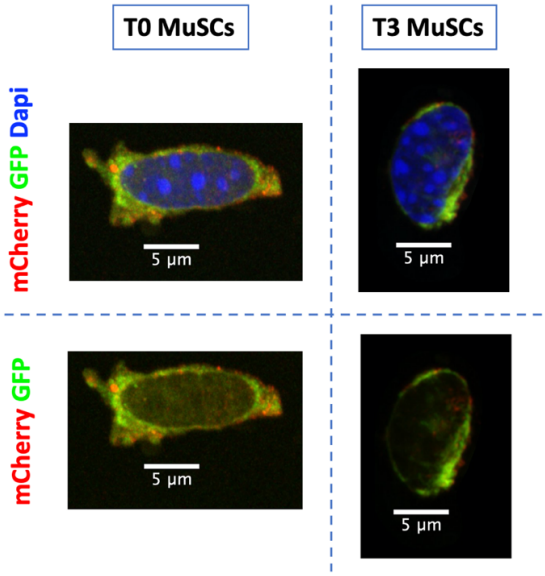
T0 MuSCs
T3 MuSCs
mCherry GFP Dapi
mCherry GFP
5 µm
5 µm
5 µm
5 µm

G

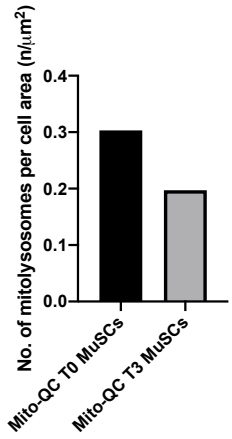
No. of mitolysosomes per cell area (n/µm²)
Mito-QC T0 MuSCs
Mito-QC T3 MuSCs

Fig. 9: Mitophagy is required for maintenance of quiescence in MuSCs

A-B, Scatter plots representing the gating strategy used to identify MuSCs represented by a double positive cell population of VCAM-1-PE-Cy7 and Integrin α7-Alexa Fluor 647. **C**, Representative confocal images of nuclei of FACS-sorted, *in situ*-fixed (T0 MuSCs) and 3 hours post isolation-fixed (T3 MuSCs) *mito*-QC MuSCs. Magnification: 63X. **D**, Quantification of length of nuclei of T0 and T3 MuSCs (μm) (n=1 independent experiment). **E**, Quantification of area of nuclei of T0 and T3 MuSCs (μm^2) (n=1 independent experiment). **F**, Representative confocal images of T0 and T3 isolated *mito*-QC MuSCs. Magnification: 63X. **G**, Quantification of number of mitolysosomes per MuSC area ($n/\mu m^2$) of T0 and T3 MuSCs assessed by the *mito*-QC counter on ImageJ (n=1 independent experiment).

3.4. Loss of PINK1 impairs muscle regeneration upon chronic injury

To study the importance of mitophagy in muscle regeneration, we used a CTX injury model of the TA muscle in mice harboring a KO of PINK1 gene, an important regulator of mitophagy. CTX is a purified snake venom toxin which causes myonecrosis thereby triggering muscle regeneration and it has been widely used to examine cellular and molecular players in muscle regeneration[27; 161]. CTX acts as a protein kinase C-specific inhibitor which causes membrane depolarization of myofibers and muscle contraction resulting in changes in ion fluxes, loss of protein content, degradation of organelles and eventually extensive necrosis of muscle fibers[24; 27; 162]. Several studies have reported that the toxicity of CTX is specific to muscle fibers and thus does not affect the basal lamina and the activity of MuSCs therefore making it an ideal injury model to study satellite cells during muscle regeneration[13; 27].

First of all, we observed no difference in the mean myofiber size of the uninjured muscles between WT and PINK1 KO mice, however, a significant decrease in the number of bigger myofibers (8000-9000 μm^2) was seen in the fiber distribution suggesting that PINK1 deficiency at the germline level had little to no effect on muscle fiber morphology at baseline (**Fig. 10B-E**). Surprisingly, our data revealed a significant increase in the number of myofibers at 4 days post injury (DPI) in PINK1-deficient mice compared to WT mice indicating that impaired PINK1-mediated mitophagy could be possibly leading to increased regenerative capacity (**Fig. 10M**). Nevertheless, we observed no changes in mean muscle fiber size at 4DPI and no changes in myofiber number or mean muscle fiber size at later timepoints, 7DPI and 14DPI indicating that PINK1 loss of function could be influencing the fate decisions of the MuSCs and not muscle differentiation (**Fig. 10B, D, M**). To have a more detailed assessment of the size of myofibers, we analysed the distribution of the muscle fiber size. Here we observed no difference in the size distribution of myofibers at 4DPI between WT and PINK1 KO mice (**Fig. 10F**), but we revealed a trend towards a decrease in the number of smaller myofibers and relative increase in the number of bigger myofibers at 7DPI in the PINK1 KO mice vs WT possibly showing increased differentiation (**Fig. 10G**). Although no difference was observed

in the myofiber size distribution at 14DPI (**Fig. 10H**), our theory of increased differentiation and regenerative capacity in the PINK KO mice correlates with our data at 14DPI where we observed a slight decrease in the number of central nuclei per fiber in PINK1 KO muscle fibers. This data suggests that the PINK1-deficient MuSCs moved to the periphery of the muscle fiber faster than WT MuSCs thus displaying increased differentiation and regenerative capacity (**Fig. 10B, L**). Moreover, loss of PINK1 in response to acute CTX injury after 21 days resulted in a trend towards an increase in TA muscle weight (compared to contralateral uninjured muscle) (**Fig. 10A**) and significantly greater mean cross-sectional area (CSA) of muscle fibers (**Fig. 10C, D**) compared to the WT mice indicating that PINK1 KO injured muscles regenerated with greater efficiency therefore in line with the trends observed at 4DPI, 7DPI and 14DPI. Additionally, further quantification of fiber distribution at 21DPI showed significant decrease in the number of small myofibers and increase in the number of larger myofibers (**Fig. 10I**). Here, we thought that impaired PINK1-mediated mitophagy may have favored MuSC differentiation at the expense of self-renewal thus resulting in muscle hypertrophy and fewer MuSCs for future muscle regeneration. To test this possibility, we used a repetitive injury model (three cycles of CTX-injury) each separated by 21 days and found that the regenerative advantage in response to acute injury was gradually lost in the PINK1 KO mice. Indeed, after a significant increase in CSA of PINK1 KO muscle fibers after a 1st injury at 21DPI, the size of the muscle fibers gradually decreased after a 2nd injury to finally result in a significant decrease in the CSA of the myofibers after a 3rd injury thereby indicating a significant impairment in muscle regeneration following repeated injuries (**Fig. 10A, C, D, I, J, K, M**).

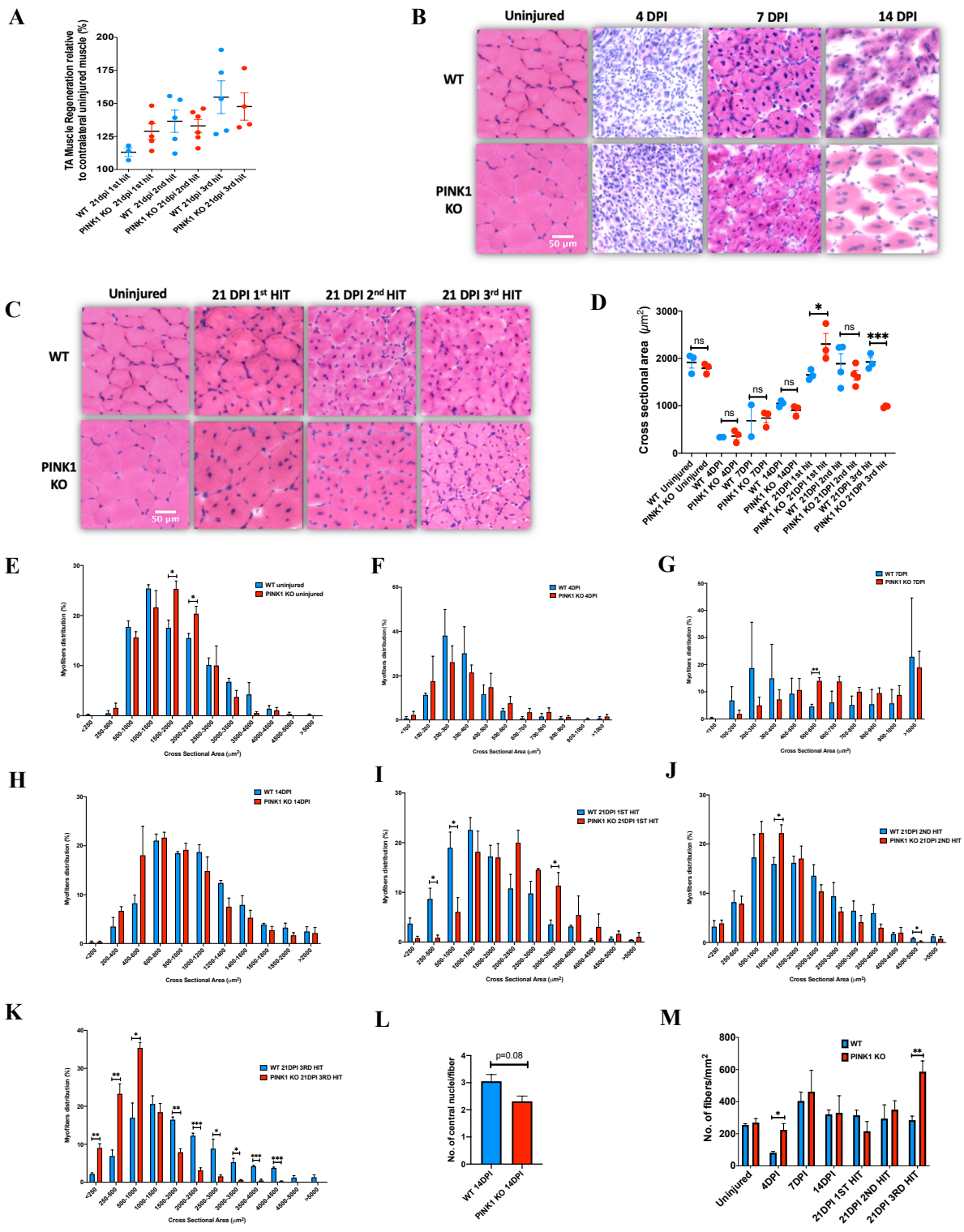
A
TA Muscle Regeneration relative to contralateral uninjured muscle (%)
WT 21dpi 1st hit
PINK1 KO 21dpi 1st hit
WT 21dpi 2nd hit
PINK1 KO 21dpi 2nd hit
WT 21dpi 3rd hit
PINK1 KO 21dpi 3rd hit
B
Uninjured
4 DPI
7 DPI
14 DPI
WT
PINK1 KO
50 µm
C
Uninjured
21 DPI 1st HIT
21 DPI 2nd HIT
21 DPI 3rd HIT
WT
PINK1 KO
50 µm
D
Cross sectional area (µm²)
E
WT uninjured
PINK1 KO uninjured
Myofibers distribution (%)
Cross Sectional Area (µm²)
F
WT 4DPI
PINK1 KO 4DPI
G
WT 7DPI
PINK1 KO 7DPI
H
WT 14DPI
PINK1 KO 14DPI
I
WT 21DPI 1ST HIT
PINK1 KO 21DPI 1ST HIT
J
WT 21DPI 2ND HIT
PINK1 KO 21DPI 2ND HIT
K
WT 21DPI 3RD HIT
PINK1 KO 21DPI 3RD HIT
L
p=0.08
No. of central nuclei/fiber
WT 14DPI
PINK1 KO 14DPI
M
WT
PINK1 KO
No. of fibers/mm²
Uninjured
4DPI
7DPI
14DPI
21DPI 1ST HIT
21DPI 2ND HIT
21DPI 3RD HIT

Fig. 10: Loss of PINK1 *in vivo* impairs muscle regeneration following repetitive injuries

A, TA Muscle regeneration relative to contralateral uninjured muscle (%) at 21DPI 1^{st} ,2^{nd},3^{rd} hit of WT vs PINK1 KO injured mice (n≥3 mice). **B-C**, Representative H&E images of TA muscle sections of uninjured, 4DPI, 7DPI, 14DPI, 21DPI 1^{st} ,2^{nd},3^{rd} hit WT vs PINK1 KO mice. Magnification: 20X. **D**, Quantification of mean CSA of muscle fibers (μm^2) of uninjured, 4DPI, 7DPI, 14DPI, 21DPI 1^{st} ,2^{nd},3^{rd} hit WT vs PINK1 KO mice (4DPI, 7DPI: n≥2 mice; 14DPI, 21DPI 1^{st} ,2^{nd},3^{rd} hit: n≥3 mice). **E-K**, Fiber size distribution of muscle fibers of uninjured, 4DPI, 7DPI, 14DPI, 21DPI 1^{st} ,2^{nd},3^{rd} hit WT vs PINK1 KO mice (4DPI, 7DPI: n≥2 mice; 14DPI, 21DPI 1^{st} ,2^{nd},3^{rd} hit: n≥3 mice). **L**, Quantification of central nuclei per myofiber at 14DPI WT vs PINK1 KO mice. **M**, Quantification of number of fibers/mm^2 of 4DPI, 7DPI, 14DPI, 21DPI 1^{st} ,2^{nd},3^{rd} hit WT vs PINK1 KO mice (4DPI, 7DPI: n≥2 mice; 14DPI, 21DPI 1^{st} ,2^{nd},3^{rd} hit: n≥3 mice). Statistics were realized using an unpaired t test. Statistical significance is displayed as ns: not significant, *$p < 0.05$, **$p < 0.01$, ***$p < 0.001$, ****$p < 0.0001$. Data are presented as mean ± SEM.

3.5. PINK1 deficiency *in vivo* promotes commitment and impairs self-renewal of MuSCs

To test our theory that impaired PINK1-mediated mitophagy may have caused an imbalance in MuSC stem cell fate by favoring MuSC commitment and impairing self-renewal, we performed immunostaining with muscle-specific transcription factors, Pax7 as a marker for undifferentiated MuSCs with proliferative potential, Ki67 as a proliferation marker, MyoD as a commitment marker, MyoG as a marker of MuSCs committed to differentiation and eMyHC as a marker for early differentiation of MuSCs. Here, we observed no significant difference in the muscle specific markers (Pax7, MyoD, MyoD, eMyHC) at baseline in uninjured TA muscles of WT and PINK1 KO mice (**Fig. 11A**). Compared to WT mice, a slight increase in the number of Pax7+ve cells was observed at 4DPI in the PINK1 KO mice, this correlated with a significant increase in MuSC proliferation as assessed by Pax7+ve, Ki67+ve MuSCs (**Fig. 11B, C, H, I**). At a later timepoint, 7DPI, we observed a trend towards a decline in the number of Pax7+ve cells and a robust increase in proliferating MuSCs (Pax7+ve, Ki67+ve) (**Fig. 11B, D, H, J**). At 14DPI, the number of Pax7+ve cells were similar in both mice (**Fig. 11B, E)**. Assessment of the myogenic progenitor markers, MyoD and MyoG revealed a significant increase in MyoD at 14DPI and high number of MyoG+ve cells at 4DPI which then leveled out at later timepoints (7DPI and 14DPI) (**Fig. 11K-P)**. Our data also showed a trend whereby a higher proportion of myofibers turned off the early differentiation marker, eMyHC at 7DPI in the PINK1 KO mice compared to the WT mice (**Fig. 11Q-R)**. These results suggest that PINK1 deficiency promotes MuSC proliferation, myogenic commitment and differentiation compared to the WT mice in response to acute injury which is in line with our H&E data. At 21DPI, after full regeneration of the muscles, we observed a significant decrease in the number of self-renewing MuSCs as assessed by Pax7+ve cells (**Fig. 11F-G)**. The MuSC pool was further depleted as observed with a significant decrease in the number of Pax7+ve cells after two and three cycles of injury (21DPI 2nd hit and 21DPI 3rd hit) (**Fig. 11F-G)**.

Together, these findings show that PINK1-deficient MuSCs *in vivo* exhibit increased proliferation, commitment and differentiation in response to acute injury but ultimately leads to depletion of the MuSC pool as observed with a decrease in the number of self-renewing MuSCs following repetitive injuries.

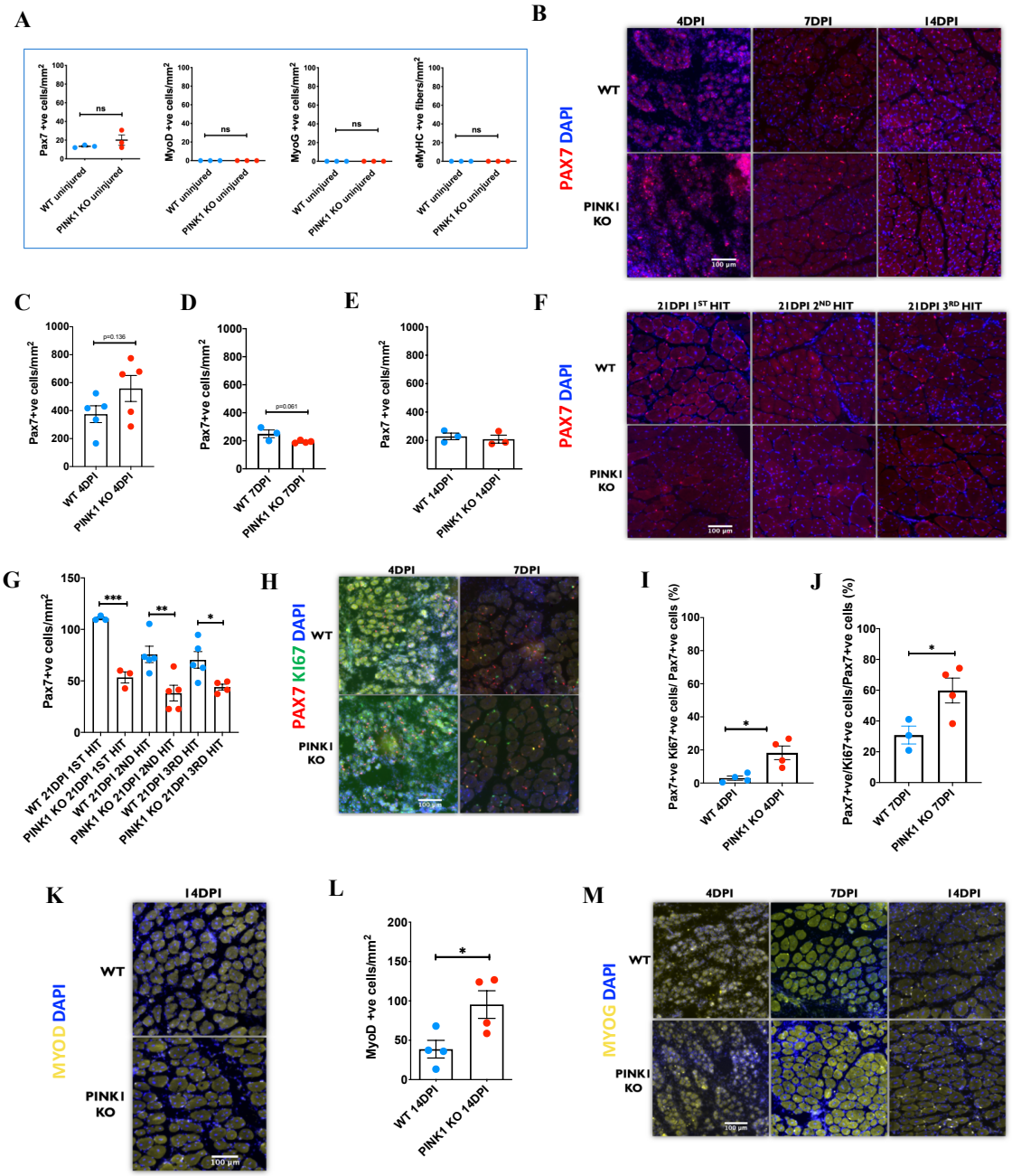
A
Pax7 +ve cells/mm2
MyoD +ve cells/mm2
MyoG +ve cells/mm2
eMyHC +ve fibers/mm2
ns
WT uninjured
PINK1 KO uninjured
B
4DPI
7DPI
14DPI
PAX7 DAPI
WT
PINK1 KO
C
Pax7+ve cells/mm2
p=0.136
WT 4DPI
PINK1 KO 4DPI
D
p=0.061
WT 7DPI
PINK1 KO 7DPI
E
WT 14DPI
PINK1 KO 14DPI
F
21DPI 1ST HIT
21DPI 2ND HIT
21DPI 3RD HIT
G
***
**
*
WT 21DPI 1ST HIT
PINK1 KO 21DPI 1ST HIT
WT 21DPI 2ND HIT
PINK1 KO 21DPI 2ND HIT
WT 21DPI 3RD HIT
PINK1 KO 21DPI 3RD HIT
H
PAX7 KI67 DAPI
I
Pax7+ve Ki67+ve cells/ Pax7+ve cells (%)
J
Pax7+ve/KI67+ve cells/Pax7+ve cells (%)
K
MYOD DAPI
L
MyoD +ve cells/mm2
M
MYOG DAPI
100 µm

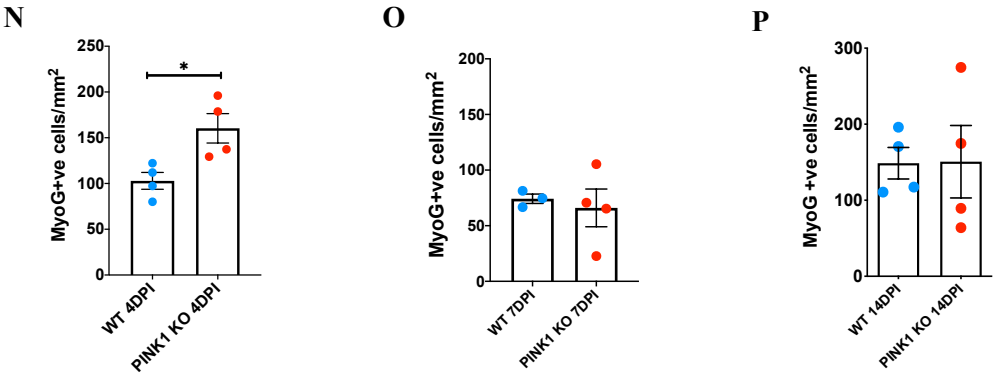
N
MyoG+ve cells/mm2
250
200
150
100
50
0
*
WT 4DPI
PINK1 KO 4DPI
O
MyoG+ve cells/mm2
200
150
100
50
0
WT 7DPI
PINK1 KO 7DPI
P
MyoG +ve cells/mm2
300
200
100
0
WT 14DPI
PINK1 KO 14DPI

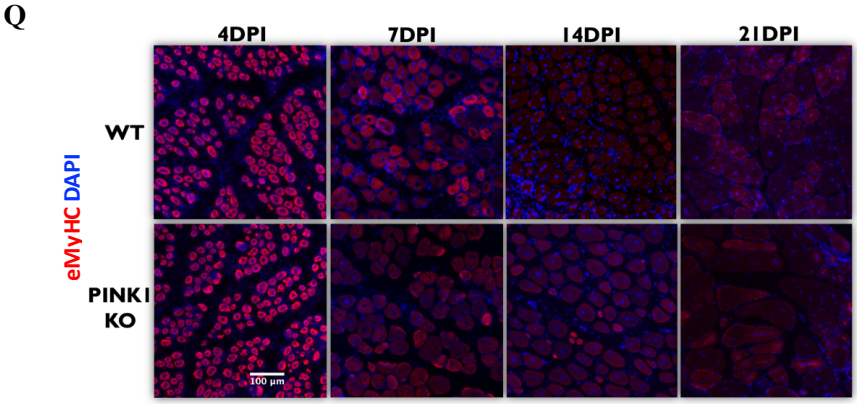
Q
4DPI
7DPI
14DPI
21DPI
WT
PINK1 KO
eMyHC DAPI
100 µm

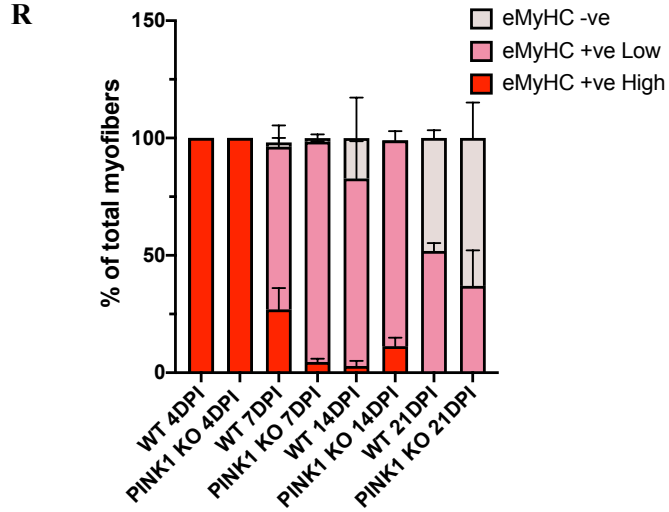
R
% of total myofibers
150
100
50
0
eMyHC -ve
eMyHC +ve Low
eMyHC +ve High
WT 4DPI
PINK1 KO 4DPI
WT 7DPI
PINK1 KO 7DPI
WT 14DPI
PINK1 KO 14DPI
WT 21DPI
PINK1 KO 21DPI

Fig. 11: Loss of PINK1 *in vivo* promotes commitment and impairs self-renewal of MuSCs

A, Immunostaining analysis of uninjured TA muscle of WT vs PINK1 KO mice stained with MuSC markers Pax7, MyoD, MyoG, eMyHC (n=3 mice) **B,** Representative immunostaining images of TA muscle sections stained with Pax7 and DAPI at 4DPI, 7DPI, 14DPI. Magnification: 20X. **C-E,** Immunostaining analysis stained with Pax7 and DAPI at 4DPI, 7DPI, 14DPI (n≥3 mice). **F,** Representative immunostaining images of TA muscle sections stained with Pax7 and DAPI at 21DPI 1st hit, 21DPI 2nd hit and 21DPI 3rd hit. Magnification: 20X. **G,** Immunostaining analysis stained with Pax7 and DAPI at 21DPI 1st hit, 21DPI 2nd hit and 21DPI 3rd hit (n≥3 mice). **H,** Representative immunostaining images of TA muscle sections stained with Pax7, Ki67 and DAPI at 4DPI and 7DPI. Magnification: 20X. **I-J,** Immunostaining analysis stained with Pax7, Ki67 and DAPI at 4DPI and 7DPI (n≥3 mice). **K,** Representative immunostaining images of TA muscle sections stained with MyoD and DAPI at 14DPI. Magnification: 20X. **L,** Immunostaining analysis stained with MyoD and DAPI at 14DPI (n=4 mice). **M,** Representative immunostaining images of TA muscle sections stained with MyoG and DAPI at 4DPI, 7DPI and 14DPI. Magnification: 20X. **N-P,** Immunostaining analysis with MyoG and DAPI at 4DPI, 7DPI and 14DPI (n≥3 mice). **Q,** Representative immunostaining images of TA muscle sections stained with eMyHC and DAPI at 4DPI, 7DPI, 14DPI and 21DPI 1st hit. Magnification: 20X. **R,** Immunostaining analysis stained with eMyHC and DAPI at 4DPI, 7DPI, 14DPI and 21DPI 1st hit (n≥3 mice). Statistics were realized using an unpaired t test. Statistical significance is displayed as ns: not significant, *$p < 0.05$, **$p < 0.01$, ***$p < 0.001$, ****$p < 0.0001$. Data are presented as mean ± SEM.

3.6. Loss of PINK1 *in vitro* promotes commitment and impairs self-renewal of MuSCs

To confirm whether PINK1 deficiency affects MuSC fate, *in vitro* single myofiber cultures from PINK1-deficient mice were isolated at different timepoints (1, 24, 48 and 72 hour(s) post isolation). We found no significant difference in the number of cells per cluster at T72 showing that the proliferation rate in *in vitro* cultures is similar in both mice (**Fig. 12A-B**). At T1, both WT and PINK1 KO MuSCs expressed only Pax7 (**Fig. 12A, C, D**). Consistent with our *in vivo* data, we observed that at T24, WT MuSCs still express Pax7 only while PINK1 KO MuSCs display increased activation (Pax7+ve, MyoD+ve) and enhanced commitment (MyoD+ve only) (**Fig. 12A, E**). At T48, PINK1-deficient MuSCs showed a trend towards an increase in commitment (MyoD+ve only) and reduced self-renewal capacity as observed by a low count of Pax7+ve only cells compared to WT MuSCs (**Fig. 12A, G**). At T72, PINK1-deficient MuSCs revealed increased commitment and impaired self-renewal as observed with an increase in MyoD+ve only cells and decrease in Pax7+ve only cells (**Fig. 12A, I**). No difference in MyoG+ve cells was seen at all timepoints between both mice (**Fig. 12A, D, F, H, J**). Furthermore, the data analysis from our Pax7/MyoG staining at T48 and T72 revealed a population of PINK1 KO MuSCs which were neither expressing Pax7 nor MyoG indicating that these cells could be MyoD+ve only cells as per our Pax7/MyoD staining results (**Fig. 12A, G-J**) further confirming an increase in myogenic commitment in the PINK1 KO mice.

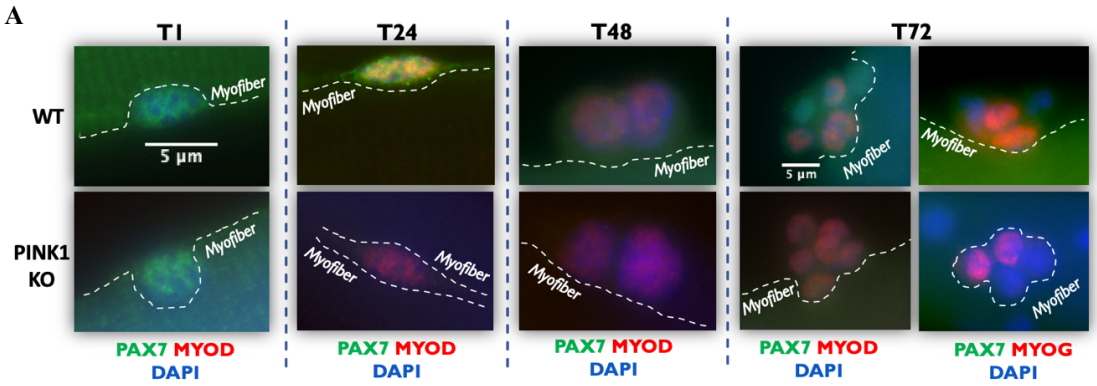
A
T1
T24
T48
T72
WT
PINK1 KO
Myofiber
5 µm
PAX7 MYOD DAPI
PAX7 MYOG DAPI

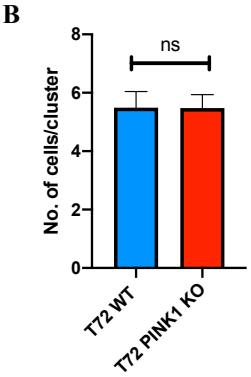
B
ns
No. of cells/cluster
0
2
4
6
8
T72 WT
T72 PINK1 KO

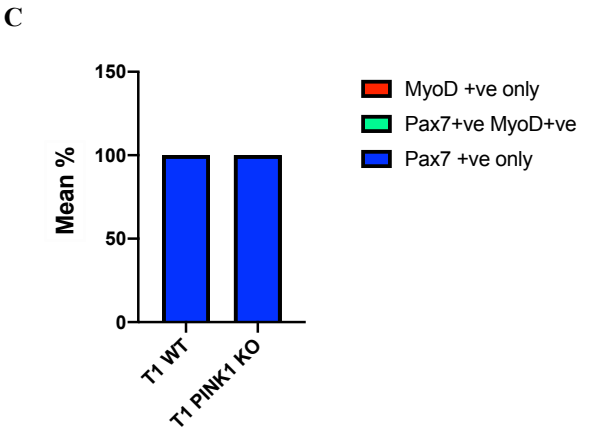
C
Mean %
0
50
100
150
T1 WT
T1 PINK1 KO
MyoD +ve only
Pax7+ve MyoD+ve
Pax7 +ve only

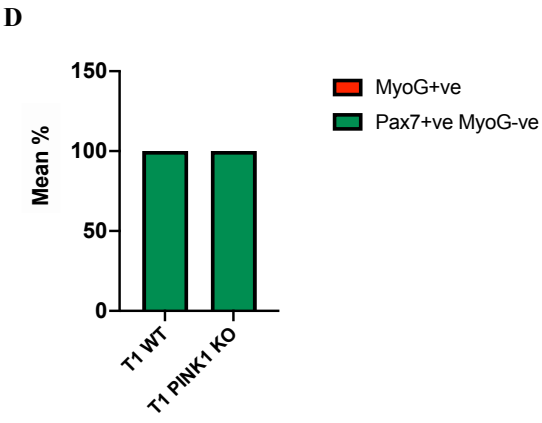
D
Mean %
0
50
100
150
T1 WT
T1 PINK1 KO
MyoG+ve
Pax7+ve MyoG-ve

E

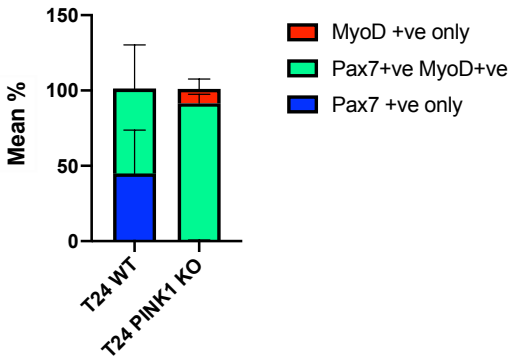
150
100
50
0
Mean %
T24 WT
T24 PINK1 KO
MyoD +ve only
Pax7+ve MyoD+ve
Pax7 +ve only

F

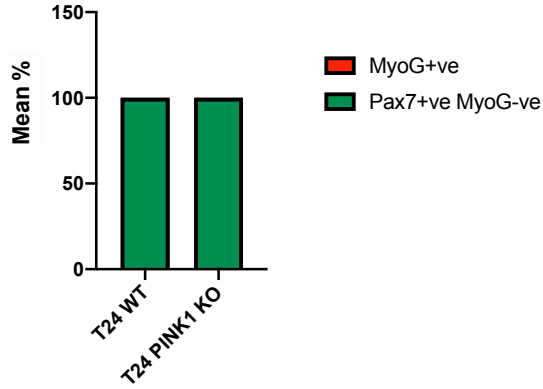
150
100
50
0
Mean %
T24 WT
T24 PINK1 KO
MyoG+ve
Pax7+ve MyoG-ve

G

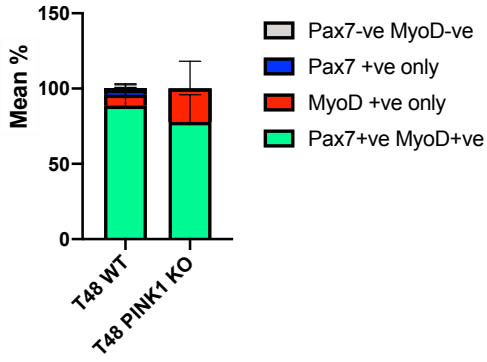
150
100
50
0
Mean %
T48 WT
T48 PINK1 KO
Pax7-ve MyoD-ve
Pax7 +ve only
MyoD +ve only
Pax7+ve MyoD+ve

H

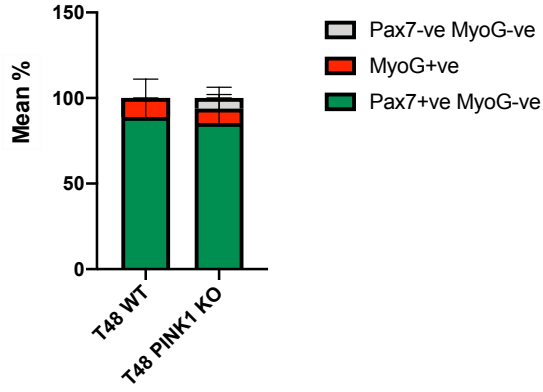
150
100
50
0
Mean %
T48 WT
T48 PINK1 KO
Pax7-ve MyoG-ve
MyoG+ve
Pax7+ve MyoG-ve

I

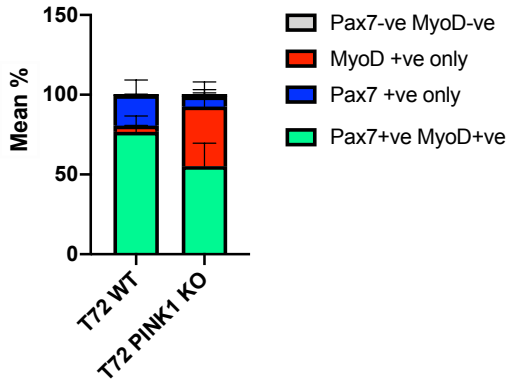
150
100
50
0
Mean %
T72 WT
T72 PINK1 KO
Pax7-ve MyoD-ve
MyoD +ve only
Pax7 +ve only
Pax7+ve MyoD+ve

J

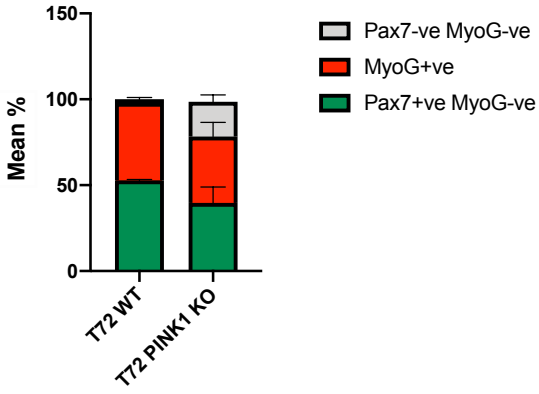
150
100
50
0
Mean %
T72 WT
T72 PINK1 KO
Pax7-ve MyoG-ve
MyoG+ve
Pax7+ve MyoG-ve

Fig. 12: PINK1 deficiency *in vitro* promotes commitment and impairs self-renewal of MuSCs

A, Representative epifluorescence images of WT vs PINK1 KO MuSCs on EDL single fibers at different isolation timepoints. (T1, T24, T48, T72) stained with Pax7/MyoD/DAPI and Pax7/MyoG/DAPI. Magnification: 20X. **B**, Number of cells per cluster in WT vs PINK1 KO EDL single fibers at T72. **C-J**, Quantification of muscle specific transcription factors, Pax7/MyoD and Pax7/MyoG in WT vs PINK1 KO EDL single fibers at T1, T24, T48, T72. Statistics in B was realized using an unpaired t test (n=3 independent experiments). Statistical significance is displayed as ns: not significant, *$p < 0.05$, **$p < 0.01$, ***$p < 0.001$, ****$p < 0.0001$. Data are presented as mean ± SEM.

3.7. Loss of PINK1 promotes MuSCs activation

We next wanted to see whether alterations in MuSC fate can be observed in freshly isolated PINK1-deficient MuSCs. We thus isolated MuSCs by FACS from WT and PINK1 KO mice. Gating of MuSCs was performed based on a double positive cell population of VCAM-1-PE-Cy7 and Integrin α7-Alexa Fluor 647, two commonly used MuSC surface markers (**Fig. 13A)**. In line with our *in vivo* and *in vitro* data, WT MuSCs still express Pax7 only while PINK1 KO MuSCs displayed increased activation, as assessed by the presence of Pax7+ve, MyoD+ve MuSCs suggesting that PINK1 MuSCs rapidly enter the cell cycle (**Fig. 13B-C).**

A

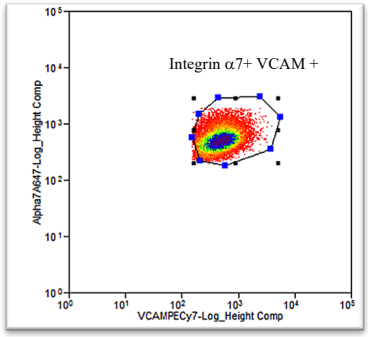
Integrin α7+ VCAM +
Alpha7/647-Log_Height Comp
VCAMPECy7-Log_Height Comp

B

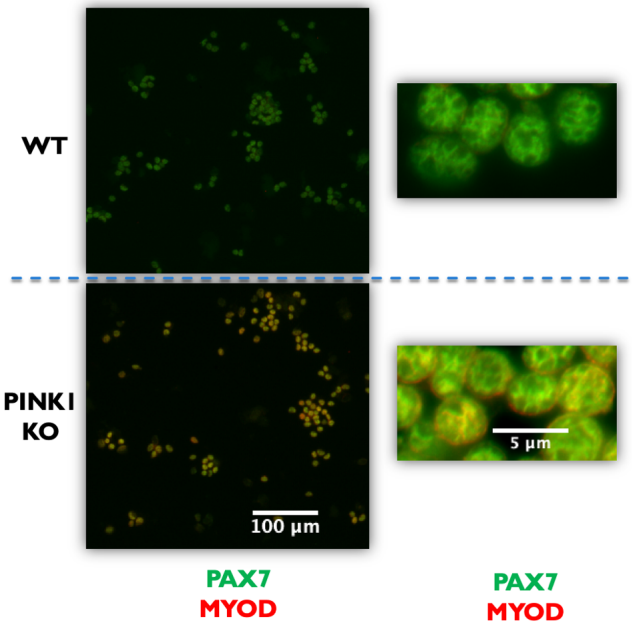
WT
PINK1 KO
100 µm
5 µm
PAX7
MYOD
PAX7
MYOD

C

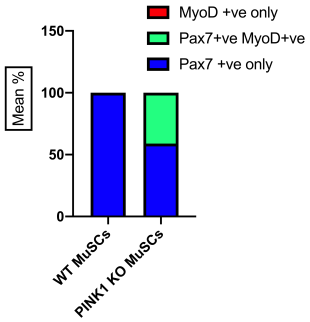
MyoD +ve only
Pax7+ve MyoD+ve
Pax7 +ve only
Mean %
150
100
50
0
WT MuSCs
PINK1 KO MuSCs

Fig. 13: PINK1-deficient MuSCs rapidly enter the cell cycle

A, Representative scatter plot demonstrating the gating strategy used to identify MuSCs. Gating of MuSCs is represented by a double positive cell population of Integrin α7-Alexa Fluor 647 and VCAM-1-PE-Cy7. **B**, Representative epifluorescence images of freshly isolated WT and PINK1 KO MuSCs stained with muscle specific marker, Pax7 and MyoD. Magnification: 100X. **C**, Quantification of Pax7 and MyoD expression in freshly isolated MuSCs from WT and PINK1 KO mice (n=1 independent experiment).

3.8. PINK1 KO mice exhibit CI and CIV deficiency in uninjured TA muscle fibers

To examine whether impairment in PINK1-mediated mitophagy results in muscle fibers with mitochondrial defects, we assessed mitochondrial dysfunction in flash frozen TA muscle sections at 21DPI by CI and COX/CIV histochemistry. Here, we revealed CI (**Fig. 14A-B**) and CIV (**Fig. 14C-D**) deficiency in uninjured TA muscle fibers of PINK1 KO mice indicating that basally PINK1-deficient muscle fibers may have dysfunctional mitochondria. However, no difference in both mitochondrial complexes was seen in injured TA muscle fibers of both mice at 21DPI (**Fig. 14A-D**).

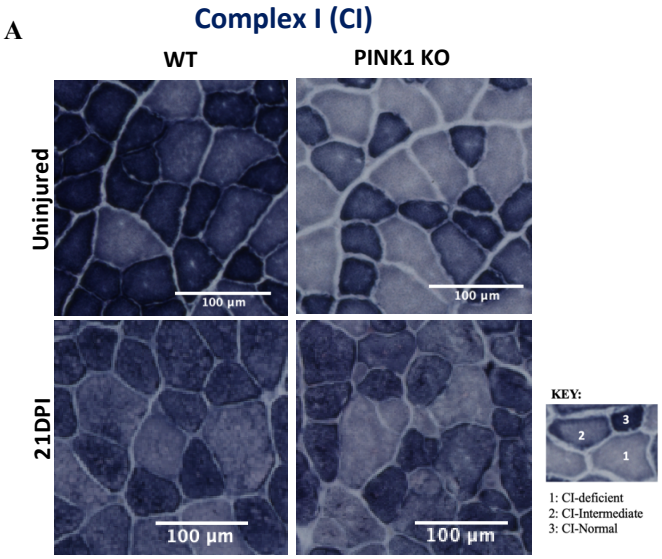
A
Complex I (CI)
WT
PINK1 KO
Uninjured
21DPI
100 µm
KEY:
1: CI-deficient
2: CI-Intermediate
3: CI-Normal

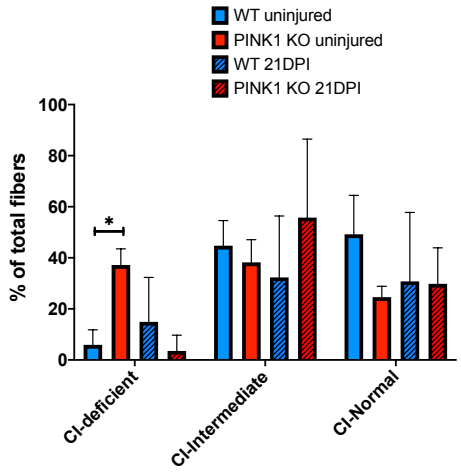
B
WT uninjured
PINK1 KO uninjured
WT 21DPI
PINK1 KO 21DPI
% of total fibers
CI-deficient
CI-Intermediate
CI-Normal

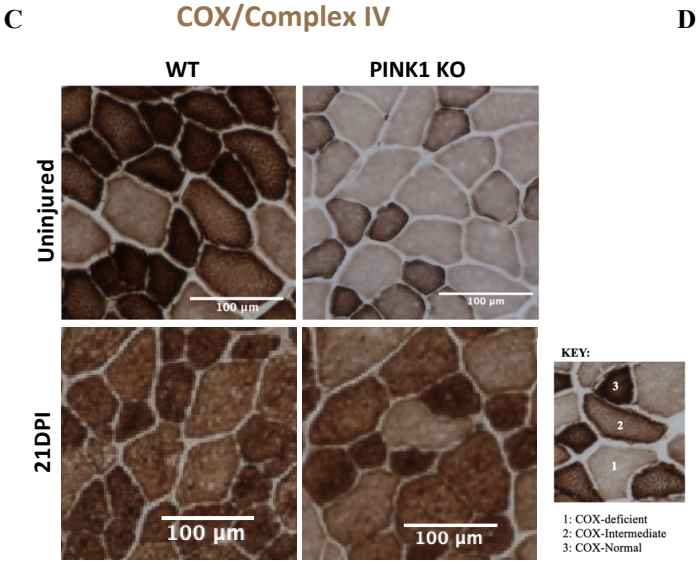
C
COX/Complex IV
WT
PINK1 KO
Uninjured
21DPI
100 µm
KEY:
1: COX-deficient
2: COX-Intermediate
3: COX-Normal

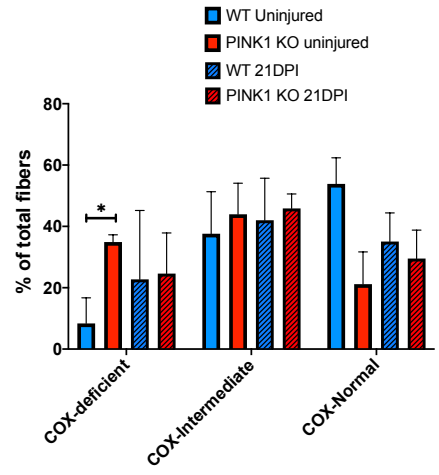
D
WT Uninjured
PINK1 KO uninjured
WT 21DPI
PINK1 KO 21DPI
% of total fibers
COX-deficient
COX-Intermediate
COX-Normal

Fig. 14: PINK1 KO mice exhibit CI and CIV deficiency in uninjured TA muscle fibers

A, Representative epifluorescence images of WT and PINK1 KO flash frozen uninjured vs 21DPI TA muscle fibers stained for CI. Magnification: 20X. **B**, Quantification of CI staining in WT vs PINK1 KO EDL flash frozen uninjured vs 21DPI TA muscle fibers (n=3 mice). **C**, Representative epifluorescence images of WT and PINK1 KO flash frozen uninjured vs 21DPI TA muscle fibers stained for CIV. Magnification: 20X. **D**, Quantification of CIV staining in WT vs PINK1 KO EDL flash frozen uninjured vs 21DPI TA muscle fibers (n=3 mice). Statistics were realized using an unpaired t test. Statistical significance is displayed as *$p < 0.05$, **$p < 0.01$, ***$p < 0.001$, ****$p < 0.0001$. Data are presented as mean ± SEM.

3.9. Parkin deletion in MuSCs results in loss of MuSCs in both uninjured contralateral muscle and injured TA muscle

Several studies in different models have shown that developmental compensation for PINK1-dependent mitophagy can occur[163; 164; 165; 166; 167]. Thus we suspected that defects in PINK1-deficient MuSC function may be masked by compensatory up-regulation of alternative PINK1-independent mitophagy pathways such as Parkin-driven mitophagy, BNIP3/NIX-mediated mitophagy and FUNDC1-dependent mitophagy, which remain functional in PINK1-deficient mice[163; 164; 165; 166; 167.] Therefore, our lab developed a tamoxifen-inducible conditional KO of Parkin in the Pax7+ adult skeletal MuSCs **(Fig 15A-B)**. Validation of Parkin KO was confirmed by immunofluorescent staining in cultured WT and Parkin KO MuSCs for the absence of Parkin (**Fig. 15C**). There was no difference in the TA muscle weight between both mice at 21DPI (**Fig. 15E**). Next, we immunostained TA muscle fibers of Parkin KO mice with Pax7 marker to quantify self-renewing MuSCs at 21DPI. Analysis of the number of fibers per tissue area showed significant differences between WT and Parkin KO mice in both uninjured and injured muscles (**Fig. 15F**). Thus, analysis of Pax7+ve MuSCs was performed relative to the number of fibers. Interestingly, we revealed a significant loss of MuSCs in uninjured contralateral muscles of Parkin KO mice and a decrease in the self-renewal capacity of Parkin-deficient MuSCs at 21DPI suggesting that muscle-specific KO of Parkin had a detrimental effect on the MuSC pool and self-renewal ability of MuSCs (**Fig. 15D, G**).

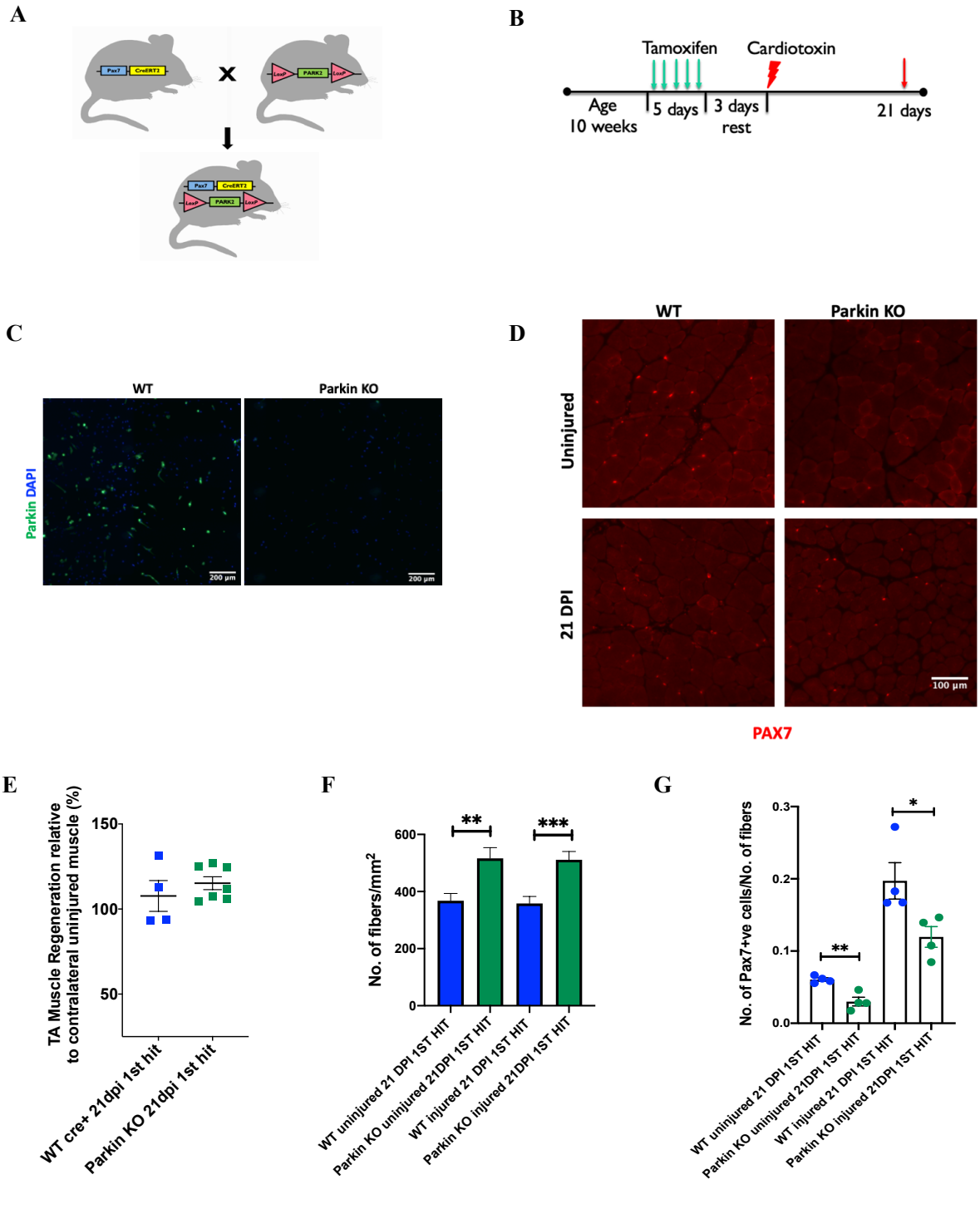
A
B
Tamoxifen
Cardiotoxin
Age
10 weeks
5 days
3 days
rest
21 days
C
WT
Parkin KO
Parkin DAPI
200 µm
D
WT
Parkin KO
Uninjured
21 DPI
100 µm
PAX7
E
TA Muscle Regeneration relative to contralateral uninjured muscle (%)
150
100
50
WT cre+ 21dpi 1st hit
Parkin KO 21dpi 1st hit
F
No. of fibers/mm2
600
400
200
0
**
***
WT uninjured 21 DPI 1ST HIT
Parkin KO uninjured 21DPI 1ST HIT
WT injured 21 DPI 1ST HIT
Parkin KO injured 21DPI 1ST HIT
G
No. of Pax7+ve cells/No. of fibers
0.3
0.2
0.1
0.0
**
*
WT uninjured 21 DPI 1ST HIT
Parkin KO uninjured 21DPI 1ST HIT
WT injured 21 DPI 1ST HIT
Parkin KO injured 21DPI 1ST HIT

Fig. 15: Loss of Parkin *in vivo* leads to a decrease in the number of MuSCs in the contralateral uninjured muscles and results in impaired self-renewal of MuSCs in response to acute injury

A, Breeding strategy to generate tamoxifen-inducible conditional KO of Parkin/PARK2 in Pax7+ adult skeletal MuSCs. **B**, Injury model paradigm. **C**, Validation of Parkin KO in MuSCs by immunostaining of cultured isolated WT and Parkin KO MuSCs. **D**, Representative immunostaining images of TA muscle sections stained with MuSC marker, Pax7 at 21DPI. Magnification: 20X. **E**, TA Muscle regeneration relative to contralateral uninjured muscle (%) at 21DPI WT vs Parkin KO injured mice (n≥4 mice). **F**, Quantification of the number of fibers/tissue area in TA muscle of WT and Parkin KO mice at 21DPI. **G**, Immunostaining analysis stained with MuSC marker, Pax7 at 21DPI normalized to number of fibers given the significant difference seen in Fig. 14F. Statistics were realized using an unpaired t test (n=4 mice). Statistical significance is displayed as $*p < 0.05$, $**p < 0.01$, $***p < 0.001$, $****p < 0.0001$. Data are presented as mean ± SEM.

3.10. Loss of Parkin *in vitro* shows decreased proliferation, increased commitment and impaired differentiation of MuSCs

To investigate whether muscle-specific deletion of Parkin affects MuSC fate, *in vitro* single myofiber cultures from Parkin-deficient mice were isolated at different timepoints (T1, T24, T48, T72). Our preliminary results demonstrated a trend towards a decline in the number of cells per cluster at T72 showing that the proliferation rate in *in vitro* cultures is impaired with loss of Parkin in MuSCs (**Fig. 16B**). At T1, WT and Parkin KO MuSCs express Pax7 only (**Fig. 16A, C-D**). Our data revealed that Parkin KO MuSCs display decreased proliferation (Pax7+ve MyoD+ve) and increased commitment (MyoD+ve only) at T24, T48 and T72 (**Fig. 16A, E, G, I**). At T48 and T72, our results pointed towards an impairment in MuSC differentiation as assessed by a decrease in the number of MyoG+ve cells (**Fig. 16A, H, J**). However, this decrease did not affect muscle regeneration as seen in our *in vivo* data (**Fig.15**). Parkin KO MuSCs also showed impaired self-renewal as assessed by the absence of Pax7+ve only cells at T72 (**Fig. 16A, I**). These preliminary findings reflect a potential role of Parkin-mediated mitophagy in fate decisions, lineage progression and differentiation of MuSCs.

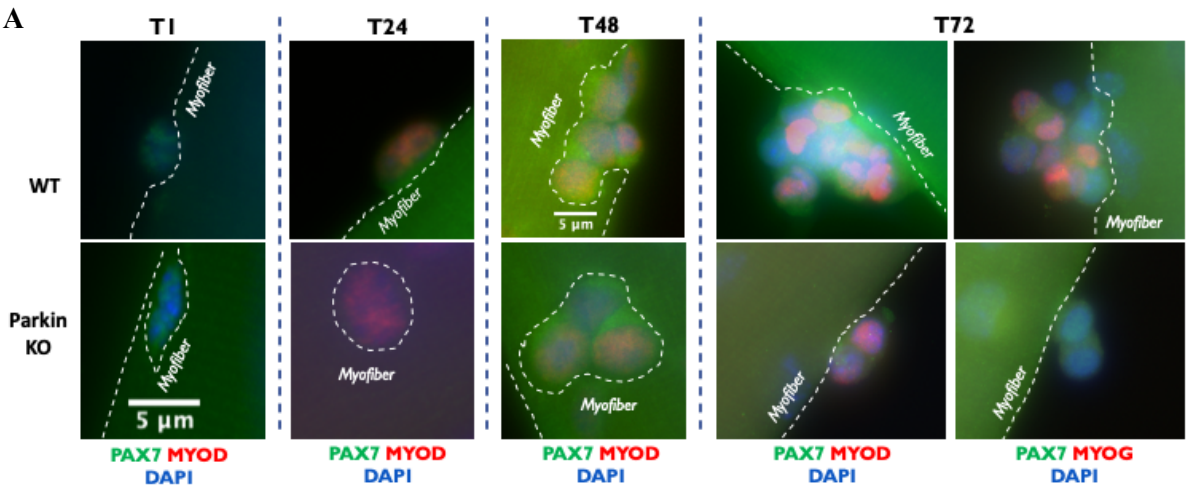
A
T1
T24
T48
T72
WT
Parkin KO
Myofiber
5 µm
PAX7 MYOD
DAPI
PAX7 MYOG
DAPI

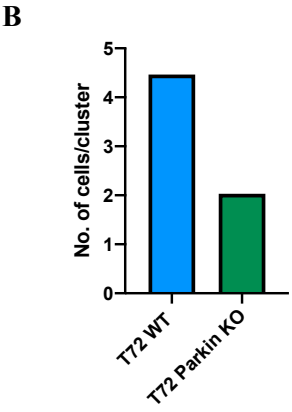
B
No. of cells/cluster
0
1
2
3
4
5
T72 WT
T72 Parkin KO

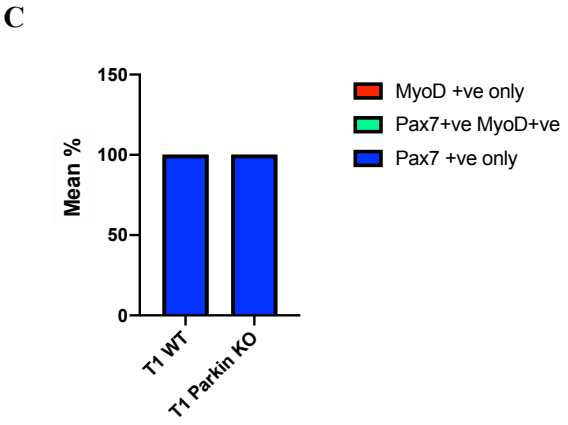
C
Mean %
0
50
100
150
T1 WT
T1 Parkin KO
MyoD +ve only
Pax7+ve MyoD+ve
Pax7 +ve only

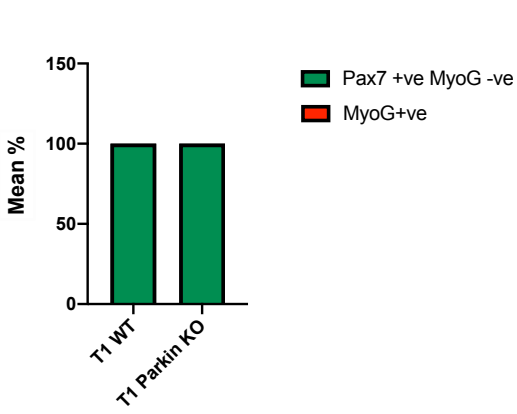
D
Mean %
0
50
100
150
T1 WT
T1 Parkin KO
Pax7 +ve MyoG -ve
MyoG+ve

E

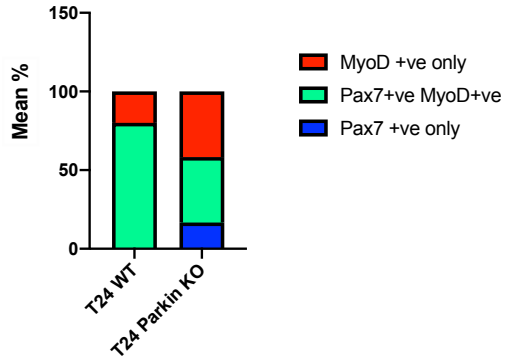
Mean %
150
100
50
0
T24 WT
T24 Parkin KO
MyoD +ve only
Pax7+ve MyoD+ve
Pax7 +ve only

F

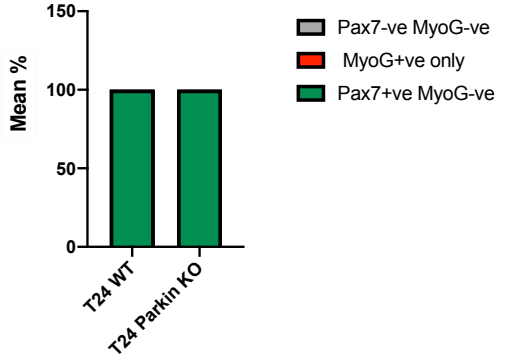
Mean %
150
100
50
0
T24 WT
T24 Parkin KO
Pax7-ve MyoG-ve
MyoG+ve only
Pax7+ve MyoG-ve

G

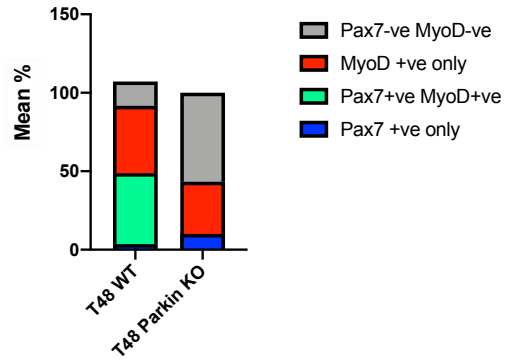
Mean %
150
100
50
0
T48 WT
T48 Parkin KO
Pax7-ve MyoD-ve
MyoD +ve only
Pax7+ve MyoD+ve
Pax7 +ve only

H

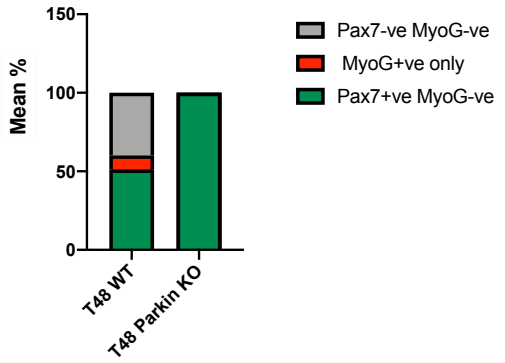
Mean %
150
100
50
0
T48 WT
T48 Parkin KO
Pax7-ve MyoG-ve
MyoG+ve only
Pax7+ve MyoG-ve

I

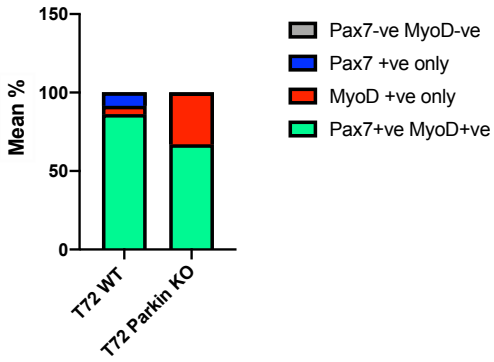
Mean %
150
100
50
0
T72 WT
T72 Parkin KO
Pax7-ve MyoD-ve
Pax7 +ve only
MyoD +ve only
Pax7+ve MyoD+ve

J

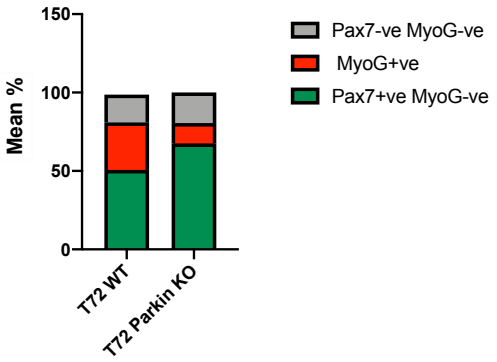
Mean %
150
100
50
0
T72 WT
T72 Parkin KO
Pax7-ve MyoG-ve
MyoG+ve
Pax7+ve MyoG-ve

Fig. 16: Parkin deficiency *in vitro* results in decreased proliferation, increased commitment and impaired differentiation of MuSCs

A, Representative epifluorescence images of WT vs Parkin KO MuSCs on EDL single fibers at different isolation timepoints. (T1, T24, T48, T72) stained with Pax7/MyoD/DAPI and Pax7/MyoG/DAPI. Magnification: 20X. **B**, Number of cells per cluster in WT vs Parkin KO EDL single fibers at T72. **C-J**, Quantification of muscle specific transcription factors, Pax7/MyoD and Pax7/MyoG in WT vs Parkin KO EDL single fibers at T1, T24, T48, T72 (n=1 independent experiment).

4. DISCUSSION

MuSCs are the main contributors of skeletal muscle regeneration[168]. A fine balance between myogenic commitment for proper regeneration and self-renewal for the maintenance of the MuSC pool is critical to ensure long-term maintenance of skeletal muscle[62; 71]. Therefore, dissecting the mechanisms regulating MuSC fate has gained significant interest and attention in the field of stem cell biology and regenerative medicine, particularly to develop new therapeutic approaches for the prevention and treatment of muscle diseases such as Duchenne muscular dystrophy and sarcopenia which are characterized by impaired regeneration and depletion of the MuSC pool[169; 170]. In this study, we investigated the role of mitochondrial quality control, particularly mitophagy, on MuSC function. Using our mitophagy reporter mouse, we provide evidence that mitophagy is active in quiescent MuSCs and is transiently down-regulated during early activation before increasing again during differentiation or self-renewal, suggesting its dynamic role in MuSC fate decision and lineage progression. Furthermore, we show that interfering with mitophagy through genetic inactivation of the PINK1/Parkin pathway promotes MuSC commitment at the expense of self-renewal, which ultimately leads to a progressive decline of the MuSC pool and tissue regeneration.

4.1. Role of mitophagy in maintenance of stemness in MuSCs

To date, direct measurement of mitophagy in MuSCs is lacking. Our work is the first to directly assess the natural course of mitophagy in MuSCs through the quantification of mitolysosomes using previously developed mitophagy reporter mice, *mito*-QC mice[119]. Firstly, to ensure that this mouse model was a reliable tool to accurately assess mitophagy in MuSCs, we treated *in vitro* single muscle fibers with 20µM of CCCP, an uncoupler of electron transport chain, to stimulate membrane depolarisation and mitophagy[171]. As a result, mitophagy was successfully induced and resulted in an increase in the number of mitolysosomes in MuSCs. Our *in vitro* single myofiber cultures isolated from the *mito*-QC mice revealed that mitophagy is active in *in-situ* fixed quiescent MuSCs. Interestingly, we also found that mitophagic events

were more frequent in MuSCs expressing high levels of Pax7 after 72 hours in culture. As cells expressing high levels of Pax7 were previously identified as self-renewing MuSCs capable of reverting back to quiescence [32], our data suggest that mitophagy remains active in MuSCs that are poised towards self-renewal.

To monitor mitophagy in a truly quiescent state, MuSCs were also purified from muscles that were fixed *in situ* prior to the normal cell dissociation procedure which, although relatively short (3h), is sufficient to initiate activation[156]. Our preliminary assessment of mitophagy in truly quiescent MuSCs (T0 MuSCs) obtained from *in situ* fixed muscle provide further evidence that active mitophagy is an inherent property of MuSC quiescence. Interestingly, as previously described by Machado *et al*., T0 MuSCs retained their *in vivo* spindle-like shape with several branches emanating from their poles suggesting that the fixation procedure was effective at preserving the native morphology of truly quiescent MuSCs[22; 156]. This could be confirmed by transcriptomic profiling in future studies.

To gain insights on the potential mechanisms involved in the regulation of mitophagy, we examined three transcriptomics datasets taken from previous murine studies comparing MuSCs in the quiescent state and early after (i.e., 2-3 days) *in vivo* activation induced by the intramuscular injection of CTX or $BaCl_2$. Importantly, in all three datasets, the expression of PINK1 and Parkin was enriched in quiescent MuSCs and down-regulated in 2-3 days activated MuSCs, supporting the idea that the PINK1/Parkin pathway could play a role in sustaining mitophagy in quiescent MuSCs and driving the acute changes in mitophagy observed during early activation.

To address this question, we studied a whole-body KO of the PINK1 gene *in vivo* and revealed a significant decrease in the number of Pax7+ve MuSCs at 21DPI, suggesting an impairment in the self-renewal capacity of MuSCs. Indeed, several studies have previously established that a loss of Pax7+ve cells in newly regenerated muscle is indicative of an impairment in the self-renewal capacity of MuSCs[172; 173; 174; 175]. Self-renewal being a key aspect for the maintenance of muscle repair capacity on the long term, we next examined

muscle regeneration after three serial CTX injuries to the TA muscle each separated by 21 days[175]. After two and three cycles of injury/regeneration, we observed a decline in the number of Pax7+ve MuSCs, a gradual reduction in the CSA of regenerated fibers in the PINK1 KO mice and progressive loss of tissue regenerative capacity which further points to a defect in the self-renewal capacity of PINK1-deficient MuSCs and a progressive depletion of the MuSC pool. Consistent with these results, single myofiber culture experiments revealed a decrease in the number of MuSCs expressing only Pax7 after 72 hours in culture, again pointing to a reduction in the number of self-renewing MuSCs[173] in absence of PINK1.

Previous studies have shown that a degree of compensation is observed in germline deletion of PINK1 and Parkin[176; 177; 178; 179; 180]. In both mouse models, only mild mitochondrial dysfunctions are present in tissues and loss of dopaminergic neurons, the hallmark of Parkinson's disease, is minimal and only occurs in aged mice suggesting the existence of developmental compensation[176; 177; 178]. In line with this hypothesis, inducible KO of Parkin in the adult brain was shown to precipitate the loss of dopaminergic neurons[179] while deletion from the heart in neonates, blocked the metabolic maturation in cardiomyocytes and precipitated dilated cardiomyopathy[180]. In order to limit the contribution of compensatory mechanisms and avoid the potential confounding effect of knocking out the PINK1/Parkin pathway in other tissues, we therefore sought to validate our findings in an inducible MuSC specific model of Parkin deficiency.

In line with our results obtained with PINK1-deficient mice, we found that deletion of Parkin in MuSCs led to a significant decrease in the number of Pax7+ve MuSCs following a single round of CTX-induced injury and regeneration. Interestingly, and in contrast to what was observed in the PINK1 model, these mice also presented a lower number of *Pax7+ve* MuSC in the contralateral uninjured muscle, which could be indicative of a defect at baseline. Furthermore, preliminary studies monitoring lineage progression in the single EDL fiber culture model at T72 showed a more rapid loss of MuSCs expressing *Pax7* only in absence of Parkin indicative of a potential defect in MuSC self-renewal. Although further experiments

are required to fully characterize the regenerative response, the muscle phenotype at baseline, and fate decisions, these preliminary results validate the observations made in the germline PINK1 KO mice, and suggest that interfering with PINK1/Parkin-mediated mitophagy impairs the capacity of MuSCs to self-renew.

While limited data is available on the PINK1/Parkin pathway in MuSCs, evidence obtained in other types of stem cells bring support to our observations. For instance, loss of PINK1-dependent mitophagy was reported to impair mitochondrial rejuvenation associated with the nuclear reprogramming of somatic cells into iPSCs[143]. Furthermore, Ito *et al*. reported that PINK1 and Parkin were highly expressed in HSCs under steady state conditions and that silencing these genes impaired the expansion and maintenance of HSCs[144]. Another study showed that knockdown of PINK1 in LSCs impaired their capacity to self-renew and that PINK1 mRNA expression was higher in subpopulations of LSCs emitting low amounts of ROS compared to subpopulations emitting larger amounts[138]. In combination with our results, these data[138; 143; 144] thus provide evidence for an important role in PINK1/Parkin-mediated mitophagy in the maintenance of multiple types of stem cells.

An interesting study by Katajisto *et al*. [64] brings additional insight on the importance of mitophagy for the preservation of stemness properties. In this study, the authors used SNAP-tag labelling of the OMM protein Omp25 to label "old" mitochondria in red and more recently synthesized "young" mitochondria in green prior to cell division. Using this approach they monitored the distribution of the labelled mitochondria upon asymmetric division and found that self-renewing stem cells predominantly retained "young" mitochondria, while stem cells with "older" mitochondria were more prone to commit and differentiate[64]. The authors also reported that mitophagy, as assessed by immunolabeling with the autophagy marker light chain 3B (LC3B), was higher in self-renewing stem cells with "younger" mitochondria. Furthermore, knock-down of Parkin was shown to deplete the population of cells displaying high stemness properties. Collectively, these results support the idea that by actively clearing mitochondria, mitophagy allows to clear "old" mitochondria and maintain a pool of recently synthesized

organelles in cells with high stemness properties. Conversely, reduced mitophagy and asymmetric segregation of "old" mitochondria appears to poise stem cells towards commitment. Therefore, changes in the rate of mitophagy appear to affect stem cell fate decisions by modulating the functional/structural properties of their mitochondrial population.

The mechanisms linking active mitophagy to the maintenance of self-renewal capacity in MuSCs are currently unclear. However, the link between mitophagy and the maintenance of stemness in other types of stem cells can provide interesting insights. For instance, Liang and colleagues found that subpopulations of HSCs with high stemness properties generally harbor mitochondria with a low MMP[181]. Interestingly, these cells also display a more fragmented mitochondrial network (due to a greater recruitment of dynamin-related protein 1 (DRP1) to mitochondria), enhanced activity of the PINK1/Parkin pathway, and increased lysosomal degradation of mitochondria compared to cycling-primed HSCs presenting high membrane potential and lower stemness properties[181]. Based on these results and our data we could speculate that low MMP, which is a well-known trigger of Parkin recruitment to mitochondria, could allow for sustaining mitophagy in quiescent MuSCs, thereby enabling active pruning of the mitochondrial pool, and maintenance of metabolic stemness traits[181;182].

Consistent with a low MMP, quiescent stem cells, including MuSCs, have very low metabolic rates[88; 92;105; 106; 183]. This allows to limit the production of ROS, which, apart from inducing oxidative damage, also act as a potent trigger for stem cell differentiation[184; 185; 186]. Therefore, active elimination of mitochondria through mitophagy could act as a protective mechanism to maintain a limited pool of healthy mitochondria with low OXPHOS activity and low levels of ROS, which would in turn favor survival and maintenance of stemness properties[105; 106; 108; 144]. To support this claim, recent studies have shown that mitophagy protects various stem cells (e.g. HSCs, BMSCs and MSCs) against oxidative damage and rescues them from ROS-induced apoptosis through elimination of damaged and dysfunctional mitochondria[146; 147;26; 59; 148].

As outlined in the introduction of this thesis, although intermediary metabolism and rates of OXPHOS are low in stem cells, their ability to oxidize fuels, particularly fatty acids, is crucial for the maintenance of stemness properties[110; 112]. As a result, promoting FAO using treatments such as peroxisome proliferator-activated receptor δ (PPARδ) (a master regulator of FAO) agonists were shown to enhance self-renewal capacity in HSCs[115; 144]. Conversely, inhibiting FAO was shown to trigger differentiation[104; 111]. Interestingly, PINK1 expression was recently shown to be transcriptionally regulated by peroxisome proliferator-activated receptor (PPAR)[144]. Moreover, in this study, the authors showed that PPARδ agonists not only stimulated FAO but also activated mitophagy through the recruitment of Parkin to mitochondria[144]. Although much remains to be learned, these results suggest the existence of a potential regulatory mechanism linking mitophagy to the reliance of FAO, which appears to be a distinctive metabolic characteristic of stemness[110; 112].

4.2. Mitophagy during MuSC activation

Our analysis of mitophagy in the *mito*-QC mouse model revealed that a rapid and transient inhibition of mitophagy naturally occurs in MuSCs upon activation. This was observed in single EDL fiber culture experiments, where a robust decrease in the number of mitophagic events was found in MuSCs at 24h *vs* 0.5 and 1 h post isolation. Moreover, mitophagic events were also less frequent in 3h-activated compared to *in situ* fixed quiescent MuSCs, suggesting that the decay kinetics of mitophagy upon activation may in fact be rapid. This was further corroborated by our analysis of transcriptomics datasets which indicated a rapid down-regulation in the expression of PINK1 and Parkin transcripts in *in vivo* activated *vs* quiescent MuSCs[139; 159]. Altogether, these data suggest that physiological down-regulation of mitophagy plays a role in MuSC activation.

Although these results clearly indicate that mitophagy is rapidly inhibited upon MuSCs activation, the underlying regulatory mechanisms remain obscure. The strong and consistent decrease in PINK1 and Parkin transcripts observed across multiple transcriptomic datasets

available in the literature suggest that a transcriptional mechanism may be involved. It is also possible that Parkin recruitment to mitochondria naturally becomes inhibited in response to the rise in MMP, and the activation of oxidative metabolism that occurs as MuSCs become activated[187; 188]. Further studies will however be required to address these questions.

An increase in ROS is thought to be required for MuSCs to exit the cell cycle[186; 189]. L'honoré *et al*. demonstrated the crucial role of ROS for cell cycle entry of MuSCs whereby activation of MuSCs during muscle regeneration was accompanied by an increase in intracellular ROS content through activation of p38α MAP kinase[186]. A recent study showed that freshly isolated MuSCs with decreased expression of Pax7 displayed high levels of ROS therefore allowing for cell cycle entry[189]. Since mitophagy plays an essential role in ROS reduction through the clearance of damaged mitochondria[190; 191; 192], we believe that a decrease in mitophagy would be necessary to allow for ROS production and consequently MuSC activation.

Interestingly, studies in MuSCs have established that macroautophagy increases upon activation and is in fact required to meet the nutrient demand of proliferation[193; 194]. This is also accompanied by a metabolic shift from glycolysis to OXPHOS, and an activation of mitochondrial biogenesis signaling to support the energy requirements of MuSC activation[194; 195; 196]. In this context, we speculate that inhibition of mitophagy during this period may allow to spare mitochondria from being degraded through macroautophagy. In conjunction with the activation of mitochondrial biogenesis, transient inhibition of mitophagy could thus constitute a mechanism to better meet the energy requirements of MuSC activation.

4.3. Mitophagy in myogenic commitment

Furthermore, our results show that in the EDL fiber culture model, MuSCs were more prone to express the myogenic progenitor markers (*e.g.* MyoD and MyoG) in absence of PINK1 or Parkin, which was accompanied by a reduced population of self-renewing cells expressing solely *Pax7* compared to WT controls. Moreover, in our *in vivo* model of CTX injury, MuSCs expressing these MRFs (MyoD or MyoG) were more numerous in PINK1-deficient mice *vs*

WT at 4DPI and 14DPI, while the number of Pax7+ve self-renewing MuSC was reduced once the muscle was fully regenerated, suggesting that commitment was favored at the expense of self-renewal. Our findings therefore suggest that impairing PINK1/Parkin-dependent mitophagy influences MuSCs fate decisions by pushing MuSCs towards commitment thereby resulting in the exhaustion of the MuSC pool. This is in line with our theory that mitophagy is required to maintain stemness of MuSCs and thus lack of mitochondrial quality control poises MuSCs towards commitment and differentiation rather than reverting them back to quiescence due to their poor mitochondrial profile. Our results are also supported by a recently published study in which Western blotting of whole muscle lysates was used to examine muscle regeneration in germline Parkin-deficient mice[197]. In this study the authors reported that Parkin deficiency led to increased myogenic commitment as assessed by an increase in the expression of the cell cycle marker, Cyclin D1 at 3 days post-CTX injury[197].

4.4. Role of mitophagy in MuSC differentiation

Previous studies in C2C12 myoblasts have shown that mitophagy is enhanced during differentiation [195; 197; 198]. For instance, Sin *et al*. reported that mitophagy was activated during early myogenic differentiation, as indicated by a decrease in the abundance of the Parkin target, translocase of outer mitochondrial membrane 70 homolog A (TOMM70A), and an increased colocalization of the autophagy adaptor protein p62/sequestosome 1 (SQSTM1) at day one into differentiation and beyond [195]. The authors suggested that activation of mitophagy, in conjunction with the activation of mitochondrial biogenesis, was required to replace immature mitochondria by more elaborated and oxidatively competent organelles that are better suited to meet the high energy requirement of differentiated muscle cells. More recently, another study performed in C2C12 myoblasts reported that mitophagy was activated during differentiation as evidenced by an increased colocalization of the autophagosome markers LC3B to mitochondria. Furthermore, the authors reported that deletion of the mitophagy receptor BNIP3 severely impaired myoblast differentiation[198].

Our time course analysis of mitophagy in single EDL fiber culture concur with these results and indicate that following a transient reduction during the early activation step (e.g., 24h time point), the number of mitophagic events increases progressively over the following 48h, which corresponds to a period where a proportion of MuSCs have engaged along the myogenic path. However, the results we obtained in PINK1-deficient mice, suggest that there is no apparent defect in MuSCs differentiation or capacity to regenerate muscle fibers *in vivo.* In fact, PINK1-deficient mice were able to mount a more robust regenerative response in response to the first injection of CTX, as evidenced by an increased proliferation of MuSC, a greater tendency to commit to the myogenic lineage, and an increased CSA of newly regenerated fibres. It is only upon repeated injury (2 and 3 CTX injections) that regenerated fibers became smaller in PINK1 KO mice, which we believe is attributable to a progressive loss of the MuSC pool rather than impaired differentiation.

Interestingly, a recently published study by Esteca *et al.* [197] reported that the CSA of fibers was reduced in germline Parkin KO mice compared to WT after a single round of CTX injury-regeneration, suggesting that the MuSC phenotype could be different and/or more severe compared to PINK1-deficient mice. This would be compatible with previous studies in the drosophila model[199] and in mammalian cell lines which showed that in absence of PINK1, the expression of endogenous Parkin is enhanced and may retain some mitophagic activity [200; 201]. It should be noted that in their study, Esteca *et al.* concluded that differentiation was impaired in Parkin-deficient MuSCs, which was not observed in our PINK1 KO mouse model. However, the experimental evidence to support their claim is open for discussion as impaired differentiation was based on the sole evidence that the proportion of MuSC expressing MyoG was reduced in Parkin KO mice muscle at 3DPI[197]. Furthermore, the expression of developmental myosin, MYH3 was enhanced in Parkin-deficient mice *vs* WT at 10DPI, which is not compatible with a gross differentiation defect[197]. The experiments initiated in this thesis using MuSC-specific inducible Parkin KO mice should allow to address these pending questions in the near future. It should also be mentioned that alternate pathways involving

mitophagy receptors could also play a role, as suggested by the dramatic effect of silencing BNIP3 on the ability of C2C12 myoblasts to differentiate [198]. These pathways deserve to be investigated in future studies.

4.5. Mitochondrial quality of PINK1-deficient muscle fibers

To examine whether defective mitophagy results in mature muscle fibers with mitochondrial defects, we assessed mitochondrial dysfunction in PINK1-deficient muscle fibers with and without injury. Our data showed that PINK1 deficiency impaired mitochondrial function as assessed by a reduction in CI and CIV activity in uninjured muscle fibers at 10 weeks of age. This data correlates with previous research and our theory that our PINK1-deficient mice display reduced mitophagy and thus an accumulation of damaged and dysfunctional mitochondria[127; 201]. PINK1 has been widely linked with mitochondrial function where its deficiency in both *D. melanogaster* and mice was reported to lead to mitochondrial dysfunction and specific reduction of CI activity [127; 132; 201]. Surprisingly, no change in CI or CIV activity was seen in newly regenerated muscle fibers of PINK1-deficient mice at 21DPI suggesting that loss of PINK1 at this specific timepoint does not result in the generation of muscle fibers with gross mitochondrial defects. Here we may speculate that the C1 and CIV defects observed in uninjured mature fibers at 10 weeks of age may take time to establish in newly regenerated fibers as they accumulate dysfunctional mitochondria over time due to impaired PINK1-mediated mitophagy. Further studies are required to gain more insights on the accumulation of mitochondrial dysfunction over time in PINK1 KO regenerated muscle fibers. These results thus suggest that mitophagy prevents the accumulation of mitochondrial defects and consequently promotes the maintenance of key mitochondrial properties that are essential to maintain MuSC function.

5. CONCLUSION

In conclusion, the experimental work performed in this thesis enabled us to document for the first time, the natural course of mitophagy in MuSCs under various states. These data and our analysis of the literature in other types of stem cells provide evidence that active mitophagy is a property of quiescent MuSCs and MuSCs that are more poised towards self-renewal. In self-renewing MuSCs, mitophagy likely contributes to maintain the metabolic properties of stemness through selective pruning of the mitochondrial pool. Our data also show that mitophagy is rapidly and transiently inhibited in MuSCs upon activation, possibly to avoid degradation through non-specific macro-autophagy and to facilitate the up-regulation of aerobic ATP production required to support the energy demand of activating MuSCs. Importantly, our data also reveal that chronic impairment of mitophagy through genetic inactivation of the PINK1/Parkin pathway predisposes MuSCs to commitment at the expense of self-renewal, thus inducing an imbalance in fate decisions and a progressive loss of muscle regenerative capacity.

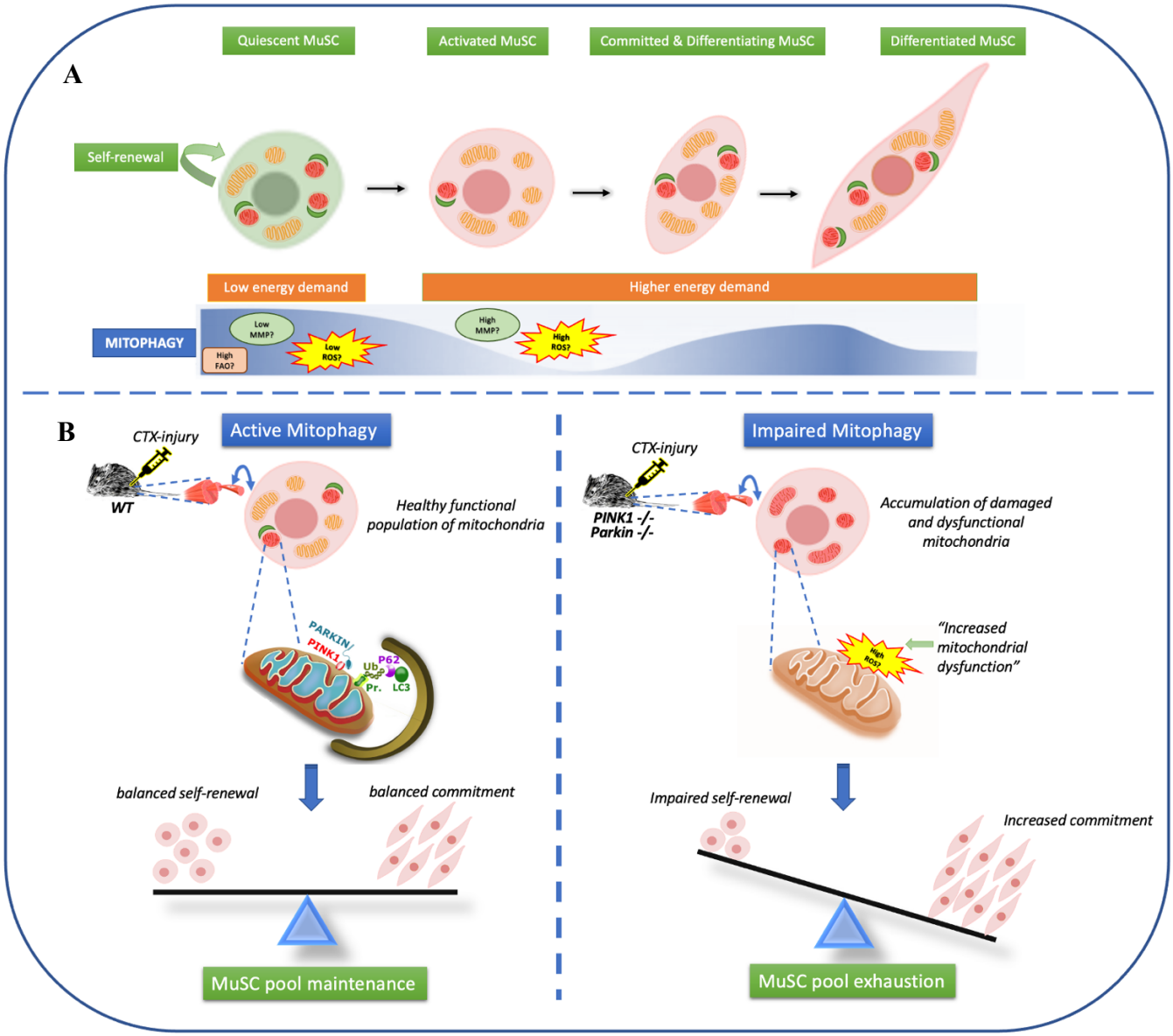
A
Quiescent MuSC
Activated MuSC
Committed & Differentiating MuSC
Differentiated MuSC
Self-renewal
Low energy demand
Higher energy demand
MITOPHAGY
Low MMP?
High FAO?
Low ROS?
High MMP?
High ROS?
B
Active Mitophagy
CTX-injury
WT
Healthy functional population of mitochondria
PARKIN/
PINK1
Ub
P62
Pr.
LC3
balanced self-renewal
balanced commitment
MuSC pool maintenance
Impaired Mitophagy
CTX-injury
PINK1 -/-
Parkin -/-
Accumulation of damaged and dysfunctional mitochondria
"Increased mitochondrial dysfunction"
High ROS?
Impaired self-renewal
Increased commitment
MuSC pool exhaustion

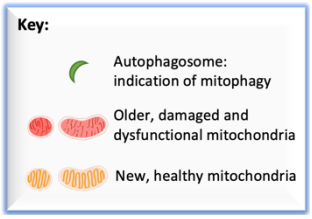
Key:
Autophagosome: indication of mitophagy
Older, damaged and dysfunctional mitochondria
New, healthy mitochondria

Fig. 17: Working model

A, Hypothesized role of mitophagy in the maintenance of MuSC stemness, lineage progression and MuSCs differentiation[131].Mitophagy is relatively active in quiescent and self-renewing MuSCs to preserve the mitochondrial profile of stemness in MuSCs and is transiently down-regulated upon MuSCs activation to allow for cell cycle entry. Up-regulation of mitophagy is also required during lineage progression and differentiation of MuSCs to meet the bioenergetic requirements of the differentiating MuSC. **B**, Mitophagy is actively involved in the modulation of MuSC fate decision during muscle regeneration by maintaining a delicate balance between MuSC commitment and self-renewal through the maintenance of a healthy pool of functional mitochondria.

6. LIMITATIONS

A limitation to our study is that we used a conventional KO of the PINK1 gene which often leads to developmental compensation[202]. Based on previous research, germline loss of PINK1 has been shown to be compensated by other mitophagy receptors such as Parkin, BNIP3, NIX and FUNDC1, which are still able to maintain the fidelity of mitochondria by inducing mitophagy of dysfunctional mitochondria in the absence of PINK1[197; 200; 201; 200; 163; 164; 199]. Therefore, the use of mice harboring conditional KO of mitophagy genes would provide further insight on the specific role of mitophagy in MuSC function.

Additionally, since MuSCs are a relatively rare population of cells in skeletal muscle, experiments requiring a large number of cells such as mitochondrial respiration activity assays using Seahorse XF Analyzer were challenging. To our knowledge, the yield of MuSCs that can be isolated from FACS experiments is approximately 120,000 cells per mouse. Thus, to overcome these limitations, the number of animals needs to be increased to obtain the desired number of cells or primary myoblast cultures could be used as an alternative model.

Moreover, while PINK1/Parkin-mediated mitophagy is the best characterized pathway of mitochondrial clearance, alternative pathways of mitophagy namely BNIP3/NIX-mediated mitophagy, FUNDC1-dependent mitophagy and many others as listed in Fig.6B have been shown to play an important role in stem cell homeostasis[166; 196]. Thus, to better understand the role of mitophagy in MuSCs, it would be worth examining PINK1/Parkin-independent pathways of mitophagy.

7. FUTURE DIRECTIONS

Further work is required using our mice harboring MuSC-specific KO of Parkin to look into the specific role of mitophagy in MuSC fate determination during regenerative myogenesis. Similar experiments performed in this thesis would thus be done to achieve this.

To provide additional and distinct information regarding mitochondrial dysfunction in MuSCs with impaired mitophagy, ROS measurement by MitoSOX™ Red staining, ATP measurement, quantification of mitochondrial length by Tom20/Pax7 staining and oxygen consumption assay by Seahorse would be performed.

To provide further insight into the role of mitophagy in truly quiescent MuSCs, MuSCs would be isolated from *in situ* fixed muscle and sorted for α-integrin-7+ve, CD34+ve double positive population (marker of quiescent MuSCs[46]) by FACS. Experiments such as qPCR, ribonucleic acid (RNA) sequencing would further explore different mitophagy genes (BNIP3, BNIP3L/NIX, FUNC1) in the maintenance of quiescence in MuSCs. Transcriptomics analysis could also be performed on quiescent MuSCs harboring a KO of mitophagy genes to examine the expression of quiescence markers like Notch ligand Delta-like protein 1 (DLL1), Spry1 and SIX1.

Further research is required to identify the mechanisms underlying the role of PINK1/Parkin-dependent mitophagy in the regulation of MuSC fate during muscle repair. As mentioned in our discussion, potential targets would be the assessment of MMP in FACS-sorted MuSCs by staining with tetramethylrhodamine, ethyl ester (TMRE) dye or 1st J-aggregate-forming cationic (JC-1) dye. Quantification of ROS in MuSCs using MitoSOX™ Red dye would also shed some light on the involvement of mitophagy through ROS signaling in dictating MuSC fate.

8. REFERENCES

1 CORNELISON, D.; PERDIGUERO, E. Muscle Stem Cells: A Model System for Adult Stem Cell Biology. **Methods Mol Biol,** v. 1556, p. 3-19, 2017. ISSN 1940-6029. Disponível em: < https://www.ncbi.nlm.nih.gov/pubmed/28247342 >.

2 CEAFALAN, L. C.; POPESCU, B. O.; HINESCU, M. E. Cellular players in skeletal muscle regeneration. **Biomed Res Int,** v. 2014, p. 957014, 2014. ISSN 2314-6141. Disponível em: < https://www.ncbi.nlm.nih.gov/pubmed/24779022 >.

3 YIN, H.; PRICE, F.; RUDNICKI, M. A. Satellite cells and the muscle stem cell niche. **Physiol Rev,** v. 93, n. 1, p. 23-67, Jan 2013. ISSN 1522-1210. Disponível em: < https://www.ncbi.nlm.nih.gov/pubmed/23303905 >.

4 CRETOIU, D. et al. Myofibers. **Adv Exp Med Biol,** v. 1088, p. 23-46, 2018 2018. ISSN 0065-2598. Disponível em: < https://www.ncbi.nlm.nih.gov/pubmed/30390246 >.

5 FRONTERA, W. R.; OCHALA, J. Skeletal muscle: a brief review of structure and function. **Calcif Tissue Int,** v. 96, n. 3, p. 183-95, Mar 2015. ISSN 1432-0827. Disponível em: < https://www.ncbi.nlm.nih.gov/pubmed/25294644 >.

6 L., S. D. **Regenerative Biology and Medicine (Second Edition). Chapter 6 - Regeneration of Musculoskeletal Tissues**: Academic press**:** 127-160, p. 2012.

7 BETTS, J. G. et al. **Anatomy and Physiology**. Houston, Texas: OpenStax, 2013. Disponível em: < https://openstax.org/books/anatomy-and-physiology/pages/1-introduction >.

8 CIAPAITE, J. et al. Fiber-type-specific sensitivities and phenotypic adaptations to dietary fat overload differentially impact fast- versus slow-twitch muscle contractile function in C57BL/6J mice. **J Nutr Biochem,** v. 26, n. 2, p. 155-64, Feb 2015. ISSN 1873-4847. Disponível em: < https://www.ncbi.nlm.nih.gov/pubmed/25516489 >.

9 TALBOT, J.; MAVES, L. Skeletal muscle fiber type: using insights from muscle developmental biology to dissect targets for susceptibility and resistance to muscle disease. **Wiley Interdiscip Rev Dev Biol,** v. 5, n. 4, p. 518-34, 07 2016. ISSN 1759-7692. Disponível em: < https://www.ncbi.nlm.nih.gov/pubmed/27199166 >.

10 FUJIMAKI, S. et al. Diabetes and Stem Cell Function. **BioMed Research International,** v. 2015, p. 16, 2015.

11 KARALAKI, M. et al. Muscle regeneration: cellular and molecular events. **In Vivo,** v. 23, n. 5, p. 779-96, 2009 Sep-Oct 2009. ISSN 0258-851X. Disponível em: < https://www.ncbi.nlm.nih.gov/pubmed/19779115 >.

12 HOWARD, E. E. et al. Divergent Roles of Inflammation in Skeletal Muscle Recovery From Injury. **Front Physiol,** v. 11, p. 87, 2020. ISSN 1664-042X. Disponível em: < https://www.ncbi.nlm.nih.gov/pubmed/32116792 >.

[13] GARRY, G. A.; ANTONY, M. L.; GARRY, D. J. Cardiotoxin Induced Injury and Skeletal Muscle Regeneration. **Methods Mol Biol,** v. 1460, p. 61-71, 2016. ISSN 1940-6029. Disponível em: < https://www.ncbi.nlm.nih.gov/pubmed/27492166 >.

[14] LAUMONIER, T.; MENETREY, J. Muscle injuries and strategies for improving their repair. **J Exp Orthop,** v. 3, n. 1, p. 15, Dec 2016. ISSN 2197-1153. Disponível em: < https://www.ncbi.nlm.nih.gov/pubmed/27447481 >.

[15] GARDNER, T.; KENTER, K.; LI, Y. **Fibrosis following Acute Skeletal Muscle Injury: Mitigation and Reversal Potential in the Clinic**: *Journal of Sports Medicine*. 2020**:** 7 p. 2020.

[16] GREISING, S. M.; CORONA, B. T.; CALL, J. A. Musculoskeletal Regeneration, Rehabilitation, and Plasticity Following Traumatic Injury. **Int J Sports Med,** v. 41, n. 8, p. 495-504, Jul 2020. ISSN 1439-3964. Disponível em: < https://www.ncbi.nlm.nih.gov/pubmed/32242332 >.

[17] JÄRVINEN, T. A.; JÄRVINEN, M.; KALIMO, H. Regeneration of injured skeletal muscle after the injury. **Muscles Ligaments Tendons J,** v. 3, n. 4, p. 337-45, Oct 2013. ISSN 2240-4554. Disponível em: < https://www.ncbi.nlm.nih.gov/pubmed/24596699 >.

[18] ZUK, P. A.; BENHAIM, P.; HEDRICK, M. H. Stem Cells from Adipose Tissue. In: (Ed.). **Handbook of Stem Cells**, v.2, 2004. cap. 40, p.Pages 425-447.

[19] JUDSON, R. N.; ROSSI, F. M. V. Towards stem cell therapies for skeletal muscle repair. **NPJ Regen Med,** v. 5, p. 10, 2020. ISSN 2057-3995. Disponível em: < https://www.ncbi.nlm.nih.gov/pubmed/32411395 >.

[20] BLAU, H. M.; COSGROVE, B. D.; HO, A. T. The central role of muscle stem cells in regenerative failure with aging. **Nat Med,** v. 21, n. 8, p. 854-62, Aug 2015. ISSN 1546-170X. Disponível em: < https://www.ncbi.nlm.nih.gov/pubmed/26248268 >.

[21] YANG, W.; HU, P. Skeletal muscle regeneration is modulated by inflammation. **J Orthop Translat,** v. 13, p. 25-32, Apr 2018. ISSN 2214-031X. Disponível em: < https://www.ncbi.nlm.nih.gov/pubmed/29662788 >.

[22] FU, X.; WANG, H.; HU, P. Stem cell activation in skeletal muscle regeneration. **Cell Mol Life Sci,** v. 72, n. 9, p. 1663-77, May 2015. ISSN 1420-9071. Disponível em: < https://www.ncbi.nlm.nih.gov/pubmed/25572293 >.

[23] SAMBASIVAN, R. et al. Pax7-expressing satellite cells are indispensable for adult skeletal muscle regeneration. **Development,** v. 138, n. 17, p. 3647-56, Sep 2011. ISSN 1477-9129. Disponível em: < https://www.ncbi.nlm.nih.gov/pubmed/21828093 >.

[24] HARDY, D. et al. Comparative Study of Injury Models for Studying Muscle Regeneration in Mice. **PLoS One,** v. 11, n. 1, p. e0147198, 2016. ISSN 1932-6203. Disponível em: < https://www.ncbi.nlm.nih.gov/pubmed/26807982 >.

[25] PUROHIT, G.; DHAWAN, J. Adult Muscle Stem Cells: Exploring the Links Between Systemic and Cellular Metabolism. **Front Cell Dev Biol,** v. 7, p. 312, 2019. ISSN 2296-634X. Disponível em: < https://www.ncbi.nlm.nih.gov/pubmed/31921837 >.

[26] FAN, P. et al. Mitophagy is a protective response against oxidative damage in bone marrow mesenchymal stem cells. **Life Sci,** v. 229, p. 36-45, Jul 2019. ISSN 1879-0631. Disponível em: < https://www.ncbi.nlm.nih.gov/pubmed/31085242 >.

[27] FORCINA, L.; COSENTINO, M.; MUSARÒ, A. Mechanisms Regulating Muscle Regeneration: Insights into the Interrelated and Time-Dependent Phases of Tissue Healing. **Cells,** v. 9, n. 5, 05 2020. ISSN 2073-4409. Disponível em: < https://www.ncbi.nlm.nih.gov/pubmed/32456017 >.

[28] GNOCCHI, V. F. et al. Further characterisation of the molecular signature of quiescent and activated mouse muscle satellite cells. **PLoS One,** v. 4, n. 4, p. e5205, 2009. ISSN 1932-6203. Disponível em: < https://www.ncbi.nlm.nih.gov/pubmed/19370151 >.

[29] ZAMMIT, P. S. et al. Pax7 and myogenic progression in skeletal muscle satellite cells. **J Cell Sci,** v. 119, n. Pt 9, p. 1824-32, May 2006. ISSN 0021-9533. Disponível em: < https://www.ncbi.nlm.nih.gov/pubmed/16608873 >.

[30] MCKAY, B. R. et al. Satellite cell number and cell cycle kinetics in response to acute myotrauma in humans: immunohistochemistry versus flow cytometry. **J Physiol,** v. 588, n. Pt 17, p. 3307-20, Sep 2010. ISSN 1469-7793. Disponível em: < https://www.ncbi.nlm.nih.gov/pubmed/20624792 >.

[31] CHANG, N. C. et al. The Dystrophin Glycoprotein Complex Regulates the Epigenetic Activation of Muscle Stem Cell Commitment. **Cell Stem Cell,** v. 22, n. 5, p. 755-768.e6, 05 2018. ISSN 1875-9777. Disponível em: < https://www.ncbi.nlm.nih.gov/pubmed/29681515 >.

[32] ROCHETEAU, P. et al. A subpopulation of adult skeletal muscle stem cells retains all template DNA strands after cell division. **Cell,** v. 148, n. 1-2, p. 112-25, Jan 2012. ISSN 1097-4172. Disponível em: < https://www.ncbi.nlm.nih.gov/pubmed/22265406 >.

[33] GUIRAUD, S. et al. Embryonic myosin is a regeneration marker to monitor utrophin-based therapies for DMD. **Hum Mol Genet,** v. 28, n. 2, p. 307-319, 01 2019. ISSN 1460-2083. Disponível em: < https://www.ncbi.nlm.nih.gov/pubmed/30304405 >.

[34] SCHULTZ, E.; MCCORMICK, K. M. Skeletal muscle satellite cells. **Rev Physiol Biochem Pharmacol,** v. 123, p. 213-57, 1994. ISSN 0303-4240. Disponível em: < https://www.ncbi.nlm.nih.gov/pubmed/8209136 >.

[35] ROCHETEAU, P.; VINET, M.; CHRETIEN, F. Dormancy and quiescence of skeletal muscle stem cells. **Results Probl Cell Differ,** v. 56, p. 215-35, 2015. ISSN 0080-1844. Disponível em: < https://www.ncbi.nlm.nih.gov/pubmed/25344673 >.

[36] WANG, Y. X.; DUMONT, N. A.; RUDNICKI, M. A. Muscle stem cells at a glance. **J Cell Sci,** v. 127, n. Pt 21, p. 4543-8, Nov 2014. ISSN 1477-9137. Disponível em: < https://www.ncbi.nlm.nih.gov/pubmed/25300792 >.

[37] EVANO, B.; TAJBAKHSH, S. Skeletal muscle stem cells in comfort and stress. **NPJ Regen Med,** v. 3, p. 24, 2018. ISSN 2057-3995. Disponível em: < https://www.ncbi.nlm.nih.gov/pubmed/30588332 >.

[38] FUKADA, S. et al. Molecular signature of quiescent satellite cells in adult skeletal muscle. **Stem Cells,** v. 25, n. 10, p. 2448-59, Oct 2007. ISSN 1549-4918. Disponível em: < https://www.ncbi.nlm.nih.gov/pubmed/17600112 >.

[39] DE MORRÉE, A. et al. Staufen1 inhibits MyoD translation to actively maintain muscle stem cell quiescence. **Proc Natl Acad Sci U S A,** v. 114, n. 43, p. E8996-E9005, 10 2017. ISSN 1091-6490. Disponível em: < https://www.ncbi.nlm.nih.gov/pubmed/29073096 >.

[40] MOURIKIS, P. et al. A critical requirement for notch signaling in maintenance of the quiescent skeletal muscle stem cell state. **Stem Cells,** v. 30, n. 2, p. 243-52, Feb 2012. ISSN 1549-4918. Disponível em: < https://www.ncbi.nlm.nih.gov/pubmed/22069237 >.

[41] FUJIMAKI, S. et al. Intrinsic ability of adult stem cell in skeletal muscle: an effective and replenishable resource to the establishment of pluripotent stem cells. **Stem Cells Int,** v. 2013, p. 420164, 2013. ISSN 1687-966X. Disponível em: < https://www.ncbi.nlm.nih.gov/pubmed/23818907 >.

[42] BJORNSON, C. R. et al. Notch signaling is necessary to maintain quiescence in adult muscle stem cells. **Stem Cells,** v. 30, n. 2, p. 232-42, Feb 2012. ISSN 1549-4918. Disponível em: < https://www.ncbi.nlm.nih.gov/pubmed/22045613 >.

[43] MOTOHASHI, N.; ASAKURA, A. Muscle satellite cell heterogeneity and self-renewal. **Front Cell Dev Biol,** v. 2, p. 1, 2014. ISSN 2296-634X. Disponível em: < https://www.ncbi.nlm.nih.gov/pubmed/25364710 >.

[44] KITAJIMA, Y.; ONO, Y. Visualization of PAX7 protein dynamics in muscle satellite cells in a YFP knock-in-mouse line. **Skelet Muscle,** v. 8, n. 1, p. 26, 08 2018. ISSN 2044-5040. Disponível em: < https://www.ncbi.nlm.nih.gov/pubmed/30139390 >.

[45] TICHY, E. D. et al. A robust Pax7EGFP mouse that enables the visualization of dynamic behaviors of muscle stem cells. **Skelet Muscle,** v. 8, n. 1, p. 27, 08 2018. ISSN 2044-5040. Disponível em: < https://www.ncbi.nlm.nih.gov/pubmed/30139374 >.

[46] BEAUCHAMP, J. R. et al. Expression of CD34 and Myf5 defines the majority of quiescent adult skeletal muscle satellite cells. **J Cell Biol,** v. 151, n. 6, p. 1221-34, Dec 2000. ISSN 0021-9525. Disponível em: < https://www.ncbi.nlm.nih.gov/pubmed/11121437 >.

[47] GARCÍA-PRAT, L. et al. FoxO maintains a genuine muscle stem-cell quiescent state until geriatric age. **Nat Cell Biol,** v. 22, n. 11, p. 1307-1318, Nov 2020. ISSN 1476-4679. Disponível em: < https://www.ncbi.nlm.nih.gov/pubmed/33106654 >.

[48] SHEA, K. L. et al. Sprouty1 regulates reversible quiescence of a self-renewing adult muscle stem cell pool during regeneration. **Cell Stem Cell,** v. 6, n. 2, p. 117-29, Feb 2010. ISSN 1875-9777. Disponível em: < https://www.ncbi.nlm.nih.gov/pubmed/20144785 >.

[49] CRUZ-MIGONI, S. B. et al. A switch in cilia-mediated Hedgehog signaling controls muscle stem cell quiescence and cell cycle progression. **bioRxiv**, p. 2019.12.21.884601, 2019. Disponível em: < https://www.biorxiv.org/content/biorxiv/early/2019/12/22/2019.12.21.884601.full.pdf >.

[50] CHEUNG, T. H. et al. Maintenance of muscle stem-cell quiescence by microRNA-489. **Nature,** v. 482, n. 7386, p. 524-8, Feb 2012. ISSN 1476-4687. Disponível em: < https://www.ncbi.nlm.nih.gov/pubmed/22358842 >.

[51] RODGERS, J. T. et al. mTORC1 controls the adaptive transition of quiescent stem cells from G0 to G(Alert). **Nature,** v. 510, n. 7505, p. 393-6, Jun 2014. ISSN 1476-4687. Disponível em: < https://www.ncbi.nlm.nih.gov/pubmed/24870234 >.

[52] ANDERSON, J. E. A role for nitric oxide in muscle repair: nitric oxide-mediated activation of muscle satellite cells. **Mol Biol Cell,** v. 11, n. 5, p. 1859-74, May 2000. ISSN 1059-1524. Disponível em: < https://www.ncbi.nlm.nih.gov/pubmed/10793157 >.

[53] ZAMMIT, P. S. et al. Muscle satellite cells adopt divergent fates: a mechanism for self-renewal? **J Cell Biol,** v. 166, n. 3, p. 347-57, Aug 2004. ISSN 0021-9525. Disponível em: < https://www.ncbi.nlm.nih.gov/pubmed/15277541 >.

[54] BRZOSKA, E. et al. Regulation of muscle stem cells activation: the role of growth factors and extracellular matrix. **Vitam Horm,** v. 87, p. 239-76, 2011. ISSN 0083-6729. Disponível em: < https://www.ncbi.nlm.nih.gov/pubmed/22127246 >.

[55] ST PIERRE, B. A.; TIDBALL, J. G. Differential response of macrophage subpopulations to soleus muscle reloading after rat hindlimb suspension. **J Appl Physiol (1985),** v. 77, n. 1, p. 290-7, Jul 1994. ISSN 8750-7587. Disponível em: < https://www.ncbi.nlm.nih.gov/pubmed/7961247 >.

[56] MILLER, K. J. et al. Hepatocyte growth factor affects satellite cell activation and differentiation in regenerating skeletal muscle. **Am J Physiol Cell Physiol,** v. 278, n. 1, p. C174-81, Jan 2000. ISSN 0363-6143. Disponível em: < https://www.ncbi.nlm.nih.gov/pubmed/10644525 >.

[57] CHRISTOV, C. et al. Muscle satellite cells and endothelial cells: close neighbors and privileged partners. **Mol Biol Cell,** v. 18, n. 4, p. 1397-409, Apr 2007. ISSN 1059-1524. Disponível em: < https://www.ncbi.nlm.nih.gov/pubmed/17287398 >.

[58] SCHULTZ, E.; JARYSZAK, D. L.; VALLIERE, C. R. Response of satellite cells to focal skeletal muscle injury. **Muscle Nerve,** v. 8, n. 3, p. 217-22, 1985 Mar-Apr 1985. ISSN 0148-639X. Disponível em: < https://www.ncbi.nlm.nih.gov/pubmed/4058466 >.

[59] ZHANG, F. et al. P53 and Parkin co-regulate mitophagy in bone marrow mesenchymal stem cells to promote the repair of early steroid-induced osteonecrosis of the femoral head. **Cell Death Dis,** v. 11, n. 1, p. 42, Jan 2020. ISSN 2041-4889. Disponível em: < https://www.ncbi.nlm.nih.gov/pubmed/31959744 >.

[60] AHLQVIST, K. J.; SUOMALAINEN, A.; HÄMÄLÄINEN, R. H. Stem cells, mitochondria and aging. **Biochim Biophys Acta,** v. 1847, n. 11, p. 1380-6, Nov 2015. ISSN 0006-3002. Disponível em: < https://www.ncbi.nlm.nih.gov/pubmed/26014347 >.

[61] SU, Y. et al. Fate decision of satellite cell differentiation and self-renewal by miR-31-IL34 axis. **Cell Death Differ,** v. 27, n. 3, p. 949-965, Mar 2020. ISSN 1476-5403. Disponível em: < https://www.ncbi.nlm.nih.gov/pubmed/31332295 >.

62 ZHANG, H.; MENZIES, K. J.; AUWERX, J. The role of mitochondria in stem cell fate and aging. **Development,** v. 145, n. 8, 04 2018. ISSN 1477-9129. Disponível em: < https://www.ncbi.nlm.nih.gov/pubmed/29654217 >.

63 MOTOHASHI, N.; ASAKURA, A. Molecular Regulation of Muscle Satellite Cell Self-Renewal. **J Stem Cell Res Ther,** v. Suppl 11, Nov 2012. ISSN 2157-7633. Disponível em: < https://www.ncbi.nlm.nih.gov/pubmed/24524010 >.

64 KATAJISTO, P. et al. Stem cells. Asymmetric apportioning of aged mitochondria between daughter cells is required for stemness. **Science,** v. 348, n. 6232, p. 340-3, Apr 2015. ISSN 1095-9203. Disponível em: < https://www.ncbi.nlm.nih.gov/pubmed/25837514 >.

65 ONO, Y. et al. Slow-dividing satellite cells retain long-term self-renewal ability in adult muscle. **J Cell Sci,** v. 125, n. Pt 5, p. 1309-17, Mar 2012. ISSN 1477-9137. Disponível em: < https://www.ncbi.nlm.nih.gov/pubmed/22349695 >.

66 LEPPER, C.; CONWAY, S. J.; FAN, C. M. Adult satellite cells and embryonic muscle progenitors have distinct genetic requirements. **Nature,** v. 460, n. 7255, p. 627-31, Jul 2009. ISSN 1476-4687. Disponível em: < https://www.ncbi.nlm.nih.gov/pubmed/19554048 >.

67 GAYRAUD-MOREL, B. et al. Myf5 haploinsufficiency reveals distinct cell fate potentials for adult skeletal muscle stem cells. **J Cell Sci,** v. 125, n. Pt 7, p. 1738-49, Apr 2012. ISSN 1477-9137. Disponível em: < https://www.ncbi.nlm.nih.gov/pubmed/22366456 >.

68 YOSHIDA, N. et al. Cell heterogeneity upon myogenic differentiation: down-regulation of MyoD and Myf-5 generates 'reserve cells'. **J Cell Sci,** v. 111 (Pt 6), p. 769-79, Mar 1998. ISSN 0021-9533. Disponível em: < https://www.ncbi.nlm.nih.gov/pubmed/9472005 >.

69 JONES, N. C. et al. The p38alpha/beta MAPK functions as a molecular switch to activate the quiescent satellite cell. **J Cell Biol,** v. 169, n. 1, p. 105-16, Apr 2005. ISSN 0021-9525. Disponível em: < https://www.ncbi.nlm.nih.gov/pubmed/15824134 >.

70 LE GRAND, F. et al. Wnt7a activates the planar cell polarity pathway to drive the symmetric expansion of satellite stem cells. **Cell Stem Cell,** v. 4, n. 6, p. 535-47, Jun 2009. ISSN 1875-9777. Disponível em: < https://www.ncbi.nlm.nih.gov/pubmed/19497282 >.

71 DUMONT, N. A.; WANG, Y. X.; RUDNICKI, M. A. Intrinsic and extrinsic mechanisms regulating satellite cell function. **Development,** v. 142, n. 9, p. 1572-81, May 2015. ISSN 1477-9129. Disponível em: < https://www.ncbi.nlm.nih.gov/pubmed/25922523 >.

72 KAWABE, Y. et al. Carm1 regulates Pax7 transcriptional activity through MLL1/2 recruitment during asymmetric satellite stem cell divisions. **Cell Stem Cell,** v. 11, n. 3, p. 333-45, Sep 2012. ISSN 1875-9777. Disponível em: < https://www.ncbi.nlm.nih.gov/pubmed/22863532 >.

73 TROY, A. et al. Coordination of satellite cell activation and self-renewal by Par-complex-dependent asymmetric activation of p38α/β MAPK. **Cell Stem Cell,** v. 11, n.

4, p. 541-53, Oct 2012. ISSN 1875-9777. Disponível em: < https://www.ncbi.nlm.nih.gov/pubmed/23040480 >.

74 EVANO, B. et al. Dynamics of Asymmetric and Symmetric Divisions of Muscle Stem Cells In Vivo and on Artificial Niches. **Cell Rep,** v. 30, n. 10, p. 3195-3206.e7, 03 2020. ISSN 2211-1247. Disponível em: < https://www.ncbi.nlm.nih.gov/pubmed/32160529 >.

75 LAAPER, M.; JAHANI-ASL, A. Regulation of neural stem cell fate decisions by mitochondrial dynamics. **Neural Regen Res,** v. 13, n. 9, p. 1548-1549, Sep 2018. ISSN 1673-5374. Disponível em: < https://www.ncbi.nlm.nih.gov/pubmed/30127113 >.

76 ITO, K. Metabolism and the Control of Cell Fate Decisions and Stem Cell Renewal. **Annu Rev Cell Dev Biol,** v. 32, p. 399-409, 10 2016. ISSN 1530-8995. Disponível em: < https://www.ncbi.nlm.nih.gov/pubmed/27482603 >.

77 OLGUIN, H. C. et al. Reciprocal inhibition between Pax7 and muscle regulatory factors modulates myogenic cell fate determination. **J Cell Biol,** v. 177, n. 5, p. 769-79, Jun 2007. ISSN 0021-9525. Disponível em: < https://www.ncbi.nlm.nih.gov/pubmed/17548510 >.

78 ONO, Y. et al. Muscle stem cell fate is controlled by the cell-polarity protein Scrib. **Cell Rep,** v. 10, n. 7, p. 1135-48, Feb 2015. ISSN 2211-1247. Disponível em: < https://www.ncbi.nlm.nih.gov/pubmed/25704816 >.

79 FOCHI, S. et al. Regulation of microRNAs in Satellite Cell Renewal, Muscle Function, Sarcopenia and the Role of Exercise. **Int J Mol Sci,** v. 21, n. 18, Sep 2020. ISSN 1422-0067. Disponível em: < https://www.ncbi.nlm.nih.gov/pubmed/32937893 >.

80 SHI, X.; GARRY, D. J. Muscle stem cells in development, regeneration, and disease. **Genes Dev,** v. 20, n. 13, p. 1692-708, Jul 2006. ISSN 0890-9369. Disponível em: < https://www.ncbi.nlm.nih.gov/pubmed/16818602 >.

81 GARRY, D. J. et al. Persistent expression of MNF identifies myogenic stem cells in postnatal muscles. **Dev Biol,** v. 188, n. 2, p. 280-94, Aug 1997. ISSN 0012-1606. Disponível em: < https://www.ncbi.nlm.nih.gov/pubmed/9268575 >.

82 THERET, M. et al. AMPKα1-LDH pathway regulates muscle stem cell self-renewal by controlling metabolic homeostasis. **EMBO J,** v. 36, n. 13, p. 1946-1962, 07 2017. ISSN 1460-2075. Disponível em: < https://www.ncbi.nlm.nih.gov/pubmed/28515121 >.

83 DING, W. X.; YIN, X. M. Mitophagy: mechanisms, pathophysiological roles, and analysis. **Biol Chem,** v. 393, n. 7, p. 547-64, Jul 2012. ISSN 1437-4315. Disponível em: < https://www.ncbi.nlm.nih.gov/pubmed/22944659 >.

84 KHACHO, M. et al. Mitochondrial Dynamics Impacts Stem Cell Identity and Fate Decisions by Regulating a Nuclear Transcriptional Program. **Cell Stem Cell,** v. 19, n. 2, p. 232-247, 08 2016. ISSN 1875-9777. Disponível em: < https://www.ncbi.nlm.nih.gov/pubmed/27237737 >.

85 KHACHO, M.; SLACK, R. S. Mitochondrial and Reactive Oxygen Species Signaling Coordinate Stem Cell Fate Decisions and Life Long Maintenance. **Antioxid Redox**

Signal, Jul 2017. ISSN 1557-7716. Disponível em: < https://www.ncbi.nlm.nih.gov/pubmed/28657337 >.

86 FORNI, M. F. et al. Murine Mesenchymal Stem Cell Commitment to Differentiation Is Regulated by Mitochondrial Dynamics. **Stem Cells,** v. 34, n. 3, p. 743-55, Mar 2016. ISSN 1549-4918. Disponível em: < https://www.ncbi.nlm.nih.gov/pubmed/26638184 >.

87 PAPA, L.; DJEDAINI, M.; HOFFMAN, R. Mitochondrial Role in Stemness and Differentiation of Hematopoietic Stem Cells. **Stem Cells Int,** v. 2019, p. 4067162, 2019. ISSN 1687-966X. Disponível em: < https://www.ncbi.nlm.nih.gov/pubmed/30881461 >.

88 SEO, B. J.; YOON, S. H.; DO, J. T. Mitochondrial Dynamics in Stem Cells and Differentiation. **Int J Mol Sci,** v. 19, n. 12, Dec 2018. ISSN 1422-0067. Disponível em: < https://www.ncbi.nlm.nih.gov/pubmed/30563106 >.

89 FU, W.; LIU, Y.; YIN, H. Mitochondrial Dynamics: Biogenesis, Fission, Fusion, and Mitophagy in the Regulation of Stem Cell Behaviors. **Stem Cells Int,** v. 2019, p. 9757201, 2019. ISSN 1687-966X. Disponível em: < https://www.ncbi.nlm.nih.gov/pubmed/31089338 >.

90 BHATTACHARYA, D.; SCIMÈ, A. Mitochondrial Function in Muscle Stem Cell Fates. **Front Cell Dev Biol,** v. 8, p. 480, 2020. ISSN 2296-634X. Disponível em: < https://www.ncbi.nlm.nih.gov/pubmed/32612995 >.

91 ZHONG, X. et al. Mitochondrial Dynamics Is Critical for the Full Pluripotency and Embryonic Developmental Potential of Pluripotent Stem Cells. **Cell Metab,** v. 29, n. 4, p. 979-992.e4, 04 2019. ISSN 1932-7420. Disponível em: < https://www.ncbi.nlm.nih.gov/pubmed/30527743 >.

92 LISOWSKI, P. et al. Mitochondria and the dynamic control of stem cell homeostasis. **EMBO Rep,** v. 19, n. 5, 05 2018. ISSN 1469-3178. Disponível em: < https://www.ncbi.nlm.nih.gov/pubmed/29661859 >.

93 SEO, N. H. et al. HSP60 is required for stemness and proper differentiation of mouse embryonic stem cells. **Exp Mol Med,** v. 50, n. 3, p. e459, 03 2018. ISSN 2092-6413. Disponível em: < https://www.ncbi.nlm.nih.gov/pubmed/29546877 >.

94 CHEN, C. T. et al. Coordinated changes of mitochondrial biogenesis and antioxidant enzymes during osteogenic differentiation of human mesenchymal stem cells. **Stem Cells,** v. 26, n. 4, p. 960-8, Apr 2008. ISSN 1549-4918. Disponível em: < https://www.ncbi.nlm.nih.gov/pubmed/18218821 >.

95 MATTES, K.; VELLENGA, E.; SCHEPERS, H. Differential redox-regulation and mitochondrial dynamics in normal and leukemic hematopoietic stem cells: A potential window for leukemia therapy. **Crit Rev Oncol Hematol,** v. 144, p. 102814, Dec 2019. ISSN 1879-0461. Disponível em: < https://www.ncbi.nlm.nih.gov/pubmed/31593878 >.

96 LI, Q. et al. The role of mitochondria in osteogenic, adipogenic and chondrogenic differentiation of mesenchymal stem cells. **Protein Cell,** v. 8, n. 6, p. 439-445, 06 2017. ISSN 1674-8018. Disponível em: < https://www.ncbi.nlm.nih.gov/pubmed/28271444 >.

[97] BECKERVORDERSANDFORTH, R. et al. Role of Mitochondrial Metabolism in the Control of Early Lineage Progression and Aging Phenotypes in Adult Hippocampal Neurogenesis. **Neuron,** v. 93, n. 3, p. 560-573.e6, Feb 2017. ISSN 1097-4199. Disponível em: < https://www.ncbi.nlm.nih.gov/pubmed/28111078 >.

[98] LUCHSINGER, L. L. et al. Mitofusin 2 maintains haematopoietic stem cells with extensive lymphoid potential. **Nature,** v. 529, n. 7587, p. 528-31, Jan 2016. ISSN 1476-4687. Disponível em: < https://www.ncbi.nlm.nih.gov/pubmed/26789249 >.

[99] JANG, Y. Y.; SHARKIS, S. J. A low level of reactive oxygen species selects for primitive hematopoietic stem cells that may reside in the low-oxygenic niche. **Blood,** v. 110, n. 8, p. 3056-63, Oct 2007. ISSN 0006-4971. Disponível em: < https://www.ncbi.nlm.nih.gov/pubmed/17595331 >.

[100] HÄMÄLÄINEN, R. H. et al. mtDNA Mutagenesis Disrupts Pluripotent Stem Cell Function by Altering Redox Signaling. **Cell Rep,** v. 11, n. 10, p. 1614-24, Jun 2015. ISSN 2211-1247. Disponível em: < https://www.ncbi.nlm.nih.gov/pubmed/26027936 >.

[101] SON, Y. W. et al. Prx2 links ROS homeostasis to stemness of cancer stem cells. **Free Radic Biol Med,** v. 134, p. 260-267, 04 2019. ISSN 1873-4596. Disponível em: < https://www.ncbi.nlm.nih.gov/pubmed/30611866 >.

[102] ROUAULT-PIERRE, K. et al. HIF-2α protects human hematopoietic stem/progenitors and acute myeloid leukemic cells from apoptosis induced by endoplasmic reticulum stress. **Cell Stem Cell,** v. 13, n. 5, p. 549-63, Nov 2013. ISSN 1875-9777. Disponível em: < https://www.ncbi.nlm.nih.gov/pubmed/24095676 >.

[103] MANDAL, S. et al. Mitochondrial function controls proliferation and early differentiation potential of embryonic stem cells. **Stem Cells,** v. 29, n. 3, p. 486-95, Mar 2011. ISSN 1549-4918. Disponível em: < https://www.ncbi.nlm.nih.gov/pubmed/21425411 >.

[104] KHACHO, M.; SLACK, R. S. Mitochondrial activity in the regulation of stem cell self-renewal and differentiation. **Curr Opin Cell Biol,** v. 49, p. 1-8, 12 2017. ISSN 1879-0410. Disponível em: < https://www.ncbi.nlm.nih.gov/pubmed/29175320 >.

[105] MARYANOVICH, M. et al. An MTCH2 pathway repressing mitochondria metabolism regulates haematopoietic stem cell fate. **Nat Commun,** v. 6, p. 7901, Jul 2015. ISSN 2041-1723. Disponível em: < https://www.ncbi.nlm.nih.gov/pubmed/26219591 >.

[106] VANNINI, N. et al. Specification of haematopoietic stem cell fate via modulation of mitochondrial activity. **Nat Commun,** v. 7, p. 13125, 10 2016. ISSN 2041-1723. Disponível em: < https://www.ncbi.nlm.nih.gov/pubmed/27731316 >.

[107] ZHANG, H. et al. NAD^+ repletion improves mitochondrial and stem cell function and enhances life span in mice. **Science,** v. 352, n. 6292, p. 1436-43, Jun 2016. ISSN 1095-9203. Disponível em: < https://www.ncbi.nlm.nih.gov/pubmed/27127236 >.

[108] JOSHI, A.; KUNDU, M. Mitophagy in hematopoietic stem cells: the case for exploration. **Autophagy,** v. 9, n. 11, p. 1737-49, Nov 2013. ISSN 1554-8635. Disponível em: < https://www.ncbi.nlm.nih.gov/pubmed/24135495 >.

[109] MENDIVIL-PEREZ, M. et al. Melatonin enhances neural stem cell differentiation and engraftment by increasing mitochondrial function. **J Pineal Res,** v. 63, n. 2, Sep 2017. ISSN 1600-079X. Disponível em: < https://www.ncbi.nlm.nih.gov/pubmed/28423196 >.

[110] WANG, L. et al. Fatty acid synthesis is critical for stem cell pluripotency via promoting mitochondrial fission. **EMBO J,** v. 36, n. 10, p. 1330-1347, 05 2017. ISSN 1460-2075. Disponível em: < https://www.ncbi.nlm.nih.gov/pubmed/28377463 >.

[111] BAHAT, A.; GROSS, A. Mitochondrial plasticity in cell fate regulation. **J Biol Chem,** v. 294, n. 38, p. 13852-13863, 09 2019. ISSN 1083-351X. Disponível em: < https://www.ncbi.nlm.nih.gov/pubmed/31383739 >.

[112] TSOGTBAATAR, E. et al. Energy Metabolism Regulates Stem Cell Pluripotency. **Front Cell Dev Biol,** v. 8, p. 87, 2020. ISSN 2296-634X. Disponível em: < https://www.ncbi.nlm.nih.gov/pubmed/32181250 >.

[113] KNOBLOCH, M. et al. A Fatty Acid Oxidation-Dependent Metabolic Shift Regulates Adult Neural Stem Cell Activity. **Cell Rep,** v. 20, n. 9, p. 2144-2155, Aug 2017. ISSN 2211-1247. Disponível em: < https://www.ncbi.nlm.nih.gov/pubmed/28854364 >.

[114] UMEMOTO, T. et al. Ca. **J Exp Med,** v. 215, n. 8, p. 2097-2113, 08 2018. ISSN 1540-9538. Disponível em: < https://www.ncbi.nlm.nih.gov/pubmed/29946000 >.

[115] ITO, K. Hematopoietic stem cell fate through metabolic control. **Exp Hematol,** v. 64, p. 1-11, 08 2018. ISSN 1873-2399. Disponível em: < https://www.ncbi.nlm.nih.gov/pubmed/29807063 >.

[116] KIM, I.; RODRIGUEZ-ENRIQUEZ, S.; LEMASTERS, J. J. Selective degradation of mitochondria by mitophagy. **Arch Biochem Biophys,** v. 462, n. 2, p. 245-53, Jun 2007. ISSN 0003-9861. Disponível em: < https://www.ncbi.nlm.nih.gov/pubmed/17475204 >.

[117] LEMASTERS, J. J. Selective mitochondrial autophagy, or mitophagy, as a targeted defense against oxidative stress, mitochondrial dysfunction, and aging. **Rejuvenation Res,** v. 8, n. 1, p. 3-5, 2005. ISSN 1549-1684. Disponível em: < https://www.ncbi.nlm.nih.gov/pubmed/15798367 >.

[118] LEMASTERS, J. J. et al. The mitochondrial permeability transition in cell death: a common mechanism in necrosis, apoptosis and autophagy. **Biochim Biophys Acta,** v. 1366, n. 1-2, p. 177-96, Aug 1998. ISSN 0006-3002. Disponível em: < https://www.ncbi.nlm.nih.gov/pubmed/9714796 >.

[119] MCWILLIAMS, T. G. et al. mito-QC illuminates mitophagy and mitochondrial architecture in vivo. **J Cell Biol,** v. 214, n. 3, p. 333-45, 08 2016. ISSN 1540-8140. Disponível em: < https://www.ncbi.nlm.nih.gov/pubmed/27458135 >.

[120] GARCÍA-PRAT, L.; MARTÍNEZ-VICENTE, M.; MUÑOZ-CÁNOVES, P. Methods for Mitochondria and Mitophagy Flux Analyses in Stem Cells of Resting and Regenerating Skeletal Muscle. **Methods Mol Biol,** v. 1460, p. 223-40, 2016. ISSN 1940-6029. Disponível em: < https://www.ncbi.nlm.nih.gov/pubmed/27492176 >.

121 HE, Y.-L. et al. BNIP3 phosphorylation by JNK1/2 promotes mitophagy via enhancing its stability under hypoxia. **bioRxiv**, 2020.

122 RODGER, C. E.; MCWILLIAMS, T. G.; GANLEY, I. G. Mammalian mitophagy - from in vitro molecules to in vivo models. **FEBS J,** v. 285, n. 7, p. 1185-1202, 04 2018. ISSN 1742-4658. Disponível em: < https://www.ncbi.nlm.nih.gov/pubmed/29151277 >.

123 CHEN, G.; KROEMER, G.; KEPP, O. Mitophagy: An Emerging Role in Aging and Age-Associated Diseases. **Front Cell Dev Biol,** v. 8, p. 200, 2020. ISSN 2296-634X. Disponível em: < https://www.ncbi.nlm.nih.gov/pubmed/32274386 >.

124 KILLACKEY, S. A.; PHILPOTT, D. J.; GIRARDIN, S. E. Mitophagy pathways in health and disease. **J Cell Biol,** v. 219, n. 11, Nov 2020. ISSN 1540-8140. Disponível em: < https://www.ncbi.nlm.nih.gov/pubmed/32926082 >.

125 GISPERT, S. et al. Rodent Models of Autosomal Recessive Parkinson Disease. In: (Ed.). **Movement Disorders: Genetics and Models**. 2nd, 2015. cap. 19, p.Pages 329-343.

126 IMAI, Y.; HATTORI, N. Autophagy: Cancer, Other Pathologies, Inflammation, Immunity, Infection, and Aging. Volume 4: Mitophagy. Chapter 15 - Mitophagy Controlled by the PINK1-Parkin Pathway Is Associated with Parkinson's Disease Pathogenesis. In: (Ed.). **Title: Autophagy: Cancer, Other Pathologies, Inflammation, Immunity, Infection, and Aging.** , v.4, 2014. cap. 15, p.Pages 227-238.

127 CEBRIÁN, C.; SULZER, D. I. **Parkinson's DiseaseMolecular Mechanisms Underlying Pathology: Chapter 8 - Neuroinflammation as a Potential Mechanism Underlying Parkinsons Disease**. 2017.

128 WANG, Y. et al. PINK1/Parkin-mediated mitophagy is activated in cisplatin nephrotoxicity to protect against kidney injury. **Cell Death Dis,** v. 9, n. 11, p. 1113, Nov 2018. ISSN 2041-4889. Disponível em: < https://www.ncbi.nlm.nih.gov/pubmed/30385753 >.

129 GE, P.; DAWSON, V. L.; DAWSON, T. M. PINK1 and Parkin mitochondrial quality control: a source of regional vulnerability in Parkinson's disease. **Mol Neurodegener,** v. 15, n. 1, p. 20, 03 2020. ISSN 1750-1326. Disponível em: < https://www.ncbi.nlm.nih.gov/pubmed/32169097 >.

130 KING, L.; PLUN-FAVREAU, H. **Parkinson's DiseaseMolecular Mechanisms Underlying Pathology: Chapter 5 - Mitophagy:** Pages 139-177 p. 2017.

131 CAIRNS, G. et al. Mitophagy: A New Player in Stem Cell Biology. **MDPI,** v. 9, p. 481, 2020.

132 SHAMCHUK, A. L.; TIERNEY, K. B. The Importance of Olfactory and Motor Endpoints for Zebrafish Models of Neurodegenerative Disease. In: (Ed.). **Animal Models for the Study of Human Disease.** , 2013. p.651-678.

133 WANG, H. L. et al. PARK6 PINK1 mutants are defective in maintaining mitochondrial membrane potential and inhibiting ROS formation of substantia nigra dopaminergic

neurons. **Biochim Biophys Acta,** v. 1812, n. 6, p. 674-84, Jun 2011. ISSN 0006-3002. Disponível em: < https://www.ncbi.nlm.nih.gov/pubmed/21421046 >.

134 BRUN, C. E.; WANG, Y. X.; RUDNICKI, M. A. Single EDL Myofiber Isolation for Analyses of Quiescent and Activated Muscle Stem Cells. **Methods Mol Biol,** v. 1686, p. 149-159, 2018. ISSN 1940-6029. Disponível em: < https://www.ncbi.nlm.nih.gov/pubmed/29030819 >.

135 PARGANLIJA, D. et al. Loss of PINK1 impairs stress-induced autophagy and cell survival. **PLoS One,** v. 9, n. 4, p. e95288, 2014. ISSN 1932-6203. Disponível em: < https://www.ncbi.nlm.nih.gov/pubmed/24751806 >.

136 GAO, A. et al. Bnip3 in mitophagy: Novel insights and potential therapeutic target for diseases of secondary mitochondrial dysfunction. **Clin Chim Acta,** v. 506, p. 72-83, Jul 2020. ISSN 1873-3492. Disponível em: < https://www.ncbi.nlm.nih.gov/pubmed/32092316 >.

137 WU, H.; CHEN, Q. Hypoxia activation of mitophagy and its role in disease pathogenesis. **Antioxid Redox Signal,** v. 22, n. 12, p. 1032-46, Apr 2015. ISSN 1557-7716. Disponível em: < https://www.ncbi.nlm.nih.gov/pubmed/25526784 >.

138 PEI, S. et al. AMPK/FIS1-Mediated Mitophagy Is Required for Self-Renewal of Human AML Stem Cells. **Cell Stem Cell,** v. 23, n. 1, p. 86-100.e6, Jul 2018. ISSN 1875-9777. Disponível em: < https://www.ncbi.nlm.nih.gov/pubmed/29910151 >.

139 GARCÍA-PRAT, L. et al. Autophagy maintains stemness by preventing senescence. **Nature,** v. 529, n. 7584, p. 37-42, Jan 2016. ISSN 1476-4687. Disponível em: < https://www.ncbi.nlm.nih.gov/pubmed/26738589 >.

140 GARCÍA-PRAT, L.; SOUSA-VICTOR, P.; MUÑOZ-CÁNOVES, P. Functional dysregulation of stem cells during aging: a focus on skeletal muscle stem cells. **FEBS J,** v. 280, n. 17, p. 4051-62, Sep 2013. ISSN 1742-4658. Disponível em: < https://www.ncbi.nlm.nih.gov/pubmed/23452120 >.

141 MOHIUDDIN, M. et al. Critical Limb Ischemia Induces Remodeling of Skeletal Muscle Motor Unit, Myonuclear-, and Mitochondrial-Domains. **Sci Rep,** v. 9, n. 1, p. 9551, 07 2019. ISSN 2045-2322. Disponível em: < https://www.ncbi.nlm.nih.gov/pubmed/31266969 >.

142 NAIK, P. P.; BIRBRAIR, A.; BHUTIA, S. K. Mitophagy-driven metabolic switch reprograms stem cell fate. **Cell Mol Life Sci,** v. 76, n. 1, p. 27-43, Jan 2019. ISSN 1420-9071. Disponível em: < https://www.ncbi.nlm.nih.gov/pubmed/30267101 >.

143 VAZQUEZ-MARTIN, A. et al. Mitophagy-driven mitochondrial rejuvenation regulates stem cell fate. **Aging (Albany NY),** v. 8, n. 7, p. 1330-52, 07 2016. ISSN 1945-4589. Disponível em: < https://www.ncbi.nlm.nih.gov/pubmed/27295498 >.

144 ITO, K. et al. Self-renewal of a purified Tie2+ hematopoietic stem cell population relies on mitochondrial clearance. **Science,** v. 354, n. 6316, p. 1156-1160, 12 2016. ISSN 1095-9203. Disponível em: < https://www.ncbi.nlm.nih.gov/pubmed/27738012 >.

145 KUHIKAR, R. et al. Transforming growth factor β1 accelerates and enhances in vitro red blood cell formation from hematopoietic stem cells by stimulating mitophagy. **Stem**

Cell Res Ther, v. 11, n. 1, p. 71, Feb 2020. ISSN 1757-6512. Disponível em: < https://www.ncbi.nlm.nih.gov/pubmed/32075694 >.

146 ZHU, W. et al. Mesenchymal stem cells ameliorate hyperglycemia-induced endothelial injury through modulation of mitophagy. **Cell Death Dis,** v. 9, n. 8, p. 837, 08 2018. ISSN 2041-4889. Disponível em: < https://www.ncbi.nlm.nih.gov/pubmed/30082798 >.

147 FENG, J. et al. SIRT3 Facilitates Amniotic Fluid Stem Cells to Repair Diabetic Nephropathy Through Protecting Mitochondrial Homeostasis by Modulation of Mitophagy. **Cell Physiol Biochem,** v. 46, n. 4, p. 1508-1524, 2018. ISSN 1421-9778. Disponível em: < https://www.ncbi.nlm.nih.gov/pubmed/29689547 >.

148 YOON, Y. M. et al. Melatonin Enhances Mitophagy by Upregulating Expression of Heat Shock 70 kDa Protein 1L in Human Mesenchymal Stem Cells under Oxidative Stress. **Int J Mol Sci,** v. 20, n. 18, Sep 2019. ISSN 1422-0067. Disponível em: < https://www.ncbi.nlm.nih.gov/pubmed/31540288 >.

149 JIN, G. et al. Atad3a suppresses Pink1-dependent mitophagy to maintain homeostasis of hematopoietic progenitor cells. **Nat Immunol,** v. 19, n. 1, p. 29-40, Jan 2018. ISSN 1529-2916. Disponível em: < https://www.ncbi.nlm.nih.gov/pubmed/29242539 >.

150 YIN, F. et al. Bone marrow mesenchymal stem cells repair Cr (VI)- injured kidney by regulating mitochondria-mediated apoptosis and mitophagy mediated via the MAPK signaling pathway. **Ecotoxicol Environ Saf,** v. 176, p. 234-241, Jul 2019. ISSN 1090-2414. Disponível em: < https://www.ncbi.nlm.nih.gov/pubmed/30939403 >.

151 MURPHY, M. M. et al. Satellite cells, connective tissue fibroblasts and their interactions are crucial for muscle regeneration. **Development,** v. 138, n. 17, p. 3625-37, Sep 2011. ISSN 1477-9129. Disponível em: < https://www.ncbi.nlm.nih.gov/pubmed/21828091 >.

152 PARISE, G.; MCKINNELL, I. W.; RUDNICKI, M. A. Muscle satellite cell and atypical myogenic progenitor response following exercise. **Muscle Nerve,** v. 37, n. 5, p. 611-9, May 2008. ISSN 0148-639X. Disponível em: < https://www.ncbi.nlm.nih.gov/pubmed/18351585 >.

153 LIM, C. L.; LING, K. H.; CHEAH, P. S. Isolation, cultivation and immunostaining of single myofibers: An improved approach to study the behavior of satellite cells. **J Biol Methods,** v. 5, n. 1, p. e87, 2018. ISSN 2326-9901. Disponível em: < https://www.ncbi.nlm.nih.gov/pubmed/31453240 >.

154 PASUT, A.; JONES, A. E.; RUDNICKI, M. A. Isolation and culture of individual myofibers and their satellite cells from adult skeletal muscle. **J Vis Exp**, n. 73, p. e50074, Mar 2013. ISSN 1940-087X. Disponível em: < https://www.ncbi.nlm.nih.gov/pubmed/23542587 >.

155 SINCENNES, M. C.; WANG, Y. X.; RUDNICKI, M. A. Primary Mouse Myoblast Purification using Magnetic Cell Separation. **Methods Mol Biol,** v. 1556, p. 41-50, 2017. ISSN 1940-6029. Disponível em: < https://www.ncbi.nlm.nih.gov/pubmed/28247344 >.

156 MACHADO, L. et al. In Situ Fixation Redefines Quiescence and Early Activation of Skeletal Muscle Stem Cells. **Cell Rep,** v. 21, n. 7, p. 1982-1993, Nov 2017. ISSN 2211-1247. Disponível em: < https://www.ncbi.nlm.nih.gov/pubmed/29141227 >.

157 ROSS, J. M. Visualization of mitochondrial respiratory function using cytochrome c oxidase/succinate dehydrogenase (COX/SDH) double-labeling histochemistry. **J Vis Exp**, n. 57, p. e3266, Nov 2011. ISSN 1940-087X. Disponível em: < https://www.ncbi.nlm.nih.gov/pubmed/22143245 >.

158 DE PAEPE, B.; DE BLEECKER, J. L.; VAN COSTER, R. Histochemical methods for the diagnosis of mitochondrial diseases. **Curr Protoc Hum Genet,** v. Chapter 19, p. Unit19.2, Oct 2009. ISSN 1934-8258. Disponível em: < https://www.ncbi.nlm.nih.gov/pubmed/19806589 >.

159 LIU, L. et al. Chromatin modifications as determinants of muscle stem cell quiescence and chronological aging. **Cell Rep,** v. 4, n. 1, p. 189-204, Jul 2013. ISSN 2211-1247. Disponível em: < https://www.ncbi.nlm.nih.gov/pubmed/23810552 >.

160 MCWILLIAMS, T. G.; GANLEY, I. G. Investigating Mitophagy and Mitochondrial Morphology In Vivo Using mito-QC: A Comprehensive Guide. **Methods Mol Biol,** v. 1880, p. 621-642, 2019. ISSN 1940-6029. Disponível em: < https://www.ncbi.nlm.nih.gov/pubmed/30610727 >.

161 GUARDIOLA, O. et al. Induction of Acute Skeletal Muscle Regeneration by Cardiotoxin Injection. **J Vis Exp**, n. 119, 01 2017. ISSN 1940-087X. Disponível em: < https://www.ncbi.nlm.nih.gov/pubmed/28117768 >.

162 CHANG, C. C. et al. Role of cardiotoxin and phospholipase A in the blockade of nerve conduction and depolarization of skeletal muscle induced by cobra venom. **Br J Pharmacol,** v. 44, n. 4, p. 752-64, Apr 1972. ISSN 0007-1188. Disponível em: < https://www.ncbi.nlm.nih.gov/pubmed/5041453 >.

163 VINCOW, E. S. et al. The PINK1-Parkin pathway promotes both mitophagy and selective respiratory chain turnover in vivo. **Proc Natl Acad Sci U S A,** v. 110, n. 16, p. 6400-5, Apr 2013. ISSN 1091-6490. Disponível em: < https://www.ncbi.nlm.nih.gov/pubmed/23509287 >.

164 KUBLI, D. A. et al. PINK1 Is Dispensable for Mitochondrial Recruitment of Parkin and Activation of Mitophagy in Cardiac Myocytes. **PLoS One,** v. 10, n. 6, p. e0130707, 2015. ISSN 1932-6203. Disponível em: < https://www.ncbi.nlm.nih.gov/pubmed/26110811 >.

165 KOENTJORO, B.; PARK, J. S.; SUE, C. M. Nix restores mitophagy and mitochondrial function to protect against PINK1/Parkin-related Parkinson's disease. **Sci Rep,** v. 7, p. 44373, 03 2017. ISSN 2045-2322. Disponível em: < https://www.ncbi.nlm.nih.gov/pubmed/28281653 >.

166 CHOI, G. E. et al. BNIP3L/NIX-mediated mitophagy protects against glucocorticoid-induced synapse defects. **Nat Commun,** v. 12, n. 1, p. 487, 01 2021. ISSN 2041-1723. Disponível em: < https://www.ncbi.nlm.nih.gov/pubmed/33473105 >.

167 PARK, S. Y.; KOH, H. C. FUNDC1 regulates receptor-mediated mitophagy independently of the PINK1/Parkin-dependent pathway in rotenone-treated SH-SY5Y

cells. **Food Chem Toxicol,** v. 137, p. 111163, Mar 2020. ISSN 1873-6351. Disponível em: < https://www.ncbi.nlm.nih.gov/pubmed/32001317 >.

168 SCHMIDT, M. et al. Adult stem cells at work: regenerating skeletal muscle. **Cell Mol Life Sci,** v. 76, n. 13, p. 2559-2570, Jul 2019. ISSN 1420-9071. Disponível em: < https://www.ncbi.nlm.nih.gov/pubmed/30976839 >.

169 CRUCIANI, S. et al. Orchestrating stem cell fate: Novel tools for regenerative medicine. **World J Stem Cells,** v. 11, n. 8, p. 464-475, Aug 2019. ISSN 1948-0210. Disponível em: < https://www.ncbi.nlm.nih.gov/pubmed/31523367 >.

170 CHANG, N. C.; CHEVALIER, F. P.; RUDNICKI, M. A. Satellite Cells in Muscular Dystrophy - Lost in Polarity. **Trends Mol Med,** v. 22, n. 6, p. 479-496, 06 2016. ISSN 1471-499X. Disponível em: < https://www.ncbi.nlm.nih.gov/pubmed/27161598 >.

171 MCLELLAND, G. L. et al. Mfn2 ubiquitination by PINK1/parkin gates the p97-dependent release of ER from mitochondria to drive mitophagy. **Elife,** v. 7, 04 2018. ISSN 2050-084X. Disponível em: < https://www.ncbi.nlm.nih.gov/pubmed/29676259 >.

172 ADDICKS, G. C. et al. MLL1 is required for PAX7 expression and satellite cell self-renewal in mice. **Nat Commun,** v. 10, n. 1, p. 4256, 09 2019. ISSN 2041-1723. Disponível em: < https://www.ncbi.nlm.nih.gov/pubmed/31534153 >.

173 WEN, Y. et al. Constitutive Notch activation upregulates Pax7 and promotes the self-renewal of skeletal muscle satellite cells. **Mol Cell Biol,** v. 32, n. 12, p. 2300-11, Jun 2012. ISSN 1098-5549. Disponível em: < https://www.ncbi.nlm.nih.gov/pubmed/22493066 >.

174 YARTSEVA, V. et al. Heterogeneity of Satellite Cells Implicates DELTA1/NOTCH2 Signaling in Self-Renewal. **Cell Rep,** v. 30, n. 5, p. 1491-1503.e6, 02 2020. ISSN 2211-1247. Disponível em: < https://www.ncbi.nlm.nih.gov/pubmed/32023464 >.

175 LALA-TABBERT, N. et al. CCAAT/enhancer binding protein β is required for satellite cell self-renewal. **Skelet Muscle,** v. 6, n. 1, p. 40, 12 2016. ISSN 2044-5040. Disponível em: < https://www.ncbi.nlm.nih.gov/pubmed/27923399 >.

176 VON COELLN, R. et al. Loss of locus coeruleus neurons and reduced startle in parkin null mice. **Proc Natl Acad Sci U S A,** v. 101, n. 29, p. 10744-9, Jul 2004. ISSN 0027-8424. Disponível em: < https://www.ncbi.nlm.nih.gov/pubmed/15249681 >.

177 KITADA, T. et al. Impaired dopamine release and synaptic plasticity in the striatum of PINK1-deficient mice. **Proc Natl Acad Sci U S A,** v. 104, n. 27, p. 11441-6, Jul 2007. ISSN 0027-8424. Disponível em: < https://www.ncbi.nlm.nih.gov/pubmed/17563363 >.

178 MCWILLIAMS, T. G. et al. Basal Mitophagy Occurs Independently of PINK1 in Mouse Tissues of High Metabolic Demand. **Cell Metab,** v. 27, n. 2, p. 439-449.e5, 02 2018. ISSN 1932-7420. Disponível em: < https://www.ncbi.nlm.nih.gov/pubmed/29337137 >.

179 SHIN, J. H. et al. PARIS (ZNF746) repression of PGC-1α contributes to neurodegeneration in Parkinson's disease. **Cell,** v. 144, n. 5, p. 689-702, Mar 2011.

ISSN 1097-4172. Disponível em: < https://www.ncbi.nlm.nih.gov/pubmed/21376232 >.

180 GONG, G. et al. Parkin-mediated mitophagy directs perinatal cardiac metabolic maturation in mice. **Science,** v. 350, n. 6265, p. aad2459, Dec 2015. ISSN 1095-9203. Disponível em: < https://www.ncbi.nlm.nih.gov/pubmed/26785495 >.

181 LIANG, R. et al. Restraining Lysosomal Activity Preserves Hematopoietic Stem Cell Quiescence and Potency. **Cell Stem Cell,** v. 26, n. 3, p. 359-376.e7, 03 2020. ISSN 1875-9777. Disponível em: < https://www.ncbi.nlm.nih.gov/pubmed/32109377 >.

182 VIVES-BAUZA, C. et al. PINK1-dependent recruitment of Parkin to mitochondria in mitophagy. **Proc Natl Acad Sci U S A,** v. 107, n. 1, p. 378-83, Jan 2010. ISSN 1091-6490. Disponível em: < https://www.ncbi.nlm.nih.gov/pubmed/19966284 >.

183 PALA, F. et al. Distinct metabolic states govern skeletal muscle stem cell fates during prenatal and postnatal myogenesis. **J Cell Sci,** v. 131, n. 14, 07 2018. ISSN 1477-9137. Disponível em: < https://www.ncbi.nlm.nih.gov/pubmed/30054310 >.

184 HU, Q. et al. Oxidative stress promotes exit from the stem cell state and spontaneous neuronal differentiation. **Oncotarget,** v. 9, n. 3, p. 4223-4238, Jan 2018. ISSN 1949-2553. Disponível em: < https://www.ncbi.nlm.nih.gov/pubmed/29423117 >.

185 SCHMELTER, M. et al. Embryonic stem cells utilize reactive oxygen species as transducers of mechanical strain-induced cardiovascular differentiation. **FASEB J,** v. 20, n. 8, p. 1182-4, Jun 2006. ISSN 1530-6860. Disponível em: < https://www.ncbi.nlm.nih.gov/pubmed/16636108 >.

186 L'HONORÉ, A. et al. The role of Pitx2 and Pitx3 in muscle stem cells gives new insights into P38α MAP kinase and redox regulation of muscle regeneration. **Elife,** v. 7, 08 2018. ISSN 2050-084X. Disponível em: < https://www.ncbi.nlm.nih.gov/pubmed/30106373 >.

187 MATSUDA, N. et al. PINK1 stabilized by mitochondrial depolarization recruits Parkin to damaged mitochondria and activates latent Parkin for mitophagy. **J Cell Biol,** v. 189, n. 2, p. 211-21, Apr 2010. ISSN 1540-8140. Disponível em: < https://www.ncbi.nlm.nih.gov/pubmed/20404107 >.

188 KURODA, Y. et al. Parkin interacts with Klokin1 for mitochondrial import and maintenance of membrane potential. **Human Molecular Genetics,** v. 21, n. 5, p. 991-1003, 2011. ISSN 0964-6906. Disponível em: < https://doi.org/10.1093/hmg/ddr530 >. Acesso em: 2/11/2021.

189 YANG, B. A. et al. Sestrins regulate age-induced deterioration of muscle stem cell homeostasis. 2020.

190 SEBORI, R. et al. Resveratrol Decreases Oxidative Stress by Restoring Mitophagy and Improves the Pathophysiology of Dystrophin-Deficient. **Oxid Med Cell Longev,** v. 2018, p. 9179270, 2018. ISSN 1942-0994. Disponível em: < https://www.ncbi.nlm.nih.gov/pubmed/30510631 >.

191 SAKELLARIOU, G. K. et al. Mitochondrial ROS regulate oxidative damage and mitophagy but not age-related muscle fiber atrophy. **Sci Rep,** v. 6, p. 33944, Sep 2016.

ISSN 2045-2322. Disponível em: < https://www.ncbi.nlm.nih.gov/pubmed/27681159 >.

192 KURIHARA, Y. et al. Mitophagy plays an essential role in reducing mitochondrial production of reactive oxygen species and mutation of mitochondrial DNA by maintaining mitochondrial quantity and quality in yeast. **J Biol Chem,** v. 287, n. 5, p. 3265-72, Jan 2012. ISSN 1083-351X. Disponível em: < https://www.ncbi.nlm.nih.gov/pubmed/22157017 >.

193 LEEMAN, D. S. et al. Lysosome activation clears aggregates and enhances quiescent neural stem cell activation during aging. **Science,** v. 359, n. 6381, p. 1277-1283, 03 2018. ISSN 1095-9203. Disponível em: < https://www.ncbi.nlm.nih.gov/pubmed/29590078 >.

194 TANG, A. H.; RANDO, T. A. Induction of autophagy supports the bioenergetic demands of quiescent muscle stem cell activation. **EMBO J,** v. 33, n. 23, p. 2782-97, Dec 2014. ISSN 1460-2075. Disponível em: < https://www.ncbi.nlm.nih.gov/pubmed/25316028 >.

195 SIN, J. et al. Mitophagy is required for mitochondrial biogenesis and myogenic differentiation of C2C12 myoblasts. **Autophagy,** v. 12, n. 2, p. 369-80, 2016. ISSN 1554-8635. Disponível em: < https://www.ncbi.nlm.nih.gov/pubmed/26566717 >.

196 LAMPERT, M. A. et al. BNIP3L/NIX and FUNDC1-mediated mitophagy is required for mitochondrial network remodeling during cardiac progenitor cell differentiation. **Autophagy,** v. 15, n. 7, p. 1182-1198, 07 2019. ISSN 1554-8635. Disponível em: < https://www.ncbi.nlm.nih.gov/pubmed/30741592 >.

197 ESTECA, M. V. et al. Loss of Parkin Results in Altered Muscle Stem Cell Differentiation during Regeneration. **Int J Mol Sci,** v. 21, n. 21, Oct 2020. ISSN 1422-0067. Disponível em: < https://www.ncbi.nlm.nih.gov/pubmed/33126429 >.

198 BAECHLER, B. L.; BLOEMBERG, D.; QUADRILATERO, J. Mitophagy regulates mitochondrial network signaling, oxidative stress, and apoptosis during myoblast differentiation. **Autophagy,** v. 15, n. 9, p. 1606-1619, 09 2019. ISSN 1554-8635. Disponível em: < https://www.ncbi.nlm.nih.gov/pubmed/30859901 >.

199 PARK, J. et al. Mitochondrial dysfunction in Drosophila PINK1 mutants is complemented by parkin. **Nature,** v. 441, n. 7097, p. 1157-61, Jun 2006. ISSN 1476-4687. Disponível em: < https://www.ncbi.nlm.nih.gov/pubmed/16672980 >.

200 CHU, C. T. A pivotal role for PINK1 and autophagy in mitochondrial quality control: implications for Parkinson disease. **Hum Mol Genet,** v. 19, n. R1, p. R28-37, Apr 2010. ISSN 1460-2083. Disponível em: < https://www.ncbi.nlm.nih.gov/pubmed/20385539 >.

201 DAGDA, R. K. et al. Loss of PINK1 function promotes mitophagy through effects on oxidative stress and mitochondrial fission. **J Biol Chem,** v. 284, n. 20, p. 13843-55, May 2009. ISSN 0021-9258. Disponível em: < https://www.ncbi.nlm.nih.gov/pubmed/19279012 >.

202 CHEN, J. et al. A Convenient Cas9-based Conditional Knockout Strategy for Simultaneously Targeting Multiple Genes in Mouse. **Sci Rep,** v. 7, n. 1, p. 517, 03

2017. ISSN 2045-2322. Disponível em: < https://www.ncbi.nlm.nih.gov/pubmed/28364122 >.